2023

Phosphorus Release and Recovery from Simulated Ferric Wastewater Sludge

Aseel Alnimer
alni3770@mylaurier.ca

Phosphorus Release and Recovery from Simulated Ferric Wastewater Sludge

By

Aseel Ahmad Alnimer

Bachelor of Science, Chemistry, Yarmouk University, 1999
Master of Science, Chemistry, The University of Jordan, 2002

A thesis

Submitted to the Biological and Chemical Sciences Program

Faculty of Science

In partial fulfilment of the requirements for the

Doctor of Philosophy in Biological and Chemical Sciences

Wilfrid Laurier University

Waterloo, Ontario, Canada, 2023

Settle for nothing but the stars,

If you venture for a noble aim,

Whether a great or a trifling death,

The bitter cup tastes the same.

"Al-Mutanabbi"

"المتنبي"

DECLARATION OF CO-AUTHORSHIP

Chapter 3

This chapter contains my contribution to the paper that was published in *Journal of Environmental Chemical Engineering* and can be found online at the following link: https://www.sciencedirect.com/science/article/abs/pii/S2213343723009983.

Alnimer A., Scott Smith, D., Parker W., **2023**. Insight into direct phosphorus release from simulated wastewater ferric sludge: Influence of physiochemical factors. *Journal of Environmental Chemical Engineering*, Volume 11, Issue 3, 110259, doi.org/10.1016/j.jece.2023.110259. The paper is co-authored by myself, my supervisors Dr. D. Scott Smith and Dr. Wayne J. Parker. I did the literature search, planned, prepared, modeled and executed all experiments, analyzed data, and drafted the paper.

Chapter 4

This chapter contains my contribution to the paper that was published in *Chemosphere* and can be found online at the following DOI (doi.org/10.1016/j.chemosphere.2023.140500): Alnimer A., Scott Smith, D., Parker W., **2023**. Phosphorus release and recovery by reductive dissolution of chemically precipitated phosphorus from simulated wastewater, Chemosphere. The paper is co-authored by myself, my supervisors Dr. D. Scott Smith and Dr. Wayne J. Parker. I did the literature search, planned, prepared, modeled and executed all experiments, analyzed data, and drafted the paper.

Chapter 5

This chapter contains my contribution to the paper in preparation to be submitted to *Water Research*. "Impact of organic matter on chemical phosphorus removal and recovery in synthetic wastewater matrix". The paper is co-authored by myself, my supervisors Dr. D. Scott Smith and Dr. Wayne J. Parker. I did the literature search, planned, prepared, modeled and executed all experiments, analyzed data, and drafted the paper.

ABSTRACT

Phosphorus (P) is a fundamental element necessary for all life forms and a key component in the fertilizer industry. Meanwhile, the excessive load of P to water bodies due to human activities has the potential to promote eutrophication. Wastewater treatment plants remove P either biologically or chemically and produce P rich sludge which could be a potential renewable source for P. At present, commercial technologies exist for P recovery from biological wastewater sludge. However, P recovery from chemical sludge particularly iron(III)-phosphate (Fe-P) sludge generated in chemical P removal plants that use iron(III) salts remains a challenge.

This study explored, in lab bench scale, the influence of pH, competing anions (Cl^-), and Fe redox chemistry using reducing agents like ascorbic acid (AA) on direct P and Fe(III) release and recovery from simulated Fe-P sludge. Initial tests were performed in the absence of organic matter interferences followed up by tests in more realistic matrices where the effect of organic matter (OM) (carbonaceous and nitrogenous constituents) on chemical phosphorus removal and recovery is investigated.

Fe-P sludge was prepared to mimic the inorganic fraction of real Fe-P sludge using ferric additions to synthetic wastewater. The impacts of acidic/basic wet treatment (pH effect) and competing anions (Cl^-) on P and soluble Fe release from Fe-P sludge were assessed. Factors influencing recovery, such as sludge age and Fe/P molar ratio were also investigated. Results revealed that alkaline treatment had minimal effectiveness in releasing iron (<3%), but significantly facilitated phosphorus release, especially at a controlled pH of 10, where the percentage of phosphorus release reached (90±2%). The chloride effect in releasing P from Fe-P sludge was negligible. At ages less than 5 days, sludge ageing did not influence P release from Fe-P sludge. However, a noticeable decline in %P release (i.e., 50% reduction) was observed at ages of 9 and 11 days for pH values of 9-10. The reduction in P release by aging was best described by a zero-order kinetic model. Moreover, the internalization of surface bound P during aging was a proposed mechanism for the decrease in P release during ageing which was qualitatively supported by arsenic extraction and HFO surface area determination. The utilization of the PHREEQC geochemical software did not consistently align with the measured phosphorus release from the Fe-P sludge. This discrepancy can be attributed to PHREEQC's assumption that all surface sites for phosphorus are exchangeable, which neglects the representation of phosphorus that may be trapped within HFO particles.

The impact of reductive dissolution using AA under acidic conditions on P and Fe release from lab simulated Fe-P sludge was examined. To find the optimum conditions for Fe-P reductive solubilization and vivianite precipitation, factors like AA/Fe molar ratio, pH, and Fe-P sludge age were tested. Moreover, the reductive, chelating, and acidic effects of AA, were evaluated by comparing them with hydroxylamine (a reducing agent), oxalic acid (a chelating agent), and inorganic acids (to assess pH effects), including HNO_3, HCl, and H_2SO_4. At pH values of 3 and 4, and with Fe/AA molar ratios of 1:2 and 1:4, complete solubilization of Fe-P sludge and reduction

of Fe(III) were observed. The sludge age, up to 11 days, did not affect the reductive solubilization of Fe-P when AA was added. Hydroxylamine treatment resulted in negligible reductive dissolution of Fe-P sludge, while oxalic acid treatment at an Fe/oxalic acid molar ratio of 1:2 and pH 3 facilitated non-reductive dissolution, leading to solubilization of both phosphorus (95±2%) and Fe(III) (90±1%). Inorganic acids treatment at pH 3 resulted in very low P and Fe release (<10%) compared to AA and oxalic acid treatments. After complete solubilization of Fe-P sludge via AA treatment at pH 3, it became feasible to recover phosphorus and iron as vivianite by adjusting the pH to 7. Remarkably, this simple pH adjustment led to P and Fe recoveries of 88±2% and 90±1%, respectively. XRD analysis, Fe/P molar ratio measurements, and magnetic attraction confirmed the formation of vivianite. PHREEQC modeling exhibited reasonable agreement with the measured P and Fe release from Fe-P sludge and vivianite formation, highlighting its potential as a valuable tool for interpreting and predicting P and Fe release and recovery systems.

The influence of OM on P removal performance was tested using different synthetic wastewater recipes containing model carbonaceous and nitrogenous constituents and combination of them. Carbonaceous constituents including meat extract (ME), potato starch, glycerol, and Luther Marsh concentrate (LM) represented proteins, carbohydrates, lipids, and natural organic matter respectively. Peptone, urea, and ammonium chloride represented nitrogenous constituents. Results showed insignificant effect of nitrogenous constituents, potato starch and glycerol on P removal performance. However, ME and LM possessed a remarkable reduction in P removal performance of (3.0±0.4%) and (23±1%) respectively. No change in P removal performance observed for carbonaceous constituents in the presence of nitrogen source except for LM which exhibited a substantial increase by (23%). The higher measurements for soluble Fe (SFe) residuals for ME (87±5%) and LM (51±1%) indicated occurrence of interactions between Fe(III) cations and the negatively charged functional groups like hydroxyl, carboxyl, and phenolic groups available in ME and LM. This suggested Fe solubilization as the mechanism responsible for reducing P removal. Wet alkaline (pH 10) and ascorbic acid treatments showed no influence of OM on P release from Fe-P sludge.

ACKNOWLEDGMENT

First and foremost, I should offer my thanks, obedience, and gratitude to **ALLAH** the great from whom I receive my guidance and help.

-One of the most beautiful blessings of God comes to us as people-

I would like to express my deepest and heartiest thanks and appreciation to my supervisors Dr. Scott Smith and Dr. Wayne Parker for their supervision, continuous encouragement, unlimited patience and advise, and for their constant belief in me throughout the duration of this research. I am grateful for the opportunities you have given me to publish, present my work in eventful conferences, and to be a successful scientific researcher. Without your profound knowledge, tireless efforts and friendly relationship I could not be able to go through all the challenges in my Ph.D. study and stand where I am today. Working with you has been a great privilege to me.

My sincere thanks go to the members of my committee Dr. Vladimir Kitaev and Dr. Chris Parsons for providing valuable feedback and constructive suggestions throughout each stage of my research. My sincere thanks are also for Dr. Kevin Stevens (internal examiner) and Dr. Yves Comeau (external examiner) for their valuable time and contribution to my research journey. It is a great pleasure to have you as my examiners.

I would like to extend my thanks to Dr. Lillian DeBruin, Gena Braun, Victoria Jarvis, Ron Danial and Alaa Alsherbi for their help and support. My heartiest thanks to Jane Davidson; your constant friendship and support always helped me overcome the ups and downs I was facing throughout my study journey.

I would like also to thank the Graduate and Postdoctoral Studies, Department of Chemistry and Biochemistry, and William Nikolaus Martin Science Scholarship, Wilfrid Laurier University, for their financial support. Also, thanks to Ontario Government for the Queen Elizabeth II Graduate Scholarship in Science and Technology Award.

Finally, I want to express my heartiest thanks to my husband, Muhammad and my sons Elias and Yousif for their encouragement, patience and care they have shown during my study. I am also grateful to my brothers Waleed and Wael, my sisters, Lamees, Dana, and Farah, my sister-in-law Reham and my dearest friend Zoulina for their moral support, inspiration, and encouragement throughout my whole study journey.

DEDICATION

For the soul of my dear parents

Ahmad Alnimer & Khairia Marie

And to those who care about my success

LIST OF ABBREVIATIONS

AA	Ascorbic Acid
AD	Anerobic Digestion
ADP	Adenosine Diphosphate
ATP	Adenosine Triphosphate
BET	Brunauer-Emmett-Teller
BOD	Biochemical Oxygen Demand
COD	Chemical Oxygen Demand
CPR	Chemical Phosphorus Removal
DHA	Dehydroascorbic Acid
DIRB	Dissimilatory Iron-Reducing Bacteria
DMRB	Dissimilatory Metal-Reducing Bacteria
DOC	Dissolved Organic Carbon
DOM	Dissolved Organic Matter
EBPR	Enhanced Biological Phosphorus Removal
EDTA	Ethylenediaminetetraacetic Acid
EET	Extracellular Electron Transfer
HFO	Hydrous Ferric Oxide
HS	Humic Substance
ICP-OES	Inductively Coupled Plasma Optical Emission Spectroscopy
LM	Luther Marsh
Mt/year	Million metric tonnes per Year

NIST	National Institute of Standards and Technology
NOM	Natural Organic Matter
nRP	non-Reactive Phosphorus
OM	Organic Matter
ORPs	Oxidation Reduction Potentials
Ox	Oxalic Acid
P_{ortho}	Orthophosphate
POC	Particulate Organic Matter
PXRD	Powder X-Ray Diffraction (PXRD)
PZC	Point of Zero Charge
RP	Reactive Phosphorus
RPM	Round Per Minute
SI	Saturation Index
TFe	Total Iron
TN	Total Nitrogen
TOC	Total Organic Carbon
TP	Total Phosphorus
TSS	Total Suspended Solids
USGS	US Geological Survey
WRRFs	Water Resource Recovery Facilities
WWTPs	Wastewater Treatment Plants
XAS	X-ray absorption spectroscopy
XRD	X-Ray Diffraction

TABLE OF CONTENTS

Page

LIST OF FIGURES

LIST OF TABLES

Chapter 1 - Introduction

1.1 Problem statement

The demand for fertilizers has increased in the last 75 years as a result of increasing global food production accompanied by the green revolution (Childers et al., 2011; Kok et al., 2018). Phosphorus (P) is a fundamental key ingredient in the fertilizer industry. Phosphate rock mining has commonly been the main source of P. The approximate annual mining of P is 21±4 million metric tonnes per year (Mt P/year) where 18±4 Mt P/year are used for fertilizer production. (Cordell and White, 2014). However, many studies have predicted that due to excessive mining, easy to extract deposits of this non-renewable source are expected to be reduced in a few decades (Cordell et al., 2009; Cordell and White, 2014; Kok et al., 2018). As a result of this reduction, to meet P needs, it will become necessary to utilize poor quality, high impurity, hard rock phosphate deposits, which would escalate mining and processing costs. Furthermore, phosphorus reserves are not evenly distributed globally. A small number of countries, such as China, the United States, and Morocco, possess a significant portion of the world's phosphorus resources. This concentration can lead to geopolitical tensions and competition for access to these resources. Therefore, ecological, economical, and geopolitical factors prioritize searching for alternative sources of P (Peng et al., 2018b).

Municipal wastewater treatment plants (WWTPs) are significantly a large anthropogenic pool for P where 1.3 Mt P/year is removed globally from wastewater streams (Vuuren et al., 2010; Wilfert et al., 2015). Therefore, upon P recovery WWTPs could provide 15-20% of the world's P demand (Peng et al., 2018a). In fact, trends toward P recovery from sewage sludge generated in WWTPs through water resource recovery facilities (WRRFs) has gained considerable attention.

At present the greatest fraction of P recovered from WWTPs is limited to enhanced biological phosphorus removal (EBPR) plants where struvite ($MgNH_4PO_4.6H_2O$) crystallization is utilized (Wilfret et al., 2015). Although P recovery from EBPR plants is practiced around the world in full scale applications (i.e., in North America there are six WRRFs operating struvite crystallization) (Latimer et al., 2015), EBPR plants might not be the optimal place for P recovery because of complex operating conditions, soluble P concentration needs to be >100 mg P/L, higher costs compared to low-value product, and unsatisfactory recovery efficacy (10-50%) (Hao et al., 2013; Egle et al., 2015; Xie et al., 2016; Lin et al., 2017a).

On the contrary, chemical P removal (CPR) plants are more widespread than EBPR plants in North America and Europe, as only CPR can achieve lowest limits of P removal often required for sensitive receiving waters (Szabó et al., 2008). CPR plants generate iron-phosphate (Fe-P) rich sludge due to the interaction of the iron(III) cations with phosphate ions in wastewater (Peng et al., 2018b). The different forms of Fe-P minerals produced include strengite ($FePO_4.2H_2O$), iron-hydroxyphosphate ($Fe_nPO_4(OH)_{3n-3}$), and vivianite ($Fe_3(PO_4)_2.8H_2O$). Phosphate can also bind to the surfaces of hydrous ferric oxide (HFO) formed during wastewater treatment (Smith et al., 2008). The iron phosphorus solids are retained, and concentrated in the sludge and make CPR plants a potential source for P recovery. Moreover, direct release of P from Fe-P sludge can potentially provide soluble P in concentrations greater than 100 mg P/L required for efficient struvite crystallization. For example, Monea et al, (2020) reported direct solubilization of 600 mg P/L from tertiary Fe-P sludge by wet acidic treatment (pH<1.5). In addition, P could be recovered from CPR sludge directly as solid vivianite (Wilfert et al., 2016; Wu et al., 2019; Port et al., 2022).

While several approaches have been used to effectively extract P from Fe-P sludge, P recovery from CPR plants is still challenging and needs more investigations in terms of the

performance of direct P release from the inorganic fraction of Fe-P sludge, and the different physiochemical factors affecting it, particularly in the absence of interferences found in real wastewater media such as bacteria and organic matter. Moreover, it is important to explore the effect of organic matter on the performance of chemical P removal which could significantly affect the amount of Fe-P sludge generated. Obtaining such knowledge will facilitate developing effective technologies for P release and recovery from CPR plants.

1.2 Objectives & research questions

Currently, adoption of P recovery technologies for CPR plants is increasing gradually. For example, in 2016, 26% of the total generated Fe-P rich biosolids from four CPR plants in Toronto city (Canada) were recycled for land application, 49% were made into fertilizer pellets, and 25% were stabilized by alkaline treatment to treat acidic soils (City of Toronto, 2023). As mentioned earlier, it is important to study and understand the behaviour of direct P release and recovery from the inorganic fraction of Fe-P sludge in the absence of wastewater interferences, and the effect of organic matter on chemical P removal and recovery. Different physiochemical factors play a vital role in P release and recovery form Fe-P sludge such as solution pH, Fe/P molar ratio, competing anions, sludge age, and iron redox chemistry. Therefore, a systematic investigation for these factors is required.

The primary objectives of this PhD dissertation are: (i) to investigate the effectiveness and describe the mechanism of direct P release from simulated Fe-P sludge that mimic the inorganic composition of real Fe-P sludge in CPR plants after acid/alkali and NaCl treatment under the influence of Fe/P molar ratio and sludge aging time; (ii) to explore the role of iron redox chemistry on P release and recovery from Fe-P sludge by chemically mediated reduction of Fe(III) to Fe(II)

using different chemical reducing agents and the potential for P recovery as vivianite; (iii) to evaluate the influence of organic matter (carbonaceous and nitrogenous constituents) on the efficiency of P removal by iron(III) salts and on P recovery from inorganic Fe-P sludge using model compounds and different simulated wastewater recipes.

In order to accomplish these objectives, the following research questions were set:

1- What are the effects of acid/alkali wet treatment, chloride anion, and Fe/P molar ratio on the performance of direct P release from the inorganic fraction of Fe-P sludge? (Chapter 3)

2- Dose Fe-P sludge age affect P release? If yes, what mechanism explains this effect? (Chapter 3)

3- Can P be recovered from Fe-P sludge as vivianite using chemical reducing agents? (Chapter 4)

4- In wastewater, how does organic matter affect chemical P removal and recovery? (Chapter 5)

In this doctoral research, the above questions have been covered and described one by one, in laboratory bench testing scale under different experimental conditions.

1.3 Significance

Using simulated wastewater of increasing complexity, these studies provide insight into the chemistry of P release from inorganic Fe-P sludge generated in CPR plants, both in the absence of interferences from organic wastewater components (Chapters 3 and 4) as well as with Fe-P sludge generated in the presence of organic matter of variable composition (Chapter 5). By starting from simple inorganic solids, the experiments provide knowledge about the influence of different physiochemical factors (i.e., pH, Fe:P molar ratio, chloride ion, sludge age, and redox potential) on direct P release from Fe-P sludge and the more complex matrices demonstrate the effect of

different organic matter constituents on chemical P removal and recovery in more realistic simulated wastewater. Taken as a whole, these experiments help demonstrate what might be practically implemented to achieve P release and recovery from CPR plants. Moreover, the investigations made in these studies toward using chemical reducing agents to release and recover P will help to set the basis for a new promising route for P recovery as vivianite from raw and activated Fe-P sludge in CPR plants. Overall, the results of this detailed study will help determine the theoretical and practical potential for P release and recovery from wastewater ferric sludge.

1.4 Thesis structure

This thesis includes six different chapters and three appendices. Chapter 1 establishes the research problem and objectives. Chapter 2 contains background information related to Fe and P chemistry in wastewater and research related to removal and recovery. Chapter 3 to Chapter 5 present three different experimental projects that are written in manuscript format. Finally, Chapter 6 summarizes the overall conclusions and discusses recommendations for future directions followed by appendices. The content for each chapter of my thesis is stated as follows: Chapter 1 introduce the problem statement, research questions and objectives, significance, and thesis structure. Chapter 2 describes general background information. It talks about phosphorus in environment, chemical P removal in CPR plants and Fe-P sludge generation, organic matter in wastewater and its interactions with iron (III), factors influencing P release and recovery, P recovery products, and finally, geochemical modeling approach. Chapter 3 contains paper "Insight into direct phosphorus release from simulated wastewater ferric sludge: Influence of physiochemical factors". This paper describes the effects of sludge age, NaCl, and Fe/P molar ratio on pH-induced phosphorus release from simulated Fe-P sludge that had Fe/P molar ratios which mimic the inorganic composition of actual Fe-P sludge in CPR plants. Chapter 4 includes the paper

"Phosphorus release and recovery by reductive dissolution of chemically precipitated phosphorus from simulated wastewater". This paper illustrates the use of chemical reducing agents like ascorbic acid to induce iron(III) reduction to iron(II) for the purpose of releasing P from Fe-P sludge and recover it as vivianite by solution pH adjustment. It also, compares the performance of ascorbic acid with other reducing agents (hydroxylamine) and complexing agents (oxalic acid) for P release and recovery. Chapter 5 represents paper "Impact of organic matter on chemical phosphorus removal and recovery from a synthetic wastewater matrix". This paper investigates the effect of different carbonaceous and nitrogenous constituents on P removal efficiency by iron(III) salts and P release from Fe-P sludge by alkaline (pH 10) and ascorbic acid treatment in synthetic wastewater. The last chapter in this thesis is Chapter 6 which compiles the various conclusions and recommendations for future directions. Appendices 1, 2, and 3 contain the supplementary material for chapters 3, 4, and 5 respectively while appendix 4 contains some aspects of Chapter 3 that attained after it was published and include extra discussion for PHREEQC modeling, effect of NaCl, and effect of aging.

1.5 References

Cordell, D., Jan Olof D., and Stuart W., **2009**. The Story of Phosphorus: Global Food Security and Food for Thought. Global Environmental Change 19 (2): 292–305. doi:10.1016/j.gloenvcha.2008.10.009.

Cordell, D., and White, S., **2014**. Life's Bottleneck: Sustaining the World's Phosphorus for a Food Secure Future. Annu Rev Environ Resour 39:161–188. doi:10.1146/annurev-environ-010213-113300.

Childers, D. L., **2011**. Response from Childers: Phosphorus Challenges beyond the Food System. BioScience, (61), 8:582–583, doi.org/10.1525/bio.2011.61.8.19.

City of Toronto, **2023**. *Biosolids Management*. < https://www.toronto.ca/services-payments/water-environment/managing-sewage-in-toronto/biosolids-management/>. (Retrieved July 25, 2023).

Egle, L., Rechberger, H., Zessner, M., **2015**. Overview and description of technologies for recovering phosphorus from municipal wastewater. Resour. Conserv. Recycl. 105, 325-346. doi.org/10.1016/j.resconrec.2015.09.016.

Egle, L., Rechberger, H., Krampe, J., Zessner, M., **2016**. Phosphorus Recovery from Municipal Wastewater: An Integrated Comparative Technological, Environmental and Economic Assessment of P Recovery Technologies. Science of The Total Environment 571. Elsevier: 522–42. doi:10.1016/J.SCITOTENV.2016.07.019.

Hao, X., Wang, C., van Loosdrecht, M.C.M., Hu, Y., **2013**. Looking beyond struvite for P-recovery. Environmental Science Technology. 47 (10), 4965-4966.

Kok, D. D., van Lier,J. B., Uhlenbrook, S., Ortigara, A. R.C., Pande, S., Savenije, H., **2018**. Global Phosphorus Recovery for Agricultural Reuse. Hydrology and Earth System Sciences Discussions, 1–18. doi:10.5194/hess-2018-176.

Latimer, R., Rohrbacher, J., Nguyen, V., Khunjar, W. O., Jeyanayagam, S., **2015**. Towards a Renewable Future: Assessing Resource Recovery as a Viable Treatment Alternative (NTRY1R12b). Water Environment Research Foundation. doi.org/10.2166/9781780407883.

Lin, L., Li, R.-h., Li, Y., Xu, J., Li, X.-y., **2017a**. Recovery of organic carbon and phosphorus from wastewater by Fe-enhanced primary sedimentation and sludge fermentation. Process Biochem. 54, 135-139. doi:10.1016/j.procbio.2016.12.016.

Monea, M.C., Löhr, D.K., Meyer, C., Preyl, V., Xiao, J., Steinmetz, H., Schönberger, H., Drenkova-Tuhtan, A., **2020a**. Comparing the leaching behavior of phosphorus, aluminum and iron from post-precipitated tertiary sludge and anaerobically digested sewage sludge aiming at phosphorus recovery. J. Clean. Prod. 247, 119129. doi.org/10.1016/j.jclepro.2019.119129.

Peng, Lihong, Hongliang Dai, Yifeng Wu, Yonghong Peng, and Xiwu Lu., **2018b**. A Comprehensive Review of the Available Media and Approaches for Phosphorus Recovery from Wastewater. Water, Air, & Soil Pollution 229 (4). doi:10.1007/s11270-018-3706-4.

Prot T., Pannekoek W., Belloni C., Dugulan A.I., Hendrikx R., Korving L., Loosdrecht M.C.M., **2022**. Efficient formation of vivianite without anaerobic digester: Study in excess activated sludge. Journal of Environmental Chemical Engineering (10) 107473. doi.org/10.1016/j.jece.2022.107473.

Szabó, A., Takács, I., Murthy, S., Daigger, G. T., Licskó, I., Smith, S. D., **2008**. Significance of Design and Operational Variables in Chemical Phosphorus Removal. Water Environment Research 80 (5): 407–16. doi:10.2175/106143008X268498.

Vuuren, D. P. Van, Bouwman A. F., Beusen, A. H. W., **2010**. Phosphorus Demand for the 1970–2100 Period: A Scenario Analysis of Resource Depletion. Global Environmental Change 20 (3): 428–39. doi:10.1016/j.gloenvcha.2010.04.004.

Wilfert, P., A Mandalidis, A., Dugulan, A. I., Goubitz, K., Korving, L., Temmink. H., **2016**. Vivianite as an Important Iron Phosphate Precipitate in Sewage Treatment Plants. Water Research 104. 449–60. doi:10.1016/j.watres.2016.08.032.

Wilfert, P., Prashanth S. K., Korving, L., Witkamp, G. J., van Loosdrecht, M.C.M., **2015**. The Relevance of Phosphorus and Iron Chemistry to the Recovery of Phosphorus from Wastewater: A Review. Environmental Science and Technology 49 (16): 9400–9414. doi:10.1021/acs.est.5b00150.

Wu Y., Luo J. Y., Zhang Q., Aleem M., Fang F., Xue Z. X., Cao J. S., **2019**. Potentials and challenges of phosphorus recovery as vivianite from wastewater: a review. Chemosphere. 226:246–258. doi.org/10.1016/j.chemosphere.2019.03.138.

Xie, M., Shon, H. K., Gray, S. R., Elimelech, M., **2016**. Membrane-based processes for wastewater nutrient recovery: technology, challenges and future direction. Water Research, 89; 210 -221. doi.org/10.1016/j.watres.2015.11.04.

Chapter 2 - Background Information

2.1 Phosphorus

Phosphorus (P) is a non-metallic element located in group 5 and period 3 in the periodic table with atomic number 15. It is the 11th most available element in the Earth's crust and has three main allotropic forms including red, white, and black phosphorus (Smil, 2000; Prasad and Majeti, 2016). In living organisms, P is a main building block of DNA and RNA; the nucleic acids that store and replicate all genetic codes and information. Also, the cycling of P based bond (phosphate bond) between adenosine diphosphate (ADP) and adenosine triphosphate (ATP) generates energy; necessary for complex molecules production in living systems (Westheimer, 1987; Smil, 2000). In addition, P is unsubstituted and essential key nutrient for crops production, which makes it a basic ingredient in fertilizer industry along with potassium and nitrogen (Prasad and Majeti, 2016). Therefore, P is crucial element for all life forms.

Owing to its high reactivity and instability, P is commonly found in nature in the form of phosphate containing minerals such as apatite ($Ca_5(PO_4)_3(F,Cl,OH)$) and other P-bearing minerals where P atom exhibits oxidation state of +5 (Smil, 2000; Prasad and Majeti, 2016). However, other reduced forms of P including phosphite ($H_2PO_3^-$), hypophosphite ($H_2PO_2^-$), and phosphine (PH_3) with P oxidation states of +3, +1, and -3 respectively are known to occur in nature (Pasek et al., 2014) (Figure 2.1).

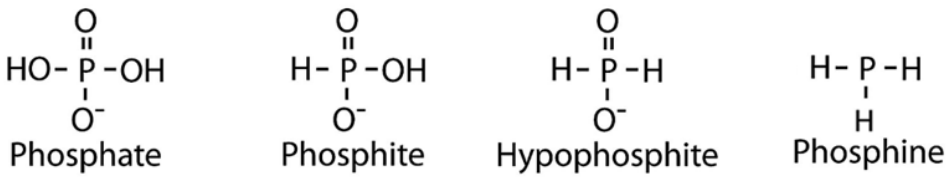

Figure 2.1 Phosphorus compounds with different oxidation numbers; phosphate (+5), phosphite (+3), hypophosphite (+1), and phosphine (-3).

Looking at natural P cycle (Figure 2.2) (Cordell et al., 2011) the initial source and largest pool of P on the Earth are lithospheric phosphate rocks where about 85% are contained in sedimentary rocks, and 15% in igneous rocks (Johanston, 2000). Phosphorus transfers to hydrosphere (oceans & freshwater) in soluble and particulate forms via weathering, soil erosion, runoff, and mineralization (Yuan et. al., 2018; Smil, 2000). At natural conditions, P loadings to freshwater and ocean (through riverine runoff) were estimated to be 6.5 ± 1.5 Mt P/year and 4.5 ± 1.5 Mt P/year respectively (Yuan et al., 2018; Beusen et al. 2016, Smil, 2000). When P enters the biosphere, it transfers between ecosystems and biota via organic cycles that take place on land and water, and moves within the living organisms through food chains (Yuan et al., 2018; Smil, 2000). However, most of P is only one way flow starting from lithosphere and ending as neritic sediments that lost to deep sea sediments. In fact, P takes very long timescales (millions to billions of years) to be exposed to lithosphere surface again via geological uplift and tectonic processes.

Figure 2.2 Phosphorus cycle in nature.

Phosphorus exists in nature at levels that maintain the balance between its availability and consumption demand by living organisms in ecosystems (Johanston, 2000; Smil, 2000). Eutrophication is the term used to describe the environmental problem occurring when these natural conditions are out of balance due to anthropogenic increase of P levels in freshwater (Ansari and Gill, 2014a). As a limiting nutrient, $\geq$10 μg P/L is the threshold concentration of dissolved P where eutrophication can potentially occurs (Ansari and Gill, 2014a; Smil, 2000).

Phosphate rock mining has traditionally been the main source of P where the approximate annual mining of P is 21$\pm$4 Mt P/year; 18$\pm$3.5 Mt P/year are used for fertilizer production and 6.3$\pm$3.2 Mt P/year of P used for fertilizer production enters the environment (Cordell and White, 2014). This non-renewable source is expected to be depleted in a few decades due to excessive mining that is estimated to reach its peak by 2035 (Cordell et al., 2009; Cordell and White, 2014; Kok et al., 2018). As a result of this depletion, in the future only a poor quality phosphate rocks will be available, which will lead to higher mining and processing costs. Moreover, phosphate rock

mining has the potential to release greenhouse gases through various processes and activities associated with its extraction and processing such as energy consumption, chemical processing, and transportation. In addition, natural P resources are limited to a number of counties (China, US, and Morocco) which control global P availability. So, it is clear that ecological, economical, and geopolitical factors demand looking for alternative sources of P (Peng et al., 2018b).

Municipal wastewater effluents are sustainable anthropogenic source for P that could cover around 15-20% of the global P demand. Approximately 1.3 Mt P/year is treated globally from municipal WWTPs (Vuuren et al., 2010; Wilfert et al., 2015; Peng et al., 2018a). Some example sources that contribute to P loads in wastewaters include human wastes (30-50% P), detergents, and household cleaning products (50-70% P), and residual P after crop production (Ruzhitskaya and Gogina, 2017; Prasad and Majeti, 2016; Zhou et al., 2018).

In WWTPs P is treated and removed from wastewater effluents before discharging them to surface water to prevent eutrophication and control mobilization of P to the environment (Carey and Migliaccio, 2009). Due to the high demand for fertilizers as a result of increasing global food production, trends toward integrating P removal and recovery in municipal WWTPs have gained remarkable attention (Cooper et al., 2011; Kok et al., 2018). Simply, direct application of P rich sewage sludge to agricultural lands has been utilized globally. However, heavy metals contamination, microplastics, pathogens, and transport costs are some of the key drawbacks and challenges associated with using P rich sewage sludge as fertilizer. Therefore, it is important to extract and recycle P from sewage sludge to more value-added products to ensure its safe use as fertilizer. Typically, in modern WWTPs P is recycled through WRRFs (Peng et al., 2018a ; Mayer et al., 2016). Such facilities are designed to directly contribute to a circular economy by producing clean water, recovering nutrients (i.e., carbon, nitrogen, and phosphorus) to value-added products,

treating biosolids, and generating renewable energy (Vu et al., 2023). The advanced WWTP Blue Plains (Washington, D.C., US), serves as a prime example of WRRFs. It is globally recognized as one of the largest facilities of its kind, employing advanced techniques for nutrients recovery, energy production via anaerobic digestion, and effective management of biosolids.

2.2 Chemical phosphorus removal (CPR) in WWTPs

In municipal wastewater the typical concentration of total P (TP) ranges between 6 and 12 mg/L (Di Capua et al., 2022). Phosphorus in the form of orthophosphates (P_{ortho}, see Figure 2.3) is removed during the treatment of wastewater via chemical precipitation by addition of coagulant salts (chlorides or sulphates) of iron(II), iron(III), aluminum and calcium (Thistleton et al., 2001; Ruzhitskaya and Gogina 2017). Such metal ions can form (through different mechanisms) stable insoluble solids with P_{ortho} that can be settled out and removed physically by sedimentation, filtration, centrifugation, and membrane separation (WEF, 2011).

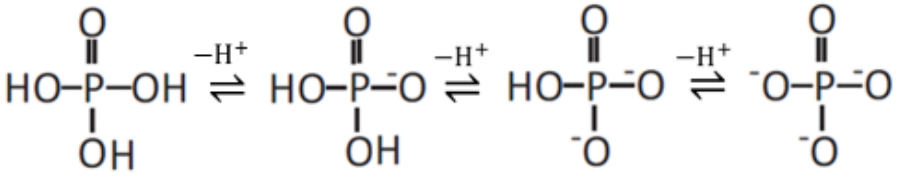

Figure 2.3 Chemical structures of protonated and deprotonated orthophosphates derived from dissociation of triprotic phosphoric acid H_3PO_4 ($pK_{a1} = 2.15$, $pK_{a2} = 7.20$, $pK_{a3} = 12.33$). Phosphate anion (PO_4^{3-}) is the product of full dissociation of H_3PO_4.

In terms of implementation, there is flexibility in the CPR process which allows for the addition of coagulants at different points in the treatment train, including upstream, within and downstream of aerobic biological treatment. For example, coagulants could be added to the primary effluent, to the aeration tank, before the final clarifier during secondary treatment, or

during tertiary treatment (Figure 2.4) (Magrí et al., 2020; Mores et al., 1998). In CPR plants that use iron salts, P is precipitated as iron(III) phosphate (Fe-P) sludge. For many CPR plants, iron salts are preferred because they are efficient and cheap (Mores et al., 1998).

The performance of P_{ortho} precipitation is governed by different factors including wastewater characteristics such as pH, total organic carbon (TOC), TP concentration, and alkalinity. Other factors influencing performance include type, amount, point and mode of application of the metal salt, mixing intensity, and concentration of total suspended solids (TSS) (Mores et al., 1998; Thistleton et al., 2001; Szabo´ et al., 2008; WEF, 2011). Based on the engineering design of the plant, which determines the requirements of the metal salt used, a residual TP ranged between 10 to 50 µg P/L can be achieved. (Kroiss et al., 2011; WEF, 2011).

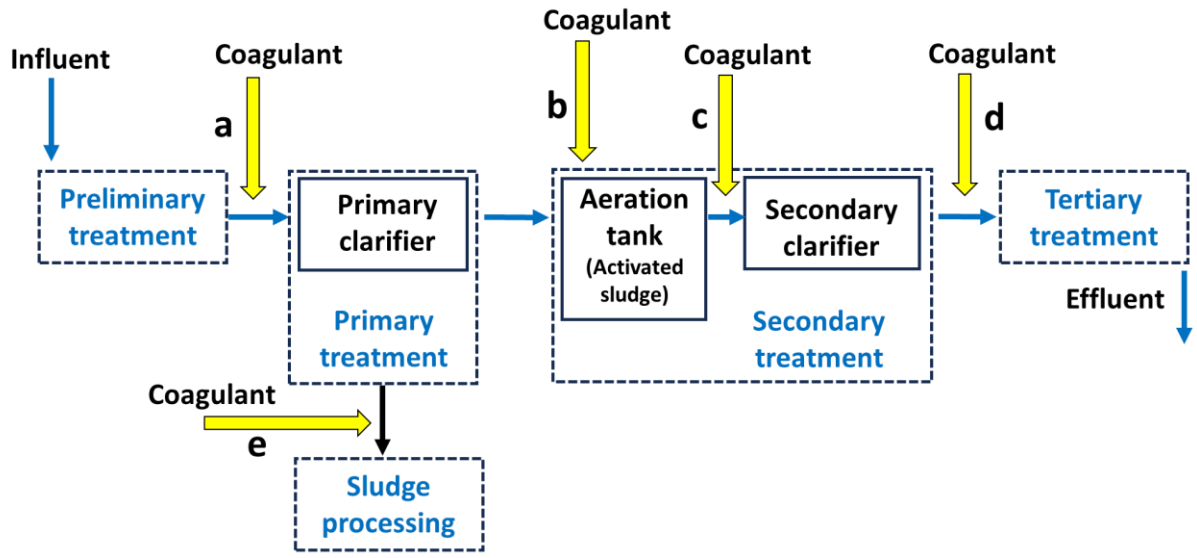

Figure 2.4 A schematic diagram for typical CPR process. Yellow arrows show possible points of chemical addition depending on CPR design. (a) After preliminary treatment, (b) Aeration tank, (c) Before the secondary clarifier during secondary treatment, (d) Before tertiary treatment, and (e) Before raw sludge processing.

2.3 Formation of Fe-P sludge in CPR process

In aqueous systems Fe(III) ion undergoes hydrolysis where the Fe atom coordinates with 6 water molecules and forms an octahedral hexacoordinated aquo complex $[Fe(H_2O)_6]^{3+}$ known as the hydrated iron(III) cation (Flynn, 1984). Different soluble and insoluble hydrolysis products of iron(III) may be generated where their formation, stability, and solubility depend on solution pH, oxidation-reduction potential (ORP), and total Fe concentration (Cornell et al., 1989; Wilfert et al., 2015). For example, as solution pH increase, hydrolysis to soluble $[Fe(H_2O)_6]^{3+}$ takes place where hydroxyl ions replace water molecules and form mononuclear ($[Fe(H_2O)_5(OH)]^{2+}$, $[Fe(H_2O)_4(OH)_2]^{+}$, $[Fe(H_2O)_3(OH)_3]$ and $[Fe(H_2O)_3(OH)_4]^{-}$) hydroxyl complexes. However, at total iron increase hydroxyl and/or oxo bridging may occur and form binuclear ($[Fe_2(H_2O)_8(OH)_4]^{2+}$) that continue to associate and precipitate as solid polynuclear hydroxyl complexes (Cornell et al., 1989; Flynn, 1984). Moreover, when iron(III) hydrates come in to contact with dissolved oxygen in water they form insoluble iron (III) oxides, iron (III) oxyhydroxides, and iron (III) hydroxide (Table 2.1) (Flynn, 1984; Cornell and Schwertmann, 2003; Wilfert et al., 2015).

Iron oxides can be characterized in terms of surface area, active sites, porosity, reducibility, and solubility according to their structure as either crystalline or amorphous. Typically, amorphous iron oxides have higher adsorption intensity because of their higher surface area (Cornell and Schwertmann, 2003; Wilfert et al., 2015).

Table 2.1 Examples of iron oxide compounds (Cornell and Schwertmann, 2003).

Iron(III) oxides		Iron(III) oxyhydroxides		Iron(III) hydroxides
hematite	α-Fe_2O_3	goethite	α-FeOOH	ferric hydroxide
maghemite	γ-Fe_2O_3	akaganeite	β-FeOOH	$Fe(OH)_3$
		lepidocrocite	γ-FeOOH	
		2-line ferrihydrite	$(Fe_5HO_8 \cdot 4H_2O)$[a]	
		6-line ferrihydrite	$(5Fe_2O_3.9H_2O)$[b]	

[a] This is one proposed chemical formula for 2-line ferrihydrite known as hydrous ferric oxide (HFO) (Jambor & Dutrizac,1998).
[b] This is one proposed chemical formula for 6-line ferrihydrite (Jansen et al., 2002).

Phosphorus exists in municipal wastewater in organic and inorganic forms. Organic P commonly originated from natural sources (i.e., plant components, animal manure, and microbial cellular materials) and anthropogenic sources (i.e., pesticides and herbicides) (Petzoldt et al., 2020) and commonly comprise 15% of TP (Parsons and Smith, 2008). It consists of a diverse range of compounds, such as ATP, phosphonate, phosphoproteins, phospholipids, phosphoamides, sugar phosphates, amino phosphoric acids, and other condensed organic phosphorus species. (Lu et al., 2014; Venkiteshwaran et al., 2018). In the other hand, orthophosphates and condensed phosphates represent the inorganic form of P and comprise 50% and 35% of TP respectively (Parsons and Smith, 2008). Based on reactivity under acidic conditions and at high temperatures, organic P and condensed phosphates are classified as non-reactive P (nRP), while orthophosphates considered the reactive P (RP) which can be removed from wastewater by chemical precipitation (Standard methods, 2012; Venkiteshwaran et al., 2018).

In WWTPs during CPR process Fe interacts with P_{ortho} through different routes including precipitation, co-precipitation, and adsorption (Wilfert et al., 2015). During precipitation, dissolved Fe cations react simultaneously with phosphate anions and form Fe-P minerals that vary

depending on ambient conditions. For example, strengite [$Fe(PO_4).2H_2O$], and vivianite [$Fe_3(PO_4)_2.8H_2O$] are different Fe-P minerals forming in oxic and anoxic environments, respectively (Equations 2-1 and 2-2) (Nriagu, 1984; Cornell and Schwertmann, 2003). The formation and solubility of Fe-P minerals are governed by the pH and oxidation-reduction conditions. For instance, solid ferric phosphate ($FePO_{4\,(s)}$) precipitates typically around pH 3.5 with no evidence of occurrence at pH higher that 5 (Smith et al., 2008).

$$Fe^{3+}_{(aq)} + PO^{3-}_{4\,(aq)} + 2H_2O \rightarrow Fe(PO_4).2H_2O_{(s)} \qquad \text{strengite} \qquad (2\text{-}1)$$

$$3Fe^{2+}_{(aq)} + 2PO^{3-}_{4\,(aq)} + 8H_2O \rightarrow Fe_3(PO_4)_2.8H_2O_{(s)} \qquad \text{vivianite} \qquad (2\text{-}2)$$

The co-precipitation route takes place when P_{ortho} is incorporated (trapped) into the structure of Fe(III) hydrolysis precipitates (see Table 2.1) to form iron hydroxyphosphate solids with general formula $Fe_xPO_4(OH)_{3x-3}$ (Ping et al., 2022). However, in the pH range between 6 to 8 typical to CPR process, hydrous ferric oxide (HFO) is considered to be the dominant form of iron oxyhydroxides in wastewater after direct hydrolysis of Fe(III) in the presence of sufficient alkalinity (WEF, 2011). The active sites on HFO surface allow P_{ortho} to be adsorbed onto HFOs' surface and a surface complexation reaction occurs where P_{ortho} binds directly to the surface of HFO via ligand exchange mechanism in which Fe atom acts as Lewis acid and exchanges the hydroxyl group present on the surface of HFO with oxygen atom from the P_{ortho} anion as illustrated in Equation (2-3) and Figure (2.5) (Nriagu, 1984; Cornell and Schwertmann, 2003; Smith et al., 2008; Wilfert et al., 2015).

$$\equiv FeOOH_{(s)} + HOPO_{3(aq)} \rightarrow \equiv FeOOPO_3 + H_2O \qquad (2\text{-}3)$$

A variety of surface complexation reactions could take place ending with different inner-sphere complexes. For example, single P_{ortho} molecule could binds one Fe atom through one oxygen bond (mononuclear monodentate, see Figure 2.5), two oxygen bonds (mononuclear bidentate), or it could binds two Fe atoms through two oxygen bonds (binuclear bidentate). The strength of binding between P_{ortho} molecule and HFO surface is determined by the number of oxygen atoms bonded to Fe atoms (Abdala et al., 2015; Wilfert et al., 2015).

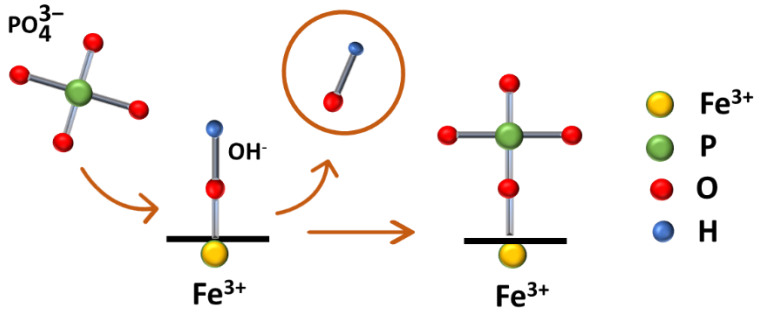

Figure 2.5 Adsorption of phosphate ion on iron oxide surface via ligand exchange mechanism and formation of mononuclear monodentate complex where one phosphate molecule binds one Fe atom via one oxygen bond.

Although the above mentioned routes may coexist in CPR process, many researchers described the mechanism of P_{ortho} removal by HFOs with fast co-precipitation reactions followed by slow complexation/adsorption reactions into HFOs' surfaces (Smith et al., 2008; Szabó et al., 2008; Carliell-Marquet et al., 2010; Li et al., 2018; Ping et al., 2022). Therefore, co-precipitation and adsorption pathways are typically the routes responsible for the formation of Fe-P solids during P removal process at circumneutral pH. Figure 2.6 illustrates how P in Fe-P solids is included (trapped) inside the amorphous structure of HFO and adsorbed onto its surface through surface complexation reactions (Smith et al., 2008; Hauduc et al., 2015).

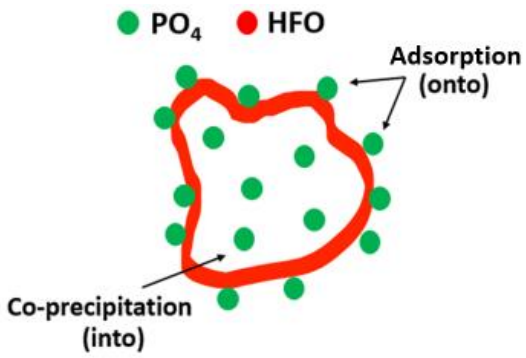

Figure 2.6 An illustrative drawing for amorphous Fe-P solid particle. The red outline indicates an HFO particle and the green dots represent surface bound and trapped phosphate molecules.

2.4 Organic matter in wastewater

Organic matter (OM) is the term applied to carbon-based compounds that are derived from living organisms or their metabolic processes. In municipal wastewater, OM composition is diverse and varies depending on origin. A variety of sources contribute to OM loading in wastewater include human wastes, food wastes, decomposition of animal and plant residues, and industrial discharges (Ghunmi et al. 2008; Metcalf and Eddy, 2014). However, depending on its origin and physical and chemical characteristics, OM in wastewater can be allocated into different categories. For example, human and food wastes contain proteins, carbohydrates, and lipids (Heukelekian and Balmat, 1959; Raunkjaer et al., 1994; Huang et al., 2004). Humic and fulvic substances are originated from soil and decay products of dead animals and plants (Stevenson,1994), while organic pollutants are more concentrated in industrial effluents (Heukelekian and Balmat, 1959; Sophonsiri and Morgenroth, 2004).

Based on particle size OM is generally classified into two main groups including dissolved (soluble), and particulate (insoluble) organic matter (Danielsson, 1982; Mara & Horan, 2003; Mopper et al., 2007; Metcalf and Eddy, 2014). Dissolved organic matter (DOC) represent organic

compounds that are soluble in water and pass through 0.45 micrometer pore size filter membrane (Sophonsiri & Morgenroth, 2004). Particulate organic matter (POC) ranges in size from 1 μm to well over 100 μm and can be separated by sedimentation, centrifugation, and filtration (Heukelekian and Balmat, 1959, Levine et al., 1985; Leenheer and Crouè, 2003; Metcalf & Eddy, 2014). Figure 2.7 illustrates the size distribution for different types of organic matter found in sewage effluents.

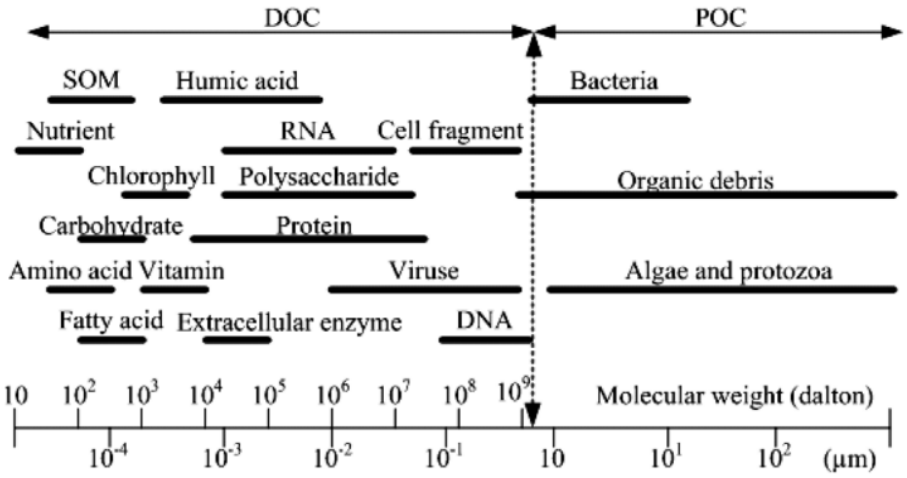

Figure 2.7 Size ranges distribution for typical organic compounds in biologically treated sewage effluents. (Adopted from Levine et al., 1985; Leenheer and Crouè, 2003).

Commonly, the DOM content in wastewater can be approximated by chemical and biochemical parameters, such as chemical oxygen demand (COD) which is a measure of the amount of oxygen required to chemically oxidize all substances in wastewater, including OM, and biochemical oxygen demand (BOD) which represents the amount of oxygen required by microorganisms to break down bioavailable OM in the wastewater over a specified period of time (Metcalf & Eddy, 2014). Moreover, dissolved organic carbon (DOC) and total organic carbon (TOC) are additional parameters used for estimating DOM in wastewater (Liu et al., 2019). However, these parameters can only quantify the total content of DOM as organic carbon

concentration (e.g., mg C/L) and are not able to identify the chemical composition and the concentration of different DOM constituents (Mesquita et al., 2017; Shi et al., 2021).

Typically, the complexity of DOM content in municipal wastewater is the highest among industrial, commercial, agricultural and surface waters. Studies aimed to characterize the molecular chemical composition of DOM in municipal wastewater indicated that the major organic macromolecules are proteins, carbohydrates, lipids, nucleic acids, and natural organic matter (NOM) (Levine et al., 1985; Raunkjaer et al., 1994; Huang et al., 2004). For instance, Narkis et al, (1980) analysed the DOC in a CPR plant and found that proteins and carbohydrates form 30% and 10% respectively of the total COD in the influent after primary sedimentation. Raunkjaer et al, (1994) pointed out that the organic composition of domestic wastewater samples after primary sedimentation includes 28% proteins, 18% carbohydrates and 31% lipids. Sophonsiri and Morgenroth, (2004) reported the major three organic constituents of the total COD in primary effluent of municipal wastewater to be 12% proteins, 6% carbohydrates, and 82% lipids. Furthermore, a study carried out by Huang et al, 2010, where chemical hydrolysis and chromatographic analysis were employed to identify the chemical composition of OMs in raw domestic wastewater influent (before screening or sedimentation), revealed that fibers, proteins, and carbohydrates accounted for 20%, 12% and 10% of TOC in the influent, respectively.

Proteins are complex organic molecules that play various essential roles in living organisms. They are made up of long chains of amino acids linked together by peptide bonds and are considered the primary constituents of animal organisms and microbial products (Tchobanoglous and Burton, 1991; Le et al., 2016). The main elemental composition of proteins includes carbon, hydrogen, and oxygen, as well as a high and constant content of nitrogen (~ 16%) (Shon et al., 2006).

The chemical structure of proteins is complex, unstable, and susceptible to various forms of decomposition (i.e., generation of foul odors). In wastewater proteins (<60% of organic matter) exists in soluble and particulate forms and considered along with urea the main sources of organic nitrogen (Bolto et al., 2004; Le et al., 2016). Moreover, proteins and their constituent amino acids can serve as potential carbon and nitrogen sources for heterotrophic bacteria responsible for breaking down organic matter in wastewater. However, membrane fouling in aerobic and anaerobic membrane reactors and disinfection by products are the main problems associated with proteins in wastewater (Bolto et al., 2004; Shon et al., 2005b; Le et al., 2016).

Carbohydrates are organic compounds containing carbon, hydrogen, and oxygen in a ratio of approximately 1:2:1 with general chemical formula of $(CH_2O)_n$ and characterized by polyhydric alcohol groups (Dignac et al., 2000; Shon et al., 2006, Huang et al., 2010). Carbohydrates are classified into different types based on their size and structure including monosaccharides, the simplest carbohydrates (i.e., glucose, fructose, and galactose), disaccharides which formed by the combination of two monosaccharides (i.e., sucrose, lactose, and maltose), and polysaccharides composed of long chains of monosaccharides (i.e., starch, cellulose, and glycogen) (Shon et al., 2006).

Different types of carbohydrates present in wastewater such as sugars, starches, cellulose, and wood fiber. Their solubility in water varies, for instance, sugars are soluble while starches are insoluble (Shon et al., 2006). In wastewater, breakdown of sugars occurs through fermentation, catalyzed by specific bacteria and yeasts, which generate carbon dioxide and alcohols. Starches are more resilient than sugars but are also converted into sugars via microbial processes and dilute mineral acids (Snyder et al., 2004; Shon et al., 2006). Generally, carbohydrates do not disrupt

conventional treatment methods. However, they are acknowledged to be fouling agents in membrane filtration techniques (Jarusutthirak, 2002; Shon et al., 2005b; Shon et al., 2006).

Lipids are the third most abundant organic matter present in wastewater and can be measured as fatty acids (Shon et al., 2006). Their composition in wastewater can vary depending on the sources of the wastewater. For example, eggs, dairy products, meats, seafood and cooking oils are the major contributors of lipids to wastewater (McCance & Widdowson, 1960; Raunkjaer et al., 1994; Huang et al., 2004). Lipids are a diverse group of organic compounds that include triglycerides, phospholipids, sterols, and waxes (Yao, 2014). Triglycerides are the most common lipid found in wastewater, and they are composed of three fatty acid chains attached to a glycerol molecule. They are often derived from fats and oils used in cooking and food processing (Beldean-Galea et al., 2013). Phospholipids are also found in wastewater, and composed of a glycerol molecule, two fatty acid chains, and a phosphate group. They are commonly found in animal and plant cell membranes and can be a by-product of the breakdown of biological matter in wastewater (Chipasa & Mędrzycka, 2006). The presence of lipids in wastewater can cause problems such as fouling of equipment, reduced treatment efficiency, and environmental pollution (Shon et al., 2006).

Humic substances (HS) are complex, relatively large, and refractory organic compounds that are formed by the degradation of OM in dead plants and animals. They are naturally occurring, and are found in soils, sediments, bodies of water such as rivers, lakes, and oceans, and wastewaters (Stevenson, 1994; Zhu et al., 2022). Humic substances are composed of a mixture of different molecules, including humic acids, fulvic acids, and humin (Stevenson, 1994; Wilfert et al., 2015; Tran et al., 2015). They are typically characterized by their dark color, high molar mass (i.e., humic acids molar mass ranged between 2000 and 130,000 g/mol) (Steelink et al., 1985), and

ability to form stable complexes with metals and other organic compounds (Stevenson, 1994; Frimmel, 1999; Wilfert et al., 2015). Humic substances play an important role in soil fertility and plant growth, and are involved in many biogeochemical processes, including nutrient cycling and carbon sequestration (Li et al., 2019; Zhu et al., 2022).

Humic substances lack well-defined chemical compositions which varies according to geographical origin, age, climate and biological conditions (de Melo et al., 2016). HS usually consist of covalently bonded molecules with aliphatic, phenolic (Boggs et al., 1985), and aromatic groups (Stevenson, 1994). It had been documented that humic acids are composed of multiple carbon rings that are linked to oxygen, nitrogen, and different functional groups such as peptide, hydroxyl, carbonyl, sulfhydryl, and carboxyl groups attached to the heterocycles at various positions as shown in Figure 2.8 (Stevenson, 1994; MacCarthy, 2001; Duan & Gregory, 2003). However, variation and arrangement of functional groups on HS impact their molecular characteristics and determine their interactions with other species (Zhu et al., 2022). In WWTPs, humic substances made up approximately 20% of the overall DOC in secondary effluents, and account for 10-20% of TOC in dry sludge (Wilfert et al., 2015).

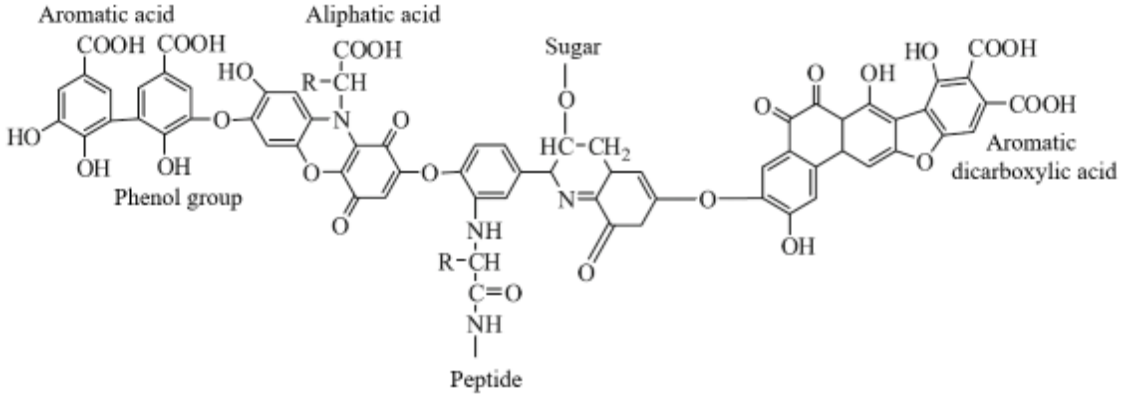

Figure 2.8 Proposed chemical structure for low molar mass (~ 2000 g/mol) humic acid molecule illustrating different functional groups. (Adopted from Stevenson, 1994).

2.4.1 Interactions of Iron and Organic Matter in Wastewater

In CPR plants, where Fe(III) salts are used for P removal, it is important to maximize the interaction between Fe(III) and P to achieve low levels of P residuals in wastewater effluents. Dissolved organic matter DOM is abundant in wastewater and contains large molecules of different species including (i.e., proteins, carbohydrates, lipids, amino acids, nucleic acids, and humic substances) (Shon et al., 2006) that have various functional groups (i.e., carboxylic, phenolic, alcoholic, amino, and amido groups) (Stevenson, 1994; MacCarthy, 2001; Duan & Gregory, 2003) capable to interact with Fe(III) and thus impact CPR process (Wilfert., et al 2015; Zhu et al., 2022). Typically, DOM interacts with Fe(III) in wastewater through different pathways such as complexation to Fe(III) ions, adsorption to Fe(III) oxides, and oxidation/reduction (Wilfert et al., 2015; Huang et al., 2021; Zhu et al., 2022).

DOM molecules can complex Fe(III) cations through out their carboxyl, hydroxyl, and phenolic groups resulting in the formation of stable soluble/insoluble organic-iron complexes (Duan & Gregory, 2003; Wilfert et al., 2015). Schwartzman et al, (2005) reported via Mössbauer spectroscopy analysis that Fe(III) can exist in the presence of organic matter as both oxides and non-oxides. Although Fe(III) can form binary complexes with DOM, it also can facilitate formation of ternary complexes between DOM and phosphate anions through cation bridging (i.e., DOM-Fe(III)-PO_4) (Audette et al., 2020).

The complexation process between Fe(III) and DOM is pH and DOM concentration dependent and the greater the acidity of the DOM molecules (determined by their functional groups), the more effectively they can chelate Fe(III) cations and heavy metals (Pandey et al., 2000). However, Fe(III) cation complexation to DOC molecules can hinder its hydrolysis and

polymerization in wastewater and affect P removal process (Karlsson & Persson, 2012; Wilfert et al., 2015).

Adsorption of DOM to iron oxides can take place through electrostatic interactions, hydrogen bonding, ligand exchange, and hydrophobic interactions depending on the type of DOM functional groups (Zhang et al., 2015, Taujale et al., 2016). For example, at pH range between 6 and 8 typical to wastewater pH, the surface charge of iron oxide is positive (beyond the point of zero charge (PZC)) and the ionization of carboxyl, hydroxyl, and phenolic groups associated with DOM develops a negative charge which induce an electrostatic interaction and leads to adsorption of DOM on solid iron oxide surface (Pullin and Cabaniss, 2003; Cabaniss et al., 2005). However, the extent of adsorption depends on the characteristics of both the DOM and the iron oxide, such as their size, shape, charge, and functional groups (Duan & Gregory, 2003; Wilfert et al., 2015).

It is clear that DOM can compete with phosphate for binding sites on iron oxides, but it could also enhance P adsorption on iron oxides. It has been reported that DOM particularly humic substances can suppress crystallization of amorphous iron oxides and thus increase their adsorption capacity toward P (Huang et al., 2005; Wilfert et al., 2015; Yang et al., 2019). Moreover, studies have revealed that humic substances possess the ability to solubilize phosphorus from wastewater Fe-P solids by forming complexes with iron(III). However, by complexing with humic substances, Fe(III) can remain in a dissolved form but would not remove P (Lobartini et al., 1998; Wilfert et al., 2015).

In addition, DOM can serve as an electron donor, promoting the reduction of iron oxides by iron reducing bacteria and increasing the concentration of soluble ferrous ions in the wastewater. This can result in a shift from ferric to ferrous iron species, which can have implications for the subsequent treatment processes (Wilfert et al., 2015; Huang et al., 2021).

Ferric is less soluble than ferrous so there would be less phosphate removal if HFO particles (for example) are solubilized by reductive dissolution.

Given the high abundance of DOM in WWTPs, their presence can significantly impact the speciation of Fe and P. Therefore, it is important to take their effects into account when studying P removal and recovery processes in wastewater.

2.5 Current approaches for P release and recovery from Fe-P sludge

In CPR plants, approximately up to 95% of soluble P in wastewater influents is captured in the sludge solids (Cornel and Schaum, 2009; Blöcher et al., 2012; Munir et al., 2017). However, 40 to 90% of treated P is potentially recovered in the solids in the form of hydroxyapatite ($Ca_5(PO_4)_3OH$), struvite ($MgNH_4PO_4.6H_2O$), white phosphorus (P_4), and vivianite ($Fe_3(PO_4)_2 \cdot 8H_2O$) from P rich sewage sludge solids and sludge ash (Egle et al., 2016; Ye et al., 2017; Li et al., 2017; Port et al., 2019; Jupp et al., 2021; Di Capua et al., 2022). At present, different technologies are employed in full and/or pilot scale for P recovery from Fe-P sludge including wet-chemical treatment, thermochemical treatment, and magnetic separation of Fe-P solids like vivianite (Ye et al., 2017; Port et al., 2019; Di Capua et al., 2022; Kaljunen et al., 2022).

A key step to achieve P recovery in CPR plants is to release P from Fe-P sludge to the liquid phase (Egle et al., 2015; Peng et al., 2018a). For example, in wet-chemical treatment technology P is extracted from wet Fe-P sludge and/or sludge ash by acid leaching (adding strong acids i.e., H_2SO_4) or alkali leaching (adding strong base i.e., NaOH). In acid leaching the dissolved metals associated with soluble P are removed from the acidified solution as sulfide precipitates by adding sodium sulfide (Na_2S) and adjusting the solution pH by NaOH (i.e., Gifhorn process) (Rashid et al., 2020) or by complexation with chelating agents like citric acid (i.e., Stuttgart

process) (Meyer et al., 2019), then the solubilized P is recovered by struvite crystallization. Alkali leaching could have an advantage that heavy metals are not soluble in basic solutions particularly at pH < 13 which allows to separate P directly from them. However, in alkali treatment the chance for some metal ions precipitation such as Mg^{2+} and Ca^{2+} is high which may affect P recovery as struvite (Ye et al., 2017). In Japan alkali leaching of P from Fe-P solids is practiced at Gifu WWTP where 60-70% of P is recovered from sewage sludge ash (Takaoka et al., 2010; Ye et al.; 2017).

In thermochemical treatment, P recovery is performed by subjecting the sewage sludge and/or sludge ash to different processes such as incineration, liquification, gasification, and pyrolysis (Munir et al., 2017). For example, the AshDec® (ASHDEC, 2008) technology which was tested in pilot-scale and put into operation from 2005 to 2008 in Leoben plant (Austria) utilized thermochemical treatment for P recovery in the form of soluble P and PK fertilizers. The sewage sludge/sludge ash is mixed with chlorides (i.e., NaCl, KCl, $MgCl_2$ and $CaCl_2$) at high temperatures (850–1000 °C) for 20 minutes in a rotary kiln. This process resulted in the removal of harmful heavy metals from sludge in the form of their corresponding volatile gaseous chlorides and concentrating P in sludge ash where potassium and nitrogen are added to produce multi-nutrient fertilizer (Ye et al., 2017; Hermann and Schaaf, 2019; Di Capua et al., 2022). However, when sodium sulfate Na_2SO_4 is added as reaction catalyst, P is recovered as Rhenania phosphates ($CaNaPO_4$) (Vogel et al., 2016). Although thermochemical treatment is an effective technology for producing fertilizers that meet the standards (i.e., Europe fertilizer standards), it requires large amounts of energy for operation (Egle et al., 2016).

Recovering P thermochemically in its pure elemental form such as white phosphorus (P_4) is another practiced approach for P recovery from Fe-P sludge and sludge ash (Jung, 2005; Di Capua et al., 2022; Kaljunen et al., 2022). Thermphos® process which was applied in a full-scale

in Netherlands (2007-2012) utilized this method where gaseous P separates from the liquid phase by heating the sewage sludge/sludge ash to high temperatures (1500-1600 °C) in a furnace via coke burning or electric means. The recovered 99.99% pure P_4 has various industrial applications, such as in the production of fertilizers, detergents, and semiconductors while the calcium-silica slag remaining in the furnace can be employed in road construction (Jupp et al., 2021; Di Capua et al., 2022). However, this process demands high energy, and the efficiency of P recovery is reduced when sludge contains high concentrations of iron due to the formation of FeP and FeP_2, causing decrease in P_4 yield. (Cossairt et al., 2010; Hoidn et al., 2021).

Recently, magnetic separation of iron(III)-phosphate mineral (vivianite) is emerging as a promising technique for P recovery from CPR plants. In fact, vivianite is reported to be the most prevalent precipitate of Fe-P solids (80-90% of P bound to vivianite) in digested sludge when iron is employed for P removal during CPR process (Wilfert et al., 2018). Lab-scale tests conducted by Port et al, (2019) on real sludge samples indicated magnetic separation concentrating the vivianite by a factor of 2–3. Investigations on pilot-scale level revealed recovery of 80% of P from sludge and 60% of the P in the wastewater treatment process influent by magnetic separation (Wijdeveld et al., 2022). However, a typical application of magnetic vivianite separation employs Jones-type low energy magnetic separator used in the mining industry, followed by optional alkaline leaching to separate P from potential heavy metals (Kaljunen et al., 2022). Vivianite as P recovery product can be applied as a slow-release fertilizer in iron poor soils. Moreover, the operational cost for vivianite recovery is very low (0.3 €/kg $P_{recovered}$) (Kaljunen et al., 2022). However, this approach is still at an early stage and further research is required towards optimization of separation efficiency which could be affected by several factors such as the size and shape of the vivianite

particles, the strength of the magnetic field, and the presence of organic matter and other minerals in the sludge (Port et al., 2019; Kaljunen et al., 2022; Di Capua et al., 2022).

Obviously, P recovery from Fe-P sludge solids in CPR plants is challenging due to the complex composition of wastewater. In spite of employing different approaches for direct P release and recovery from Fe-P sludge and/or sludge ash, many limitations prevent expanding them to full-scale application including lower quality of the obtained P-based products, low environmental sustainability, high costs, and high energy consumption (Kaljunen et al., 2022; Di Capua et al., 2022). However, a key factor to achieve the best practice of P recovery from Fe-P sludge is to address the chemistry of iron and phosphate in wastewater which is not entirely understood (Wilfert et al., 2015; Korving et al., 2019). Moreover, considering the inorganic fraction of Fe-P sludge far from the disturbance of the interfering substances such as organic matter and bacteria will provide more insights and fundamental knowledge to the performance of P release from Fe-P sludge.

2.6 Factors influencing P release from Fe-P sludge

The process of P release from Fe-P solids is affected by several factors such as solution pH, sludge age, and iron redox chemistry (Wilfert et.al, 2015; Lu et al., 2016; Li et al., 2020). In the following subsections each factor is discussed.

2.6.1 The influence of pH

In wastewater, the interaction between Fe and P occurs through coprecipitation and adsorption mechanisms which are solution pH dependent (Smith et al., 2008; Wilfert et al., 2015; Ping et al., 2022). However, solution pH can be significantly influence and control Fe and P

speciation, Fe-P minerals and iron oxides stability and solubility, and the surface charge of precipitated iron oxyhydroxides (Flynn, 1984; Cornell and Schwertmann, 2003; Smith et al., 2008; Wilfert et al., 2015; Zhang et al., 2019; Ping et al., 2022).

A strategy for P recovery from Fe-P sludge could start with liberating P from Fe-Ps through either desorption of P from HFOs' surfaces or dissolution of HFOs which could be controlled by pH. For example, at high pH (> 8) and beyond the PZC of HFO surface, desorption of P is more likely to occur because of the increase of hydroxyl ion concentration which could exchange with P on HFO surface via ligand exchange mechanism (Awual et al., 2011; Wilfert et al., 2015). In addition, at high pH, the electrostatic repulsion between the negatively charged HFO surfaces and phosphate ions facilitates P desorption (Yoon et al., 2014; Wilfert et al., 2015). On the other hand, at low pH (< 3), solubility of HFOs and iron oxides increase, and significant fractions of P are released (Petzet et al., 2011; Biswas et al., 2009). However, to achieve full dissolution of HFOs high acidic (pH=1) and basic (pH =13) conditions are necessary (Wilfert et al., 2015; Chakraborty et al., 2020; Sano et al., 2012).

In WWTPs, chemical P removal is performed at pH ranged between 6 and 8 (Metcalf and Eddy, 2014; Wilfert et al., 2015). Thus, manipulating pH treatment for Fe-P sludge above and below this range could release P. An earlier study by Rydin (1996) revealed that P release from Fe-P sludge by artificial rainwater (pH = 5) under anaerobic conditions was found to be 3.8 fold higher than aerobic conditions. Kim et al. (2016) studied the effect of pH on leaching P from Fe-P sludge obtained form vertical flow constructed wetland, where ferric salts were used as coagulants. Results revealed higher release of P under alkaline conditions (34%) than acidic (20%) which was attributed to low alkaline buffer capacity of the sludge. Lu et al. (2016) reported obvious release of P from simulated Fe-P coprecipitants ($FePO_4$) at pH range between 4 and 10 with a

greater release achieved at pH 10. Other studies also showed a potential P release from Fe-P sludge at pH 11 (Chen et al., 2019) and pH 13-14 (Sano et al., 2012). Moreover, P release from Fe-P sludge under strong acidification (pH=1) was reported (Wilfert et al., 2015; Chakraborty et al., 2020).

Although the above findings confirm the considerable role of pH in releasing P from Fe-P sludge and sludge ash, the majority of studies investigated real Fe-P sludge samples in the presence of different wastewater interferences such as organic matter and microorganisms. However, very limited studies investigate the direct P release induced by pH from the pure inorganic forms of Fe-P solids generated in CPR plants. Such basic studies are necessary in order to elucidate the details of Fe-P-pH interactions.

2.6.2 The influence of sludge age

Sludge age could have a considerable effect on P release from Fe-P solids since it affects the structure of HFO. Typically, the average residence times for Fe-P sludge in CPR plants ranged from 1 to 12 days. This could impact P release as within these residence times structural transformations of HFOs could occur. In fact, aging of HFOs has been reported to influence their reactivity (Bligh & Waite, 2010; Bligh et al., 2017), adsorptive/desorption capacity, and facilitates a transition from an amorphous to a more crystalline structure (Dzombak and Morel, 1990; Smith et al., 2008; Hauduc et al., 2015; Li et al., 2020). HFOs with amorphous structures have larger surface areas and more available active sites than crystalline structures for phosphate to bind (Smith et.al., 2008; Hauduc et al., 2015) while aged HFOs possess lower adsorptive capacity compared to fresh HFOs (Conidi & Parker, 2015). Reduction in P release and recovery from aged

Fe-P sludge under acidic conditions has been reported and attributed to an increase in HFO particle size or degree of crystallinity depending on aging periods (Georgaki et al., 2004; Li et al., 2020).

The mechanism how aging affects HFO structure and particularly its adsorption/desorption capacity depends on the time scale of aging. For example, long time spans extending from days to weeks are enough for fresh HFO structure to be crystalized resulting in lowering its surface area (Rose and Waite, 2007, Bligh and Waite, 2011) and adsorptive capacity (Conidi and Parker, 2015). Moreover, short time spans of hours to days, allow in turn aggregation and flocculation to take place among HFO particles which minimize the number of HFO accessible surfaces and active sites (Gilbert et al., 2009, Bligh et al., 2011). Li et al. (2020) conducted a study to investigate the transformation of Fe-P complexes in bioreactors under different aging periods using X-ray Absorption Near-Edge Structure Spectroscopy. The study revealed that ferrihydrite (HFO) was the primary Fe species up to day 4, and goethite was identified in the sludge after day 7, constituting 5% of the total Fe compositions, which increased to 9.4% after 30 days of aging. Therefore, it is essential to consider the impact of HFO structural morphology changes on the direct release of P from Fe-P sludge during aging, as there is a paucity of research on this subject.

2.6.3 The influence of iron redox chemistry

Iron (Fe) is the fourth most abundant element by mass in the Earth's crust (Colin and Micheal, 2012). It is found in nature in a wide range of oxidation states that vary between -2 to +6 but the most common are the ferric Fe(III) as in hematite (Fe_2O_3) and the ferrous Fe(II) as in siderite ($FeCO_3$) (Colin and Micheal, 2012, Huang et al., 2021). Iron can swing between its two common oxidation states upon interaction with water and oxygen, thus, iron plays an important

role in various environmental processes particularly those redox reactions involved in sediments, soil, and atmosphere (Cornell and Schwertmann, 2003; Huang et al., 2021).

The redox chemistry of iron has shown a noticeable effect in retaining and mobilizing P from iron-phosphate minerals occurring in soil and sediments Figure 2.9 (Smolders et al., 2006; Cornell and Schwertmann, 2003). In shallow water bodies, iron-phosphates exist in the top layer of bottom sediments where they are subjected to oxic-anoxic cycling and redox fluctuations that alter their mobilization and speciation (Parsons et al., 2017; Zaaboub et al., 2014). Similarly, at WWTPs Fe-P sludge in the bottom of sedimentation tanks could pass through aerobic-anaerobic conditions that facilitate P release from Fe-P sludge by oxidizing or reducing iron (Lu et al., 2016; Wilfert et al., 2015).

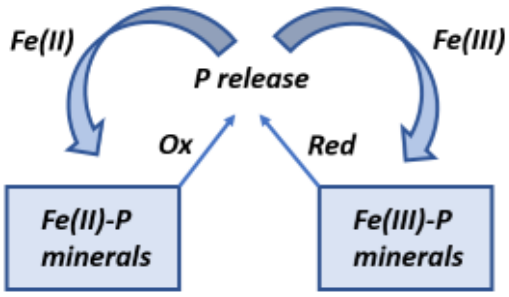

Figure 2.9 Role o f iron redox chemistry in mobilizing P

In WWTPs that use ferric salts for P removal, Fe-P sludge is exposed to a wide range of oxidation reduction potentials (ORPs) that extends from -300 mV up to +200 mV through aerobically and anaerobically treatments (Wilfert et al., 2015). This variation in ORPs along with other factors such as solution pH, sulfides, and microorganisms, could impact the redox forms and speciation of iron in wastewater. For example, ferric iron in Fe-P sludge could be reduced to ferrous iron chemically by sulfides forming sparingly soluble FeS solids, or/and biologically by

iron reducing bacteria under anaerobic conditions thus releasing P (Ge et al., 2013; Wilfert et al., 2015; Batstone et al., 2015;). However, in the absence of sulfides ferrous ion released by reduction of Fe(III) solids could bind to the released P_{ortho} and (a) precipitate as vivianite (Wilfert et al., 2016, Port et al., 2019), (b) precipitate as iron oxides that include both ferric and ferrous ions such as green rust (Weber et al., 2006; Cornell and Schwertmann, 2003; Huang et al., 2021), or (c) oxidized by electron acceptors like oxygen or nitrates and iron oxidizing bacteria in aerobic and anaerobic conditions respectively (Posth et al., 2014).

In the absence of sulfides, the speciation pathways of Fe-P solids in wastewater under different redox conditions and solution pH values is illustrated in Figure 2.10. At normal aerobic conditions and pH ranged between 6-8 Fe(III) hydrolyze in water and form HFO which bind P_{ortho} either by co-precipitation or/and adsorption forming HFO-P solids. At low solution pH values <5 direct interaction between Fe(III) and P_{ortho} occurs and strengite may form. When Fe(III) reduction takes place under anaerobic conditions the formed Fe(II) binds P_{ortho} and form vivianite at pH 7. Moreover, Fe(II) could hydrolyzes in water under circumneutral pH forming soluble Fe(II)hydroxides which become insoluble at high pH values. However, upon oxidation of Fe(II)hydroxides, HFOs are generated and bind P_{ortho} by forming HFO-P solids.

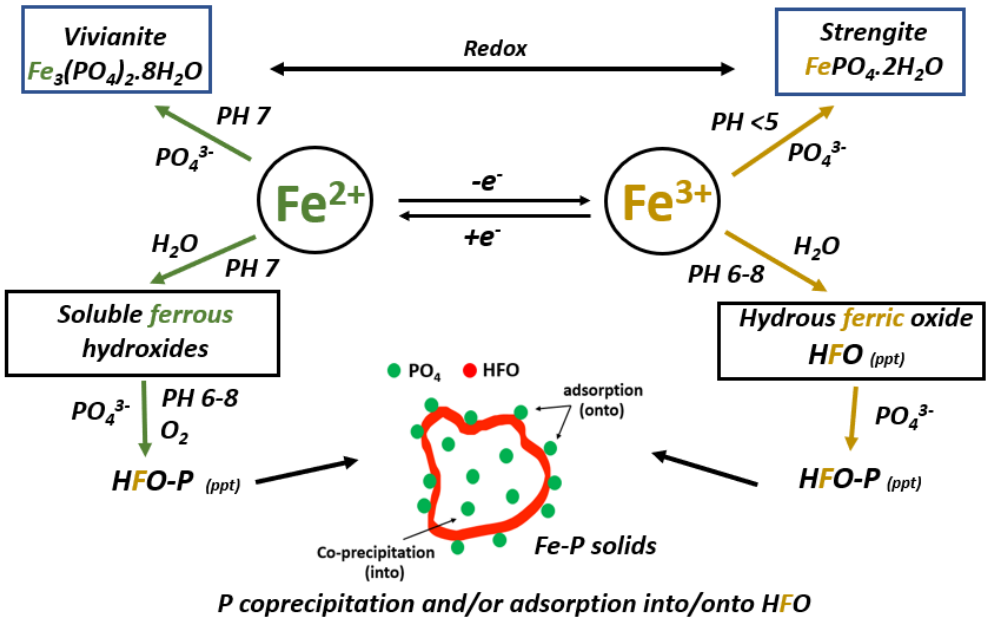

Figure 2.10 Speciation pathways of Fe-P solids under different redox conditions in the absence of sulfides. (HFO in the figure represents hydrous ferric oxide)

Different studies highlighted the role of Fe redox cycling in mobilizing P from iron Fe-P sludges in wastewater. Kim et al. (2016) studied the effect of ORPs on leaching P from Fe-P sludge obtained form vertical flow constructed wetland, where ferric salt used as coagulant. They reported that the highest release of P 39.5% was under reduced conditions of (-176 ± 113 mV/SHE). Lu et al. (2016) reported higher rates of Fe and P release from synthetized Fe-P coprecipitants at reduced conditions compared to oxidized ones under near-neutral pH. Also, a noticeable P release rates (>15%) were observed to occur after 48 hours at ORPs ranged between -261 mV and -194 mV.

The effect of sulfides on P release form Fe-P sludge has also been investigated. Kato et al. (2006) studied the addition of sulfides to pre-coagulated Fe-P sludge and lab simulated iron(III) phosphate sludge at pH range between 5.3 and 6.9 and molar ratios of S:Fe between 1.0 and 2.0. Results showed P release up to 44% and 92.8% respectively. In another study by Likosova et al. (2013), the effects of different variables including pH, sulfide dosing rate, and mixing time were

investigated on recovering P by sulfides from synthetic iron(III) phosphate sludge. For S:Fe molar ratio of 1.5, (70 ±6 %) of P release was achieved and (92 ±6 %) for 2.5 S:Fe molar ratio at pH 4. Wilfert et al, (2020) reported efficient P release (60%-92%) from different types of synthetic Fe-P solids and sewage sludge with various Fe/P molar ratios by sulfides treatment within one hour reaction time. However, this treatment has some drawbacks such as decrease in sludge dewaterability and the limited net phosphate dissolution from the Fe-P rich sewage sludge.

Currently, major fraction of research focusing on vivianite as P recovery product rely on the natural occurrence of vivianite in wastewater induced by microorganisms (O'Loughlin et al., 2013; Rothe et al., 2016; Wilfert et al., 2016; Y.Wu et al., 2019). However, introducing chemical reducing agents as an approach for releasing P from Fe-P sludge is still limited to sulfides (Wilfert et al., 2020). Recently, as an alternative, tests were performed to generate vivianite by chemically induced reduction of Fe(III) to Fe(II) using, ascorbic acid (AA) known as vitamin C (Xu et al., 2023). In this study by Xu et al, (2023) it was found that waste activated sludge can release 67.1% of its phosphorus content as vivianite through the use of AA and pH adjustment. This finding suggests that the iron-reducing activity of AA at acidic pH can be a promising approach for recovering phosphorus from Fe-P rich sludge in the form of vivianite.

2.7 Phosphorus recovery products

In WRRFs depending on the type of recovery process, P is recovered from liquid phase in the form of P-containing compounds by chemical precipitation/crystallization, and magnetic separation (Di Capua et al., 2022). Struvite ($MgNH_4PO_4.6H_2O$), hydroxyapatite ($Ca_5(OH)(PO_4)_3$), and vivianite ($Fe_3(PO_4)_2 \cdot 8H_2O$) are the most common P recovery products (Mehta et al., 2013; Hermassi et al., 2015; Liu et al., 2018). Hence, struvite and vivianite products are discussed below.

2.7.1 Struvite

The widest applied method for P recovery is through precipitating P by magnesium in the presence of ammonia at slightly basic pH (8-11). The generated product as illustrated in equation (2.4) is magnesium ammonium phosphate ($MgNH_4PO_4.6H_2O$) known as struvite (Corre et al., 2009; Kumar and Pal, 2015; Peng et al., 2018a; Li et al., 2019). This product has the advantage of also including nitrogen and magnesium as nutrients for potential application as fertilizer.

$$Mg^{2+} + NH_4^+ + H_nPO_4^{n-3} + 6H_2O \rightarrow MgNH_4PO_4.6H_2O + nH^+ \quad (2\text{-}4)$$

where n= 0, 1, or 2 (Peng et al., 2018a). Struvite precipitation is commonly practised in enhanced biological phosphorus removal (EBPR) plants where it is possible to obtain P concentrations high enough for precipitation (Rittmann et al, 2011). It is observed that under certain conditions and depending on the composition of the wastewater, unintended self-precipitation of struvite can occur causing scaling in pipes and fouling which affects WWTP efficiency and increase maintenance costs (De-bashan and Bashan 2004). However, P recovery can be deliberately managed through the process of struvite crystallization (Peng et al., 2018a).

The formation of struvite is influenced by various factors such as pH, supersaturation, molar ratios of component ions, the type of seed, sources of Mg^{2+}, and coprecipitation with Ca^{2+}. When it comes to inducing struvite crystallization, the presence of Mg^{2+}, NH_4^+, and PO_4^{3-} in wastewater triggers the precipitation of phosphorus and reduces the concentration of soluble phosphorus and ammonia within the induction period. For intentional struvite precipitation, it is recommended to maintain equimolar concentrations (1:1:1) of Mg^{2+}, P, and NH_4^+, an alkaline pH above 7.5, and low levels of suspended solids (Shepherd et al., 2016; Shih et al., 2017; Peng et al., 2018a).

The efficiency of P recovery by struvite from municipal wastewater was reported to range between 60% and 90% depending on the chosen technology (Lahav et al., 2013; Peng et al., 2018a). Moreover, struvite counts for approximately 20-50% of P recovered from the total influent P load in WWTPs (Wilfert et al., 2015; Egle et al., 2016). It is used as slow release fertilizer as it contains two major nutrients N and P (Li et al., 2019). Furthermore, struvite precipitation process is commercialised and operated with several full scale applications in WWTPs around the world (i.e., MagPrex® (formerly AirPrex®), Ostara Pearl®, Phosnix®, and PHOSPAQ™) (WEF, 2011).

Although struvite crystallization from the liquid phase of anaerobically digested wastewater sludge has been applied on a full scale through different technologies, this method has been successful in treating wastewater with P concentrations ranging from 100 to 200 mg/L and slightly alkaline conditions. However, it is not suitable when the concentrations of P and NH_4^+, as well as pH, do not meet the conditions required for the formation of struvite (Angel, 1999; Capdevielle et al. 2016).

2.7.2 Vivianite

Vivianite ($Fe_3(PO_4)_2 \cdot 8H_2O$) is a stable crystalline authigenic iron phosphate mineral, frequently found in sedimentary environments and soils, particularly under anaerobic non-sulfidic conditions with rich Fe(II) and P content (Nriagu, 1972; Rothe et al., 2014; Dijkstra et al., 2016; Y.Wu et al., 2019). It was named after the English mineralogist John Henry Vivian (1785–1855) and belongs to mineral group ($M_3(XO_4)_2 \cdot 8H_2O$, where M = divalent Mg, Mn, Fe, Co, Ni, Cu, Zn, and X = P or As) (Rouzies and Millet, 1993; Rothe et al., 2014).

Freshly formed pure vivianite appears as a colorless/white mineral, and gradually turns green and then blue when exposed to oxygen for extended periods (Rothe et al., 2014). Typically,

Fe(II) oxidizes instantly to Fe(III) at room temperature, and the oxidation process reaches equilibrium when the half concentration of Fe(II) is oxidized to Fe(III). However, under higher concentrations of Fe(III), vivianite transforms into metavivianite and with further oxidation, the mineral changes into Fe(III)-rich metavivianite, and ultimately into a black amorphous mineral containing Fe(III) and P (Rothe et al., 2016; Y.Wu et al., 2019; Zhang et al., 2022). Vivianite is stable due to its low solubility ($K_{sp}=10^{-36}$) at circumneutral pH which makes it a main sink for soluble Fe(II) in P rich environments (Miot et al. 2009; Wang et al., 2019).

Similar to the sedimentary environments and wetland soils, a spontaneous formation of vivianite is observed during anaerobic wastewater/sludge treatment in CPR plants that use iron salts (Wilfert et al., 2016, 2018;). Several researchers reported vivianite occurrence in surplus, activated, and digested sludge (Wilfert et al., 2016, 2018; Port et al., 2020; Deng et al., 2020). Moreover, vivianite scaling problems were pointed out in different zones of WWTPs such as thickened sludge pipes, heat exchangers, and around dewatering centrifuges of undigested sludge (Prot et al., 2021).

The main pathway for vivianite formation in wastewater is mediate by microbial activity where Fe(III) in Fe-P solids is reduced to Fe(II) through extracellular electron transfer (EET) induced by dissimilatory metal-reducing bacteria (DMRB), which act as electron doner species as illustrated in equation (2-5) (O'Loughlin et al., 2013; Rothe et al., 2016; Y.Wu et al., 2019). This reductive microbial process lead to the accumulation of Fe(II) and P in sludge liquor and vivianite begins to form when saturation conditions are reached (see equation (2-2) section 2.3). However, vivianite formation is primarily a chemical process that can be influenced by a range of factors, such as microorganisms, temperature, pH levels, the Fe/P molar ratio, sulfate concentration, heavy

metals, organic matter, and alkalinity (Rothe et al., 2016; Liu et al., 2018; Y.Wu et al., 2019; Zhang et al., 2022).

$$Fe(OH)_{3(s)} + 3H^{+}_{(aq)} + e^{-} \rightarrow Fe^{2+}_{(aq)} + 3H_2O_{(aq)} \quad (2\text{-}5)$$

At present, different qualitative and quantitative analysis methods are employed for vivianite detection in wastewater sludge and environmental samples (i.e., sediments) (Zhang et al., 2022; Wang et al., 2021). For example, powder X-ray diffraction (PXRD) is a common analysis technique used to identify vivianite by mineral phase. However, it is limited to only crystallized vivianite (ideally 10–50 μm particles) (Salehin et al., 2020) and requires a minimum of 5% weight of vivianite in a sample to obtain the three most intense peaks characterizing vivianite (Rothe et al., 2014). X-ray absorption spectroscopy (XAS) (Li et al., 2018), and Mössbauer spectroscopy (Wang et al., 2019; Wilfert et al., 2016) are alternative approaches used to analyze vivianite qualitatively and quantitatively but also have some limitations including oxidation of vivianite during sample preparation and the demand for synchrotron facilities for XAS and specialized instrumentation for Mössbauer spectroscopy (Li et al., 2018; Wang et al., 2021). Moreover, vivianite can be identified based on its elemental content by inductively coupled plasma-optical emission spectroscopy (ICP-OES) after acidic digestion of the samples. In addition, a quantification method that allows for separation as well as quantification of vivianite-P in sewage sludge was developed by addition of the Bipy-extraction step (0.2% 2,2′-bipyridine + 0.1 M KCl) to a sequential P extraction method (SEDEX) protocol (Gu et al., 2016; Wang et al., 2021).

Recently, P recovery via vivianite has been at the forefront research due to its advantageous characteristics such as being naturally abundant, readily available, and economically viable (Wilfert et al., 2018 , 2015 , 2016). However, comparing to struvite, vivianite possesses desirable

properties as it has a wide range of applications including agriculture (i.e., slow-release fertilizer in soils lacking Fe) (De Santiago et al., 2013; Jowett et al., 2018), electronic industry (i.e., key precursor for $LiFePO_4$ synthesis) (Rao and Varadaraju, 2015; Zhang et al., 2021), environmental remediation (i.e., removing heavy metals such as As(III)) (Taylor et al., 2008; Cai et al., 2020), and has been used as blue pigment over the years (Coccato et al., 2017). Furthermore, Zhang et al, (2022) reported higher market price for vivianite (10,000 €/ton) compared to struvite (500 €/ton). Looking at the moderate pH range for vivianite formation (6-8), thermodynamic favourability, higher recovery efficiency (82.6%) (Cao et al., 2019), and easy separation process due to magnetic properties, have made operational condition more convenient for targeting P recovery as vivianite compared to struvite (Li et al., 2021; Wijdeveld et al., 2022).

2.8 Geochemical modeling approach

Modeling is a well-established tool in science and facilitates understanding complex systems, designing experiments, making predictions, interpreting experimental results, and identifying knowledge gaps (Roman & Hartmann, 2020). For example, when it is difficult to understand a specific system through observation only, creating a model of this system will provide insights into the underlying interactions and mechanisms that drive the system's behaviour (Roman & Hartmann, 2020). Therefore, many scientific disciplines implement modeling in their contexts.

In the field of geochemistry, modeling is widely applied for understanding the chemistry and behavior of geological systems. This includes soils, groundwater, surface water, and industrial processes, such as mining and oil extraction. Basically, geochemical software models are developed to employ chemical thermodynamics and chemical kinetics for describing the

interactions between different chemical species in a system. Hence, geochemical modeling can be used to simulate chemical equilibrium systems, predict the fate and transport of contaminants in the environment (heavy metals and organic pollutants), evaluate groundwater quality, and identify mineral deposits under different environmental conditions (Zhu & Anderson, 2002). At present, different geochemical software models are available such as PHREEQC (US Geological Survey), Visual MINTEQ 3.1, and PHAST (U.S. EPA). The choice of software will depend on the specific research question and the level of complexity required for the modeling.

Modeling have been successfully used in WWTPs as significant engineering tool in research, process design, control and optimization of physical, chemical and biological processes (Henze et al. 2000). Looking at the complexity of wastewater matrix, many physiochemical processes similar to those found in geological systems are taking place in wastewater such as acid-base reactions, dissolution/precipitation reactions, chemical redox reactions, and surface complexation (sorption/desorption) reactions (Batstone et al. 2012). This allows applying geochemical models to wastewater in a number of ways to help describe, understand, and manage chemistry of wastewater. For example, to predict formation of mineral scales in wastewater treatment systems, predict the effectiveness of different types of chemical coagulants in removing specific contaminants from wastewater, and simulating the chemical reactions that occur as the wastewater mixes with the receiving water.

In this doctoral research, employing geochemical modeling are used for predicting, understanding, and interpreting the chemical behaviour of Fe-P sludge in terms of speciation at chemical equilibrium. P release and recovery processes are usually operated under stable conditions that allow the use of equilibrium models to describe these processes (Solon et al., 2019). Moreover, aqueous phase models and precipitation models could be used to describe the

interactions between phosphorus, iron and other different species in wastewater once equilibrium state is reached (Solon et al., 2019). In this study, chemical equilibrium simulations for P release and recovery from Fe-P sludge system under different experimental conditions were conducted using PHREEQC version 3.0 (US Geological Survey).

PHREEQC (PH REdox EQuilibrium (in C language)) is a geochemical modeling software that was developed by the US Geological Survey (USGS). It is broadly used in science fields to model and simulate the chemistry of aqueous systems, such as groundwater, surface water, and soil water. PHREEQC can perform numerous aqueous calculations, including ion speciation, precipitation/dissolution reactions, surface complexation reactions, chemical redox reactions, batch reactions, and saturation index (SI) calculations based on input solution characteristics such as pH, Eh, and ion concentrations. It is a versatile and powerful tool for investigating water chemistry and understanding chemical reactions in aqueous systems. In addition, the PHREEQC database is highly customizable, as it allows the users to modify thermodynamic data, reaction kinetics, and other parameters to the database to define various chemical systems. A detailed description of different PHREEQC simulations utilized in this research is provided in chapters three and four.

2.9 References

Abdala, D. B., Northrup, P. A., Arai, Y., Sparks, D. L., **2015**. Surface Loading Effects on Orthophosphate Surface Complexation at the Goethite/Water Interface as Examined by Extended X-Ray Absorption Fine Structure (EXAFS) Spectroscopy. Journal of Colloid and Interface Science 437: 297–303. doi:10.1016/j.jcis.2014.09.057.

Angel, R., **1999**. Removal of phosphate from sewage as amorphous calcium phosphate. Environmental Technology, 20(7), 709–720. doi:10.1080/09593332008616865.

Ansari, A. A., and Gill, S.S., **2014**. Eutrophication: Causes, Consequences and Control:2. Springer Dordrecht. doi:10.1007/978-94-007-7814-6.

ASHDEC, **2008**. Industrial Process and Pilot Plant. 2016. http://www.sswm.info/sites/default/files/reference_attachments/ASH%20DEC%202008%20Industrial%20Process%20and%20Pilot%20Plant.pdf (Accessed: 01.09.2016).

Audette, Y., Smith, D. S., Parsons, C. T., Chen, W., Rezanezhad, F., & Van Cappellen, P., **2020**. Phosphorus binding to soil organic matter via ternary complexes with calcium. Chemosphere, 260, 127624.

Awual, M., Rabiul, D., Jyo, A., Ihara, T., Seko, N., Tamada, M., Lim, K. T., **2011**. Enhanced Trace Phosphate Removal from Water by Zirconium(IV) Loaded Fibrous Adsorbent. Water Research 45 (15): 4592–4600. doi:10.1016/j.watres.2011.06.009.

Batstone, D. J., Amerlinck, Y., Ekama, G. A., Goel, R., Grau, P., Johnson, B., Kaya, I., Steyer, J.-P., Tait, S., Takács, I., Vanrolleghem, P.A., Brouchaert, C. J. and Volcke, E., **2012**. Towards a generalised physicochemical modelling framework. Water Science and Technology. 66(6), 1147-1161. doi: 10.2166/wst.2012.300.

Batstone, D. J., Puyol, D., Flores-Alsina, X., Rodríguez. J., **2015**. Mathematical Modelling of Anaerobic Digestion Processes: Applications and Future Needs. Reviews in Environmental Science and Bio/Technology 14 (4): 595–613. doi:10.1007/s11157-015-9376-4.

Beldean-Galea, M. S., Vial, J., Thiebaut, D., Comanc, V., **2013**. Characterization of the fate of lipids in wastewater treatment using a comprehensive GCXGC/qMS and statistical approach. Anal. Methods. 5: 2315. doi:10.1039/C3AY00060E.

Beusen, A. H. W., Bouwman, A. F., Van Beek, L. P. H., Mogollón, J. M., Middelburg, J. J., **2016**. Global riverine N and P transport to ocean increased during the 20th century despite increased retention along the aquatic continuum, Biogeosciences, 13, 2441–2451, doi.org/10.5194/bg-13-2441-2016.

Biswas, K., Kaushik, G., and Uday C. g., **2009**. Adsorption of Fluoride by Hydrous Iron(III)–tin(IV) Bimetal Mixed Oxide from the Aqueous Solutions. Chemical Engineering Journal 149 (1–3). Elsevier: 196–206. doi:10.1016/J.CEJ.2008.09.047.

Bligh, M. W., & Waite, T. D., **2010**. Role of heterogeneous precipitation in determining the nature of products formed on oxidation of Fe(II) in seawater containing natural organic matter. Environmental science & technology. 44(17), 6667–6673.doi.org/10.1021/es101046y.

Bligh, M.W., & Waite, T.D., **2011**. Formation, reactivity, and aging of ferric oxide particles formed from Fe(II) and Fe(III) sources: Implications for iron bioavailability in the marine environment. Geochimica et Cosmochimica Acta 75 (24), 7741-7758.

Bligh, M. W., Maheshwari, P., Waite, T. D., **2017**. Formation, reactivity and aging of amorphous ferric oxides in the presence of model and membrane bioreactor derived organics. Water Research, 124, 341-352. doi:10.1016/j.watres.2017.07.076.

Blöcher, C., Niewersch, C., Melin, T., **2012**. Phosphorus recovery from sewage sludge with a hybrid process of low pressure wet oxidation and nanofiltration. Water Res. 46 (6), 2009–2019. doi: 10.1016/j.watres.2012.01.022.

Boggs, S., Livermore, D., Seitz, M., **1985**. Humic macromolecules in natural waters. J. Macromol. Sci. Rev. Macromol. Chem. Phys. 25, 599–657.

Bolto, B., Dixon, D., Eldridge, R., **2004**. Ion exchange for the removal of natural organic Matter. Reactive Functional Polymers 60:171–182. doi.org/10.1016/j.reactfunctpolym.2004.02.021.

Cabaniss, S. E., Madey, G., Leff, L., Maurice, P. A., Wetzel, R. G., **2005**. A stochastic model for the synthesis and degradation of natural organic matter, Part I. Data structures and reaction kinetics. Biogeochemistry, 76, 319– 347. doi:10.1007/s10533-005-6895-z.

Cai, X., Yin, N., Wang, P., Du, H., Liu, X., Cui, Y., **2020**. Arsenate-reducing bacteria mediated arsenic speciation changes and redistribution during mineral transformations in arsenate-associated goethite. J. Hazard Mater. 398, 122886. doi:10.1016/j.jhazmat.2020.122886.

Cao, J. S., Wu, Y., Zhao, J. N., Jin, S., Aleem, M., Zhang, Q., Fang, F., Xue, Z. X., Luo, J. Y., **2019**. Phosphorus recovery as vivianite from waste activated sludge via optimizing iron source and pH value during anaerobic fermentation. Bioresour. Technol. 293, 122088. doi:10.1016/j.biortech.2019.122088

Capdevielle, A., Sýkorová, E., Béline, F., Daumer, M. L., **2016**. Effects of organic matter on crystallization of struvite in biologically treated swine wastewater. Environmental Technology, 37(7), 880–892. doi:10.1080/09593330.2015.1088580.

Carey, R. O., and Migliaccio, K. W., **2009**. Contribution of Wastewater Treatment Plant Effluents to Nutrient Dynamics in Aquatic Systems: A Review. Environmental Management 44 (2): 205–17. doi:10.1007/s00267-009-9309-5.

Carliell-Marquet, C., Smith, J., Oikonomidis, I., Wheatley, A., **2010**. Inorganic profiles of chemical phosphorus removal sludge. Water Manag. 163 (2), 65–77.

Chakraborty, T., Balusani, D., Smith, D.S., Walton, S.J., Nakhla, G., Ray, M.B., **2020**. Reusability of recovered iron coagulant from primary municipal sludge and its impact on chemically enhanced primary treatment. Separation and Purification Technology (231) 115894. doi:10.1016/j.seppur.2019.115894.

Chen, Y., Lin, H., Shen, N., Yan, W., Wang, J., Wang, G., **2019**. Phosphorus release and recovery from Fe-enhanced primary sedimentation sludge via alkaline fermentation. Bioresource technology, 278, 266–271. doi:10.1016/j.biortech.2019.01.09.

Chipasa, K. B., Mędrzycka, K., **2006**. Behavior of lipids in biological wastewater treatment processes. Journal of Industrial Microbiology and Biotechnology. (33): 8, 635–645, doi.org/10.1007/s10295-006-0099-y.

Coccato, A. , Moens, L. , Vandenabeele, P. , **2017**. On the stability of mediaeval inorganic pigments: a literature review of the effect of climate, material selection, biological activity, analysis and conservation treatments. Herit. Sci. 5 (1), 12. doi.org/10.1186/s40494-017-0125-6.

Colin, B., & Micheal, C., **2012**. Environmental Chemistry. 5th Edition; W. H. Freeman and Company, New York, ISBN: 1464113491, 9781464113499.

Conidi, D., Parker, W.J., 2015. The Effect of Solids Residence Time on Phosphorus Adsorption to Hydrous Ferric Oxide Floc. Water Research 84: 323–32. doi:10.1016/j.watres.2015.07.046.

Cooper, J., Lombardi, R., Boardman, D., Carliell-Marquet., C., **2011**. The Future Distribution and Production of Global Phosphate Rock Reserves." Resources, Conservation and Recycling 57: 78–86. doi:10.1016/J.RESCONREC.2011.09.009.

Cordell, D., Jan Olof D., and Stuart W., **2009**. The Story of Phosphorus: Global Food Security and Food for Thought. Global Environmental Change 19 (2): 292–305. doi:10.1016/j.gloenvcha.2008.10.009.

Cordell, D., Rosemarin A., J.J. Schröder, J. J., Smit, A. L., **2011**. Towards global phosphorus security: A systems framework for phosphorus recovery and reuse options. Chemosphere. 84:747–758 doi:10.1016/j.chemosphere.2011.02.032.

Cordell, D., and White, S., **2014**. Life's Bottleneck: Sustaining the World's Phosphorus for a Food Secure Future. Annu Rev Environ Resour. 39:161–188 . doi:10.1146/annurev-environ-010213-113300.

Cornel, P., & Schaum, C., **2009**. Phosphorus recovery from wastewater: needs, technologies and costs. Water Sci. Technol. 59, 1069–1076. doi.org/10.2166/WST.2009.045.

Cornell, R.M., Giovanoli, R., Schneider, W., **1989**. Review of the hydrolysis of iron(III) and the crystallization of amorphous iron(III) hydroxide hydrate. J. Chem. Technol. Biotechnol. 46 (2), 115–134.

Cornell, R. M., and Schwertmann, Udo., **2003**. The Iron Oxides : Structure, Properties, Reactions, Occurrences, and Uses. 2nd ed. Weinheim : Wiley-VCH.

Corre, K. S., Valsami-Jones, L. E., Hobbs, P., Parsons, S. A. **2009**. Phosphorus Recovery from Wastewater by Struvite Crystallization: A Review. Critical Reviews in Environmental Science and Technology 39 (6) : 433–77. doi:10.1080/10643380701640573.

Cossairt, B. M., Piro, N. A., Cummins, C. C., **2010**. Early-transition-metal-mediated activation and transformation of white phosphorus, Chem. Rev. 110 (7) (Jul.2010) 4164–4177. doi.org/10.1021/cr9003709.

Danielsson, L. G., **1982**. On the use of filters for distinguishing between dissolved and particulate fractions in natural waters. Water Research, Volume 16, Issue 2, Pages 179-182. doi.org/10.1016/0043-1354(82)90108-7.

De-Bashan, L. E., & Bashan, Y., **2004**. "Recent Advances in Removing Phosphorus from Wastewater and Its Future Use as Fertilizer (1997-2003)." Water Research 38 (19): 4222–46. doi:10.1016/j.watres.2004.07.014.

de Melo, B. A., Motta, F. L., & Santana, M. H., **2016**. Humic acids: Structural properties and multiple functionalities for novel technological developments. Materials science & engineering. C, Materials for biological applications, 62, 967–974. doi.org/10.1016/j.msec.2015.12.001.

De Santiago, A. , Carmona, E. , Quintero, J.M. , Delgado, A. , **2013**. Effectiveness of mixtures of vivianite and organic materials in preventing iron chlorosis in straw- berry. Span. J. Agric. Res. 11 (1), 208–216. doi.org/10.5424/sjar/2013111-2671.

Deng, S., Zhang, C., Dang, Y., Collins, R. N., Kinsela, A. S., Tian, J., Holmes, D. E., Li, H., Qiu, B., Cheng, X., Waite, T. D., **2020**. Iron Transformation and Its Role in Phosphorus Immobilization in a UCT-MBR with Vivianite Formation Enhancement. Environmental science & technology, 54(19), 12539–12549. doi.org/10.1021/acs.est.0c01205

Di Capua, F., de Sario, S., Ferraro, A., Petrella, A., Race, M., Pirozzi, F., Fratino, U., Spasiano, D., **2022**. Phosphorus removal and recovery from urban wastewater: Current practices and new directions. Science of The Total Environment, (823): 153750. doi.org/10.1016/j.scitotenv.2022.153750.

Dignac, M.-F., Ginestet, P., Rybacki, D., Bruchet, A., Urbain, V., Scribe, P., **2000**. Fate of wastewater organic pollution during activated sludge treatment: nature of residual organic matter. Water Research. (34): 17, 4185-4194. doi.org/10.1016/S0043-1354(00)00195-0.

Dijkstra, N., Slomp, C.P., Behrends, T., **2016**. Vivianite is a key sink for phosphorus in sediments of the Landsort Deep, an intermittently anoxic deep basin in the Baltic Sea. Chem. Geol. 438, 58-72. doi:10.1016/j.chemgeo.2016.05.025

Dzombak, D.A., Morel, F.M.M., **1990**. Surface complexation modelling: hydrous ferric oxide John Wiley and Sons, Inc., New York.

Duan, J., & Gregory, J., **2003**. Coagulation by hydrolysing metal salts. Advances in colloid and interface science, 100, 475-502. doi.org/10.1016/S0001-8686(02)00067-2.

Egle, L., Rechberger, H., Zessner, M., **2015**. Overview and description of technologies for recovering phosphorus from municipal wastewater. Resources, Conservation and Recycling. (105), Part B. 325-346. doi.org/10.1016/j.resconrec.2015.09.016.

Egle, L., Rechberger, H., Krampe, J., Zessner, M., **2016**. Phosphorus recovery from municipal wastewater: An integrated comparative technological, environmental and economic assessment of P recovery technologies. Sci. Total Environ. 571, 522–542. doi.org/10.1016/j.scitotenv.2016.07.019.

Frimmel, F., **1999**. Basic characterization of reference NOM from Central Europe-Similarities and differences. Environ. Int. (25): 2−3, 191−207. doi: 10.1016/S0160-4120(98)00116-0.

Flynn, C.M., **1984**. Hydrolysis of inorganic iron(III) salts. Chem. Rev. 84 (1), 31–41. doi: 10.1021/cr00059a003.

Ge, H., Zhang, L., Batstone, D. J., Keller, J., Yuan. Z., **2013**. Impact of Iron Salt Dosage to Sewers on Downstream Anaerobic Sludge Digesters: Sulfide Control and Methane Production. Journal of Environmental Engineering 139 (4): 594–601. doi:10.1061/(ASCE)EE.1943-7870.0000650.

Georgaki, I., Dudeney, A. L., John, M., **2004**. Characterisation of iron-rich sludge: Correlations between reactivity, density and structure. Minerals Engineering. 17. 305-316. doi:10.1016/j.mineng.2003.09.018.

Gilbert, B., Ono, R.K., Ching, K.A., Kim, C.S., **2009**. The effects of nanoparticle aggregation processes on aggregate structure and metal uptake. J. Colloid Interf. Sci. 339 (2), 285-295. doi:10.1016/j.jcis.2009.07.058.

Ghunmi, L. A., Zeeman, G., van Lier, J., Fayyed, M., **2008**. Quantitative and qualitative characteristics of grey water for reuse requirements and treatment alternatives: the case of Jordan. Water science and technology : a journal of the International Association on Water Pollution Research, 58(7), 1385–1396. doi.org/10.2166/wst.2008.444.

Gu, S., Qian, Y.G., Jiao, Y., Li, Q.M., Pinay, G., Gruau, G., **2016**. An innovative approach for sequential extraction of phosphorus in sediments: ferrous iron P as an independent P fraction. Water Res. 103, 352–361. doi.org/10.1016/j.watres.2016.07.058.

Hauduc, H., Takács, I., Smith, S., Szabo, A., Murthy, S., Daigger, G. T., Spérandio, M., **2015**. A dynamic physicochemical model for chemical phosphorus removal. Water research, 73, 157–170. doi:10.1016/j.watres.2014.12.053.

Henze, M., Gujer, W., Mino, T. van Loosdrecht, M., **2000**. Activated sludge models ASM1, ASM2, ASM2d and ASM3, IWA Publishing, London. doi:10.2166/9781780402369.

Hermann, L., & Schaaf, T., **2019**. Outotec (AshDec®) process for p fertilizers from sludge ash. In: Ohtake, H., Tsuneda, S. (Eds.), Phosphorus Recovery and Recycling. Springer, Singapore, pp. 221–233. doi.org/10.1007/978-981-10-8031-9_15.

Hermassi, M., Valderrama, C., Dosta, J., Cortina, J. L., N.H. Batis, N. H., **2015**. Evaluation of hydroxyapatite crystallization in a batch reactor for the valorization of alkaline phosphate concentrates from wastewater treatment plants using calcium chloride. Chem Eng. J. (267) :142–152. doi.org/10.1016/j.cej.2014.12.079.

Heukelekian, H., & Balmat, J. L., **1959**. Chemical Composition of the Particulate Fractions of Domestic Sewage. Sewage and Industrial Wastes, 31(4), 413–423. http://www.jstor.org/stable/25033859.

Hoidn, C. M., Scott, D. J., Wolf, R., **2021**. Transition-metal-mediated functionalization of white phosphorus, Chem. Eur. J. 27 (6) (2021) 1886–1902. doi.org/10.1002/chem.202001854.

Huang, F., Liu, H., Wen, J., Zhao, C., Dong, L., Liu, H., **2021**.Underestimated humic acids release and influence on anaerobic digestion during sludge thermal hydrolysis. Water Research. (201): 117310. doi.org/10.1016/j.watres.2021.117310.

Huang, M. H., Li, Y. M., Gu, G. W., **2010**. Chemical composition of organic matters in domestic wastewater. Desalination, vol. 262, pp. 36-42.

Huang, W., Chen, L., Peng, H., **2004**. Effect of NOM characteristics on brominated organics formation by ozonation. Environ. Int. 29 (8), 1049-1055.

Huang, P. M., Wang, M. K., Chiu, C. Y., **2005**. Soil mineral– organic matter– microbe interactions: Impacts on biogeochemical processes and biodiversity in soils, Pedobiologia, 49, 609–635, doi:10.1016/j.pedobi.2005.06.006.

Jansen, E., Kyek, A., Schäfer, W., **2002**. The structure of six-line ferrihydrite . Appl Phys A 74 (Suppl 1), s1004–s1006. doi.org/10.1007/s003390101175.

Jambor, J. L., and Dutrizac, J. E., **1998**. Occurrence and Constitution of Natural and Synthetic Ferrihydrite, a Widespread Iron Oxyhydroxide. Chemical Reviews. 98 (7), 2549-2586. doi: 10.1021/cr970105t.

Jarusutthirak, C., Amy, G., and Crouè, J.-P., **2002**. Fouling characteristics of wastewater effluent organic matter (EfOM) isolates on NF and UF membranes, Desalination. 145(1–3), 247–255. doi.org/10.1016/S0011-9164(02)00419-8.

Johanston, A.E., **2000**. Soil and Plant Phosphate. International Fertilizer Industry Association (IFA), Paris. ISBN: 2950629954, 9782950629951.

Jowett, C., Solntseva, I., Wu, L., James, C., Glasauer, S., **2018**. Removal of sewage phosphorus by adsorption and mineral precipitation, with recovery as a fertilizing soil amendment. Water Sci. Technol. 77 (8), 1967–1978. doi:10.2166/wst.2018.027.

Jung, J.-O., **2005**. Fundamental study on the recovery and removal of white phosphorus from phosphorus sludge, Environ. Eng. Res. 10 (1) 38–44. doi.org/10.4491/eer.2005.10.1.038.

Jupp, A.R., Beijer, S., Narain, G.C., Schipperc, W., Slootweg, J.C., **2021**. Phosphorus recovery and recycling – closing the loop. Chem. Soc. Rev. 50, 87–101. doi.org/10.1039/D0CS01150A.

Kaljunen, J. U., Al-Juboori, R. A., Khunjar, W., Mikola, A., Wells, G., **2022**. Phosphorus recovery alternatives for sludge from chemical phosphorus removal processes – Technology comparison and system limitations. Sustainable Materials and Technologies, 34, [100514]. doi.org/10.1016/j.susmat.2022.100514.

Karlsson, T., & Persson, P., **2012**. Complexes with aquatic organic matter suppress hydrolysis and precipitation of Fe(III). Chem. Geol. 322−323, 19−27. doi:10.1016/j.chemgeo.2012.06.003.

Kato, F., Kitakoji, H., Oshita, K., Takaoka, M., Takeda, N., Matsumoto, T. **2006**. Extraction Efficiency of Phosphate from Pre-Coagulated Sludge with NaHS. Water Science & Technology 54 (5): 119. doi:10.2166/wst.2006.554.

Kim, B., Gautier, M., Simidoff, A., Sanglar, C., Chatain, V., Philippe M., Rémy G., **2016**. pH and Eh Effects on Phosphorus Fate in Constructed Wetland's Sludge Surface Deposit. Journal of Environmental Management. 183: 175–81. doi:10.1016/j.jenvman.2016.08.064.

Kok, D. D., van Lier,J. B., Uhlenbrook, S., Ortigara, A. R.C., Pande, S., Savenije, H., **2018**. Global Phosphorus Recovery for Agricultural Reuse. Hydrology and Earth System Sciences Discussions, 1–18. doi:10.5194/hess-2018-176.

Korving, L., Van Loosdrecht, M., Wilfert, P., **2019**. Effect of iron on phosphate recovery from sewage sludge, in: H. Ohtake, S. Tsuneda (Eds.), Phosphorus Recovery and Recycling, Springer Singapore, Singapore, pp. 303–326. doi.org/ 10.1007/978-981-10-8031-9_21.

Kroiss, H., Rechberger, H., Egle, L., **2011**. Phosphorus in Water Quality and Waste Management. InTech. doi: 10.5772/18482.

Kumar, R., & Pal. P., **2015**. Assessing the Feasibility of N and P Recovery by Struvite Precipitation from Nutrient-Rich Wastewater: A Review. Environmental Science and Pollution Research 22 (22): 17453–64. doi:10.1007/s11356-015-5450-2.

Lahav, O., Telzhensky, M., Zewuhn, A., Gendel, Y., Gerth, J., Calmano, W., Birnhack, L., **2013**. Author's Personal Copy Struvite Recovery from Municipal-Wastewater Sludge Centrifuge

Supernatant Using Seawater NF Concentrate as a Cheap Mg(II) Source. doi:10.1016/j.seppur.2013.02.002.

Le, C., Kunacheva, C., Stuckey, D. C., **2016**. Protein Measurement in Biological Wastewater Treatment Systems: A Critical Evaluation. Environmental Science & Technology. 50 (6), 3074-3081. doi: 10.1021/acs.est.5b0526.

Leenheer, J.A., Crouè, J., **2003**. Peer reviewed: characterizing aquatic dissolved organic matter. Environ. Sci. Technol. 37 (1), 18A-26A.

Levine, A.D., Tchobanoglous, G., Asano, T., **1985**. Characterization of the size distribution of contaminants in wastewater: treatment and reuse implications. J. Water Pollut. Control Fed. 57 (7), 805-816.

Li, B., Boiarkina, I., Yu, W., Huang, H. M., Munir, T., Wang, G. Q., Young. B. R., **2019**. Phosphorus Recovery through Struvite Crystallization: Challenges for Future Design. Science of The Total Environment. 648: 1244–56. doi:10.1016/j.scitotenv.2018.07.166.

Li, C. Y., Sheng, Y. Q., Xu, H. D., **2021**. Phosphorus recovery from sludge by pH enhanced anaerobic fermentation and vivianite crystallization. J. Environ. Chem. Eng. 9 (1), 104663.

Li, R., Teng, W., Yanlong Li, Y., Wang, W., Cui, R., Yang. T., **2017**. Potential Recovery of Phosphorus during the Fluidized Bed Incineration of Sewage Sludge. Journal of Cleaner Production 140 (140): 964–70. doi:10.1016/j.jclepro.2016.06.177.

Li, R.H., Cui, J.L., Li, X.D., Li, X.Y., **2018**. Phosphorus removal and recovery from wastewater using Fe-dosing bioreactor and cofermentation: investigation by X-ray absorption near-edge structure spectroscopy. Environ. Sci. Technol. 52 (24), 14119–14128.

Li, R.-.H., Cui, J.-.L., Hu, J.-.H., Wang, W.-.J., Li, B., Li, X.-.D., Li, X.-.Y., **2020**. Transformation of Fe–P Complexes in Bioreactors and P Recovery from Sludge: Investigation by XANES Spectroscopy. Environmental Science and Technology 54 (7), 4641-4650. doi: 10.1021/acs.est.9b07138.

Likosova, M. E., Keller, J., Rozendal, R. A., Poussade, Y., S. Freguia. S., **2013**. Understanding Colloidal FeS_x Formation from Iron Phosphate Precipitation Sludge for Optimal Phosphorus Recovery. Journal of Colloid and Interface Science 403. Elsevier Inc.: 16–21. doi:10.1016/j.jcis.2013.04.001.

Liu, B. , Wu, J. , Cheng, C. , Tang, J. , Khan, M.F.S. , Shen, J. , **2019**. Identification of textile wastewater in water bodies by fluorescence excitation emission matrix-parallel factor analysis and high-performance size exclusion chromatography. Chemosphere 216, 617–623.

Liu, J., Cheng, X., Qi, X., Li, N., Tian, J., Qiu, B., Xu, K., Qu, D., **2018**. Recovery of phosphate from aqueous solutions via vivianite crystallization: Thermodynamics and influence of pH, Chemical Engineering Journal. 349, 37-46. doi.org/10.1016/j.cej.2018.05.064.

Lobartini, J. C., Tan, K. H., Pape, C., **1998**. Dissolution of aluminum and iron phosphate by humic acids. Commun. Soil Sci. Plant Anal. 29 (5−6), 535−544. doi:10.1080/00103629809369965.

Lu, H., Yang, L., Zhang, S., Wu, Y., **2014**. The Behavior of Organic Phosphorus under Non-Point Source Wastewater in the Presence of Phototrophic Periphyton. PLoS ONE 9(1): 185910. doi.org/10.1371/journal.pone.0085910.

Lu, J., Yang, J., Xu, K., Hao, J., Li. Y.Y., **2016**. Phosphorus Release from Coprecipitants Formed during Orthophosphate Removal with Fe(III) Salt Coagulation: Effects of pH, Eh, Temperature and Aging Time. Journal of Environmental Chemical Engineering 4 (3). Elsevier B.V.: 3322–29. doi:10.1016/j.jece.2016.07.005.

MacCarthy, P., **2001**. The principles of humic substances. Soil Sci. 166, 738–751.

Magrí, A., Carreras-Sempere, M., Biel, C., Colprim, J., **2020**. Recovery of phosphorus from wastewater profiting from biological nitrogen treatment: upstream, concomitant or downstream precipitation alternatives. Agronomy 10, 1039. doi.org/10.3390/AGRONOMY1007103.

Mara, D., & Horan, N., **2003**. Handbook of Water and Wastewater Microbiology.1-819. Academic Press. doi.org/10.1016/B978-0-12-470100-7.X5000-6.

Mayer, B. K., Baker L. A., Boyer, T. H., Drechsel, P., Mac Gifford, Hanjra, M.A., Parameswaran, P., Stoltzfus, J., Westerhoff, P., Rittmann, B. E., **2016**. Total Value of Phosphorus Recovery. Environmental Science and Technology 50 (13): 6606–20. doi:10.1021/acs.est.6b01239.

McCance, R.A & Widdowson, E.M., **1960**. The composition of foods. 3rd edition. Spec. Rep. Ser. No. 297. London, Her Majesty's Stationery Office.

Mehta, C. M., & Batstone, D. J., **2013**. Nucleation and growth kinetics of struvite crystallization, Water Res. (47): 2890–2900. doi: 10.1016/j.watres.2013.03.007.

Mesquita, D.P. , Quintelas, C. , Luis Amaral, A. , Ferreira, E.C. , **2017**. Monitoring biological wastewater treatment processes: Recent advances in spectroscopy applications. Rev. Environ. Sci. Bio-Tech. 16 (3), 395–424.

Metcalf and Eddy Inc., Tchobanoglous G., **2014**. Wastewater engineering : treatment and reuse, 5th Edition. McGraw Hill, New York.

Meyer, C., Preyl, V., Steinmetz, H., Maier, W., Mohn, R.-E., Schönberger, H., **2019**. The Stuttgart process (Germany). In: Ohtake, H., Tsuneda, S. (Eds.), Phosphorus Recovery and Recycling. Springer, Singapore. doi.org/10.1007/978-981-10-8031-9_19.

Miot, J., Benzerara, K., Morin, G., Bernard, S., Beyssac, O., Larquet, E., Kappler, A., Guyot, F., **2009**.Transformation of vivianite by anaerobic nitratereducing iron-oxidizing bacteria. Geobiology 7(3):373–384. doi:10.1111/j.1472-4669.2009.00203.x

Mopper, K., Stubbins, A., Ritchie, J. D., Bialk, H. M., Hatcher, P. G., **2007**. Advanced Instrumental Approaches for Characterization of Marine Dissolved Organic Matter: Extraction Techniques, Mass Spectrometry, and Nuclear Magnetic Resonance Spectroscopy. Chemical Reviews. 107 (2), 419-442. doi: 10.1021/cr050359b.

Mores, G.K., Brett, S.W., Guy, J.A., Lester, J.N., **1998**. Review Phosphorus Removal and Recovery Technologies. Science of the Total Environment 212: 69–81.

Munir, M. T., Li, B., Boiarkina, I., Baroutian, S., Yu, W., Young, B. R., **2017**. Phosphate recovery from hydrothermally treated sewage sludge using struvite precipitation. Bioresource Technology. (239):171–179. doi: 10.1016/j.biortech.2017.04.129.

Narkis, N., Henefeld-Fourrier, S., Rebhun, M., **1980**. Volatile organic acids in raw wastewater and in physico-chemical treatment. Water Research, Volume 14, Issue 9, Pages 1215-1223. doi.org/10.1016/0043-1354(80)90179-7.

Nriagu, J.O., **1972**. Stability of vivianite and ion-pair formation in the system $Fe_3(PO_4)_2$-H_3PO_4-H_2O. Geochim. Cosmochim. Acta 36 (4), 459–470. doi.org/10.1016/00167037(72)90035-X.

Nriagu, J. O., **1984**. Phosphate Minerals: Their Properties and General Modes of Occurrence. In Photosphate Minerals, 1–136. Berlin, Heidelberg: Springer Berlin Heidelberg. doi:10.1007/978-3-642-61736-21.

O'Loughlin, E. J., Boyanov, M. I., Flynn, T. M., Gorski, C.A., Hofmann, S. M., Mccormick, M. L., Scherer, M. M., Kemner, K. M., **2013**. Effects of bound phosphate on the bioreduction of lepidocrocite (g-FeOOH) and maghemite (g-Fe_2O_3) and formation of secondary minerals. Environ. Sci. Technol. 47 (16), 9157-9166.

Pandey, A.K., Pandey, S.D., Misra, V., **2000**. Stability constants of metal–humic acid complexes and its role in environmental detoxification. Ecotoxicol. Environ. Saf. 47, 95–200. doi: 10.1006/eesa.2000.1947.

Parsons, C. T., Rezanezhad, F., O'Connell, D. W., Van Cappellen. P., **2017**. Sediment Phosphorus Speciation and Mobility under Dynamic Redox Conditions. Biogeosciences 14 (14): 3585–3602. doi:10.5194/bg-14-3585-2017.

Parsons, S. A., and Smith. J. A., **2008**. Phosphorus Removal and Recovery from Municipal Wastewaters. Elements 4 (2). GeoScienceWorld: 109–12. doi:10.2113/GSELEMENTS.4.2.109.

Pasek, M. A., Sampson, J. M., Atlas, Z., **2014**. Redox chemistry in the phosphorus biogeochemical cycle. Proceedings of the National Academy of Sciences. 111 (43) 15468-15473. doi: 10.1073/pnas.1408134111.

Peng, L., Dai, H., Wu, Y., Peng, Y., Lu, X., **2018a**. A Comprehensive Review of Phosphorus Recovery from Wastewater by Crystallization Processes. Chemosphere 197. Elsevier Ltd:

768–81. doi:10.1016/j.chemosphere.2018.01.098.

Peng, L., Dai, H., Wu, Y., Peng, Y., Lu, X., **2018b**. A Comprehensive Review of the Available Media and Approaches for Phosphorus Recovery from Wastewater. Water, Air, & Soil Pollution 229 (4). Water, Air, & Soil Pollution: 115. doi:10.1007/s11270-018-3706-4.

Petzet, S., Peplinski, B., Bodkhe, S. Y., Cornel, P., **2011**. Recovery of Phosphorus and Aluminium from Sewage Sludge Ash by a New Wet Chemical Elution Process (SESAL-Phos-Recovery Process). Water Science and Technology : A Journal of the International Association on Water Pollution Research 64 (3): 693–99. http://www.ncbi.nlm.nih.gov/pubmed/22097049.

Petzoldt, C. S., Lezcano, J. P., Moreda, I. L., **2020**. Removal of orthophosphate and dissolved organic phosphorus from synthetic wastewater in a combined struvite precipitation-adsorption system, Journal of Environmental Chemical Engineering, Volume 8, Issue 4, 103923. doi.org/10.1016/j.jece.2020.103923.

Ping, Q., Zhang, B., Zhang, Z., Lu, K., Li, Y., **2022**. Speciation analysis and formation mechanisism of iron-phosphrous compounds during chemical phosphorus removal process. Chemosphere. 310.136852. doi.org/10.1016/j.chemosphere.2022.136852.

Posth, N.R., Canfield, D. E., Kappler, A., **2014**. Biogenic Fe(III) Minerals: From Formation to Diagenesis and Preservation in the Rock Record. Earth-Science Reviews. 135: 103–21. doi:10.1016/j.earscirev.2014.03.012.

Prot, T., Wijdeveld, W., Eshun, L. E., Dugulan, A. I., Goubitz, K., Korving, L.,Van Loosdrecht, M. C. M., **2020**. Full-scale increased iron dosage to stimulate the formation of vivianite and its recovery from digested sewage sludge. Water Research. 182, 115911. doi.org/10.1016/j.watres.2020.115911.

Prot, T., Korving, L., Dugulan, A. I., Goubitz, K., van Loosdrecht, M. C. M., **2021**. Vivianite scaling in wastewater treatment plants: Occurrence, formation mechanisms and mitigation solutions. Water research. 197, 117045. doi.org/10.1016/j.watres.2021.117045.

Prot, T., Nguyen, V. H., Wilfert, P., Dugulan, A. I., Goubitz, K., De Ridder, D. J., Korving, L., Rem, P., Bouderbala, A., Witkamp, G. J., van Loosdrecht, M. C. M., **2019**. Magnetic separation and characterization of vivianite from digested sewage sludge. Separation and Purification Technology, (224): 564-579. doi.org/10.1016/j.seppur.2019.05.057.

Prasad, M. N. & Majeti, N.V., **2016**. Environmental Materials and Waste : Resource Recovery and Pollution Prevention. 1953- Editor. London, UK ; San Diego, CA, USA : Academic Press Is an Imprint of Elsevier 2016. London: Elsevier Inc. doi:10.1016/C2014.0.05144.1.

Pullin, M. J., and Cabaniss, S. E., **2003**. The effects of pH, ionic strength, and iron-fulvic acid interactions on the kinetics of non-photochemical iron transformations. I. Iron (II) oxidation and iron colloid formation. Geochim. Cosmochim. Acta. 67, 4067 – 4077,

doi:10.1016/S0016-7037(03)00366-1.

Qualls, R. G., Sherwood, L. J., Richardson., C. J., **2009**. Effect of natural dissolved organic carbon on phosphate removal by ferric chloride and aluminum sulfate treatment of wetland waters. Water Resources Research. (45): W09414, doi:10.1029/2008WR007287.

Rao, S.R. , Varadaraju, U.V. , **2015**. Hydrothermal synthesis of $LiFePO_4$ nanorods com- posed of nanoparticles from vivianite precursor and its electrochemical perfor- mance for lithium ion battery applications. Bull. Mater. Sci. 38 (5), 1385–1388. doi:10.1007/s12034-015-1025-6. doi:10.1007/s12034-015-1025-6.

Rashid, S. S., Liu, Y. Q., Zhang, C., **2020**. Upgrading a large and centralised municipal wastewater treatment plant with sequencing batch reactor technology for integrated nutrient removal and phosphorus recovery: environmental and economic life cycle performance. Sci. Total Environ. 749, 141465. doi.org/10.1016/j.scitotenv.2020.141465.

Raunkjaer, K., Hvitvedjacobsen, T., Nielsen, P. H., 1994. Measurement of pools of protein, carbohydrate and lipid in domestic waste-water. Water Research, vol. 28, pp. 251-262.

Rittmann, B. E., Mayer, B., Westerhoff, P., Edwards, M., **2011**. Capturing the Lost Phosphorus. Chemosphere 84 (6). Elsevier Ltd: 846–53. doi:10.1016/j.chemosphere.2011.02.001.

Roman, F., & Hartmann, S., **2020**. Models in Science. The Stanford Encyclopedia of Philosophy, Edward N. Zalta (ed.), <https://plato.stanford.edu/archives/spr2020/entries/models-science/>.

Rose, A.L., Waite, T.D., 2007. Reconciling kinetic and equilibrium observations of iron(III) solubility in aqueous solutions with a polymer-based model. Geochim. Cosmochim. Acta 71, 5605-5619. doi:10.1016/j.gca.2007.02.024.

Rouzies, D., & Millet, J. M. M., **1993**. Mössbauer study of synthetic oxidized vivianite at room temperature. Hyperfine Interact. 77 (1), 19–28. doi.org/10.1007/BF02320295.

Rothe, M., Frederichs, T., Eder, M., Kleeberg, A., Hupfer, M., **2014**. Evidence for vivianite formation and its contribution to long-term phosphorus retention in a recent lake sediment: a novel analytical approach. Biogeosciences. 11 (18), 5169-5180. doi.org/10.5194/bg-11-5169-2014.

Rothe, M., Kleeberg, A., Hupfer, M., **2016**. The occurrence, identification and environmental relevance of vivianite in waterlogged soils and aquatic sediments. Earth Sci. Rev. 158, 51-64. doi.org/10.1016/j.earscirev.2016.04.008.

Ruzhitskaya, O., and Gogina, E., **2017**. Methods for Removing of Phosphates from Wastewater. MATEC Web of Conferences 106: 07006. doi:10.1051/matecconf/201710607006.

Rydin, E., **1996**. Experimental studies simulating potential phosphorus release from municipal sewage sludge deposits. Water Research. 1695-1701. doi:10.1016/0043-1354(96)00048-6.

Salehin, S., Rebosura, M., Jr, Keller, J., Gernjak, W., Donose, B. C., Yuan, Z., Pikaar, I., **2020**. Recovery of in-sewer dosed iron from digested sludge at downstream treatment plants and its reuse potential. Water research. 174, 115627.doi.org/10.1016/j.watres.2020.115627.

Sano, A., Kanomata, M., Inoue, H., Sugiura, N., Xu, K. Q., Inamori, Y., **2012**. Extraction of Raw Sewage Sludge Containing Iron Phosphate for Phosphorus Recovery. Chemosphere 89 (10). Elsevier Ltd: 1243–47. doi:10.1016/j.chemosphere.2012.07.043.

Schwartzman, U., Wagner, F., Knicker, H., **2005**. Ferrihydrite–humic associations: Magnetic hyperfine interactions. Soil Sci. Soc. Am. J. 69 (4), 1009. doi: 10.2136/sssaj2004.0274.

Shepherd, J. G., Sohi, S. P., Heal, K. V., **2016**. Optimising the recovery and re-use of phosphorus from wastewater effluent for sustainable fertiliser development. Water research, 94, 155–165. doi.org/10.1016/j.watres.2016.02.038.

Shi, W., Zhuang, W.-E., Jin Hur, J., Liyang Yang, L., **2021**. Monitoring dissolved organic matter in wastewater and drinking water treatments using spectroscopic analysis and ultra-high resolution mass spectrometry. Water Research 188, 116406. doi.org/10.1016/j.watres.2020.116406.

Shih, Y.-J., Abarca, R.M., de Luna, M. D., Huang, Y.-H., Lu, M.-C., **2017**. Recovery of Phosphorus from Synthetic Wastewaters by Struvite Crystallization in a Fluidized-Bed Reactor: Effects of PH, Phosphate Concentration and Coexisting Ions. Chemosphere 173: 466–73. doi:10.1016/j.chemosphere.2017.01.088.

Shon, H. K., Vigneswaran, S., & Snyder, S. A., **2006**. Effluent Organic Matter (EfOM) in Wastewater: Constituents, Effects, and Treatment. Critical Reviews in Environmental Science and Technology, 36(4), 327–374. doi.org/10.1080/10643380600580011.

Shon, H.K., Vigneswaran, S., Ben Aim, R., Ngo, H.H., Kim, I.S., Cho, J., **2005b**. Influence of flocculation and adsorption as pretreatment on the fouling of ultrafiltration and nanofiltration membranes: application with biologically treated sewage effluent. Environ. Sci. Technol. 39(10), 3864–3871.

Smil, V., **2000**. Phosphorus in the Environment : Natural Flows and Human Interferences. Annual Review of Energy and the Environment 25 (1): 53–88. doi:10.1146/annurev.energy.25.1.53

Smith, S., Takacs, I., Murthy, S., Daigger, G. T., Szabo, A., **2008**. Phosphate Complexation Model and Its Implications for Chemical Phosphorus Removal. Water Environ. Res. 80 (5): 428–438.

Smolders, A. P., Lamers, L. M., Lucassen, E. T., Van Der Velde, G., Roelofs, J. M., **2006**. Internal Eutrophication: How It Works and What to Do about It—a Review. Chemistry and Ecology 22 (2): 93–111. doi:10.1080/02757540600579730.

Snyder, S. A., Leising, J., Westerhoff, P., Yoon, Y., Mash, H., & Vanderford, B., **2004**. Biological

and physical attenuation of endocrine disruptors and pharmaceuticals: Implications for water reuse. Ground Water Monitoring and Remediation, 24(2), 108-118. doi.org/10.1111/j.1745-6592.2004.tb00719.x.

Solon, K., Volcke, E.I.P., Sperando, M., van Loosdercht, M. **2019**. Resource Recovery and Wastewater Treatment Modelling. Environ. Sci.:Water Res. Technol. doi.org/10.1039/C8EW00765A.

Sophonsiri, C., & Morgenroth, E., **2004**. Chemical composition associated with different particle size fractions in municipal, industrial, and agricultural wastewaters. Chemosphere, vol. 55, pp. 691-703.

Standard Methods (Standard Methods for the Examination of Water and Wastewater), **2012**. 22nd ed., American Public Health Association/American Water Works Association/Water Environment Federation, Washington, DC, USA.

Steelink, C.,**1985**. Elemental characteristics of humic substances. In Aiken GR, McKnight DM, Wershaw RL, MacCarthy P (Eds.) Humic Substances In Soil, Sediment and Water. Wiley. New York, USA. pp. 457-476.

Stevenson, F. J., 1994. Humus Chemistry: Genesis, Composition, Reactions, 2nd ed; Wiley: New York.

Szabó, A., Takács, I., Murthy, S., Daigger, G. T., Licskó, I., Smith, S. D., **2008**. Significance of Design and Operational Variables in Chemical Phosphorus Removal. Water Environment Research 80 (5): 407–16. doi:10.2175/106143008X268498.

Takaoka, M., Oshita, K., Cui, X., Matsukawa, K., Fujiwara, T., **2010**. Phosphorus material flow and its recovery from wastewater and solid waste. UNEP-DTIE-IETC, Regional. Workshop on Waste Agricultural Biomass. Global Environment Centre Foundation in Osaka. Japan Institute of Wastewater Engineering Technology (JIWET).

Taujale, S., Baratta, L. R., Huang, J., Zhang, H., **2016**. Interactions in Ternary Mixtures of MnO_2, Al_2O_3, and Natural Organic Matter (NOM) and the Impact on MnO_2 Oxidative Reactivity. Environ. Sci. Technol. 50, 2345−2353. doi: 10.1021/acs.est.5b05314.

Taylor, K. G., Hudson-Edwards, K. A. , Bennett A. J., Vishnyakov, V., **2008**. Early diagenetic vivianite [$Fe_3(PO_4)_2.8H_2O$] in a contaminated freshwater sediment and insights into zinc uptake: a μ-EXAFS, μ-XANES and Raman study. Appl Geochem 23(6):1623–1633.

Tchobanoglous, G., and Burton, F.L., **1991**. Wastewater Engineering: Treatment, Disposal, and Reuse, 3rd ed. New York: McGraw-Hill.

Thistleton, J., Clark, T., Pearce, P., Parsons, S. A., **2001**. Mechanisms of Chemical Phosphorus Removal: 1—Iron (II) Salts. Process Safety and Environmental Protection 79 (6). Elsevier: 339–44. doi:10.1205/095758201753373104.

Tran, N. H., Ngo, H. H., Urase, T., Gin, K. Y.-H., **2015**. A critical review on characterization strategies of organic matter for wastewater and water treatment processes. Bioresour. Technol. 193, 523–533. doi:10.1016/j.biortech.2015.06.091.

US Geological Survey, **2013**. PHREEQC (Version 3) – A computer program for speciation, batch-reaction, one-dimensional transport, and inverse geochemical calculations, (https://wwwbrr.cr.usgs.gov/projects/GWC_coupled/phreeqc/) (accessed on December 5th, 2021).

Venkiteshwaran, K., McNamara, P. J., K. Mayer, B. K., **2018**. Meta-Analysis of Non-Reactive Phosphorus in Water, Wastewater, and Sludge, and Strategies to Convert It for Enhanced Phosphorus Removal and Recovery. Science of the Total Environment 644. Elsevier B.V.: 661–74. doi:10.1016/j.scitotenv.2018.06.369.

Vogel, C., Krüger, O., Herzel, H., Amidani, L., Adam, C., **2016**. Chemical state of mercury and selenium in sewage sludge ash based P-fertilizers. J. Hazard. Mater. 313, 179–184.doi: 10.1016/j.jhazmat.2016.03.079.

Vu, M. T., Duong, H. C., Wang, Q., Ansari, A., Cai, Z., Hoang, N. B., Long D. Nghiem, L. D., **2023**. Recent technological developments and challenges for phosphorus removal and recovery toward a circular economy. Environmental Technology & Innovation, Volume 30, 103114. doi.org/10.1016/j.eti.2023.103114.

Vuuren, D. P. Van, Bouwman A. F., Beusen, A. H. W., **2010**. Phosphorus Demand for the 1970–2100 Period: A Scenario Analysis of Resource Depletion. Global Environmental Change 20 (3): 428–39. doi:10.1016/j.gloenvcha.2010.04.004.

Wang, Q., Kim, T. H., Reitzel, K., Almind-Jørgensen, N., Nielsen, U. G., **2021**. Quantitative determination of vivianite in sewage sludge by a phosphate extraction protocol validated by PXRD, SEM-EDS, and 31P NMR spectroscopy towards efficient vivianite recovery. Water research, 202, 117411. doi.org/10.1016/j.watres.2021.117411.

Wang, R., Wilfert, P., Dugulan, I., Goubitz, K., Korving, L., Witkamp, G.J., van Loosdrecht, M.C.M., **2019**. Fe(III) reduction and vivianite formation in activated sludge. Separ. Purif. Technol. 220, 126–135. doi.org/10.1016/j.seppur.2019.03.024.

Weber, K. A., Achenbach, L. A., Coates, J. D., **2006**. Microorganisms Pumping Iron: Anaerobic Microbial Iron Oxidation and Reduction. Nature Reviews Microbiology 4 (10): 752–64. doi:10.1038/nrmicro1490.

WEF. **2011**. Nutrient Removal - Manual of Practice. WEF Manual of Practice No. 34. (1): 72-83.

Westheimer, F. H., **1987**. Why Nature Chose Phosphates. Science. 235,1173-1178. doi:10.1126/science.2434996.

Wijdeveld, W. K., Prot, T., Sudintas, G., Kuntke, P., Korving, L., M.C.M. van Loosdrecht, M. C.

M., **2022**. Pilot-scale magnetic recovery of vivianite from digested sewage sludge, Water Res. (212): 118131. doi.org/10.1016/j.watres.2022.118131.

Wilfert, P., Dugulan, A.I., Goubitz, K., Korving, L., Witkamp, G.J., Van Loosdrecht, M. C. M., **2018**. Vivianite as the main phosphate mineral in digested sewage sludge and its role for phosphate recovery. Water Res. 144, 312–321. doi.org/10.1016/J.WATRES. 2018.07.020.

Wilfert, P., Mandalidis, A., Dugulan, A. I., Goubitz, K., Korving, L., Temmink, H., **2016**. Vivianite as an Important Iron Phosphate Precipitate in Sewage Treatment Plants. Water Research 104. Elsevier Ltd: 449–60. doi:10.1016/j.watres.2016.08.032.

Wilfert, P., Prashanth S. K., Korving, L., Witkamp, G. J., van Loosdrecht, M.C.M., **2015**. The Relevance of Phosphorus and Iron Chemistry to the Recovery of Phosphorus from Wastewater: A Review. Environmental Science and Technology 49 (16): 9400–9414. doi:10.1021/acs.est.5b00150.

Wilfert, P., Meerdink, J., Degaga, B., Temmink, H., Korving, L., Witkamp, G. J., Goubitz, K., van Loosdrecht, M. C. M., **2020**. Sulfide induced phosphate release from iron phosphates and its potential for phosphate recovery. Water Research. (171): 115389, doi.org/10.1016/j.watres.2019.115389.

Xu, X., Xu, Q., Du, Z., Gu, L., Chen, C., Huangfu, X., Shi, D., **2023**. Enhanced phosphorus release from waste activated sludge using ascorbic acid reduction and acid dissolution. Water research. 229, 119476. doi.org/10.1016/j.watres.2022.119476

Yao, Y., **2014**. Use of carbohydrate, protein and fat to characterise wastewater in terms of its major elemental constituents and energy. MSc. Thesis. The University of Manchester.

Yang, X., Chen, X., Yang, Xi., **2019**. Effect of organic matter on phosphorus adsorption and desorption in a black soil from Northeast China. Soil and Tillage Research, (187): 85-91, doi.org/10.1016/j.still.2018.11.016.

Ye, Y., Ngo, H. H., Guo, W., Liu, Y., Li, J., Liu, Y., Zhang, X., Jia, H., **2017**. Insight into Chemical Phosphate Recovery from Municipal Wastewater. Science of The Total Environment 576 : 159–71. doi:10.1016/j.scitotenv.2016.10.078.

Yoon, S.-Y., Lee, C.-G., Park, J.-A., Kim, J.-H., Kim, S.-B., Lee, S.-H., and Jae-Woo Choi, J.-W., **2014**. Kinetic, Equilibrium and Thermodynamic Studies for Phosphate Adsorption to Magnetic Iron Oxide Nanoparticles. Chemical Engineering Journal. (236): 341–47. doi:10.1016/j.cej.2013.09.053.

Yuan, Z., Jiang, S., Sheng, H., Liu, X., Hua, H., Liu, X., Zhang, Y., **2018**. Human Perturbation of the Global Phosphorus Cycle: Changes and Consequences. Environmental science & technology, 52(5), 2438–2450. doi.org/10.1021/acs.est.7b03910.

Y. Wu, Luo, J., Zhang, Q., Aleem, M., Fang, F., Xue, Z., Cao, J., **2019**. Potentials and challenges of

phosphorus recovery as vivianite from wastewater: A review. Chemosphere, 226, 246–258. doi.org/10.1016/j.chemosphere.2019.03.138.

Zaaboub, N., Ounis, A., Helali, M. A., Béjaoui, B., Lillebø, A. I., da Silva, E. F., Aleya. L., **2014**. Phosphorus Speciation in Sediments and Assessment of Nutrient Exchange at the Water-Sediment Interface in a Mediterranean Lagoon: Implications for Management and Restoration. Ecological Engineering. 73: 115–25. doi:10.1016/j.ecoleng.2014.09.017.

Zhang, H., Taujale, S., Huang, J., Lee, G.-J., **2015**. Effects of Nom on Oxidative Reactivity of Manganese Dioxide in Binary Oxide Mixtures with Goethite or Hematite. Langmuir. 31, 2790−2799. doi: 10.1021/acs.langmuir.5b00101.

Zhang, B., Wang, L., Li, Y., **2019**. Fractionation and identification of iron-phosphorus compounds in sewage sludge. Chemosphere, 223, 250–256. doi:10.1016/j.chemosphere.2019.02.052.

Zhang, C.Y., Cheng, X., Wang, M., Ma, J.X., Collins, R., Kinsela, A., Zhang, Y., Waite, T. D., **2021**. Phosphate recovery as vivianite using a flow-electrode capacitive desalination (FCDI) and fluidized bed crystallization (FBC) coupled system. Water Res. 194, 116939.

Zhang. J, Chen. Z, Liu. Y, Wei. W, Ni. B-J,. **2022**. Phosphorus recovery from wastewater and sewage sludge as vivianite, Journal of Cleaner Production. 370: 133439. doi.org/10.1016/j.jclepro.2022.133439.

Zhou, Y., Boutton, T. W., Wu, X. B., **2018**. Soil phosphorus does not keep pace with soil carbon and nitrogen accumulation following woody encroachment. Glob Change Biol. 24: 1992 – 2007. doi.org/10.1111/gcb.14048.

Zhu, C., & Anderson, G., **2002**. Environmental Applications of Geochemical Modeling. Cambridge: Cambridge University Press. doi:10.1017/CBO9780511606274.

Zhu, X., Liu, J., Li, L., Zhen, G., Lu, X., Zhang, J., Liu, H., Zhou, Z., Wu, Z., Zhang, X., **2022**. Prospects for humic acids treatment and recovery in wastewater: A review. Chemosphere, 312(Part 2). doi.org/10.1016/j.chemosphere.2022.137193.

Chapter 3 - Insight into Direct Phosphorus Release from Simulated Wastewater Ferric Sludge: Influence of Physiochemical Factors

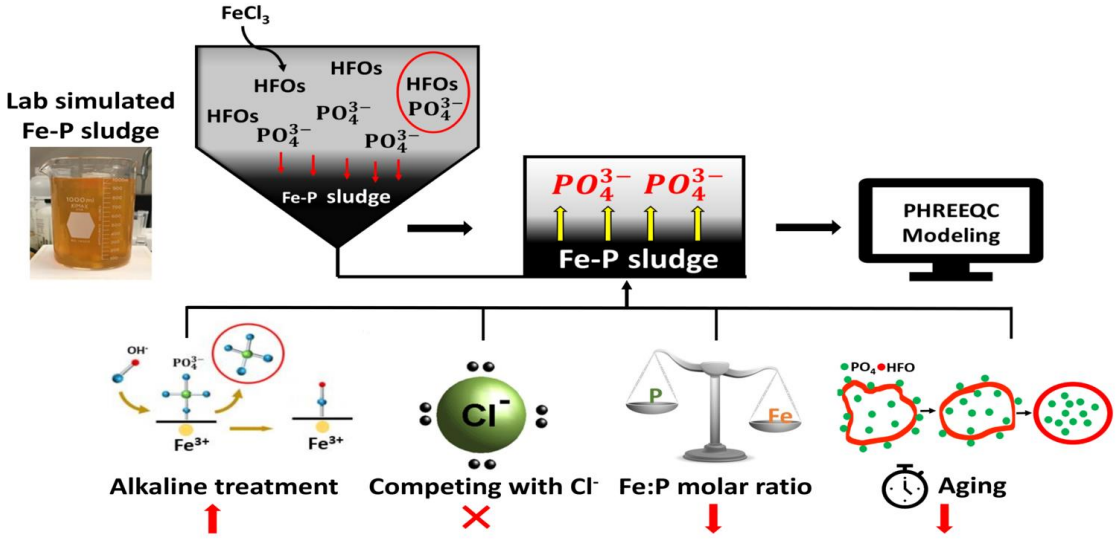

3.1 Abstract

Phosphorus recovery from chemical phosphorus removal (CPR) plants is limited. CPR plants that use iron salts for phosphorus removal generate iron phosphate (Fe-P) rich sludge. This study investigates the influence of pH and competing anions (chloride), on phosphorus and soluble iron release from lab simulated Fe-P sludge. Factors influencing recovery, such as sludge age and Fe/P molar ratio are also investigated. Results showed that alkaline treatment of Fe-P sludge was not effective in releasing Fe (<3%) but effective in releasing P, particularly at controlled pH value of 10 where the %P release was (90±2%). Sludge ageing time did not affect P release from Fe-P sludge at ages less than 5 days. However, a remarkable decrease in %P release (i.e., 50% reduction) was observed at ages of 9 and 11 days for pH values of 9-10. Arsenic extraction of exchangeable

surface bound P from Fe-P sludge and surface area determination of hydrous ferric oxide (HFO) under different aging times supported qualitatively the internalization of surface bound P during aging, which is a proposed mechanism responsible for the decrease in P release for older sludge. Chloride effect in releasing P from Fe-P sludge was negligible. The reduction in P release by aging was best described by a zero-order kinetic model. Modeling with the PHREEQC geochemical software did not always agree with the measured release of phosphorus from the Fe-P sludge. PHREEQC assumes all surface sites for phosphorus are exchangeable and has no mechanism to represent phosphorus trapped within HFO particles.

3.2 Introduction

The excessive demand on natural phosphorus (P) resources will lead to a world-wide scarcity and near depletion of these non-renewable resources in a few decades (Cordell et al., 2009; Kok et al., 2018). Hence, alternative sources of P will be required, as it is a key ingredient in the fertilizer industry, where about 18±3.5 Mt P/year are consumed (Cordell and White, 2014). Municipal wastewater contains P and could be an alternative, sustainable and renewable source, where approximately 1.3 Mt P/year is treated globally in water resource recovery facilities (WRRFs) (Wilfert et al., 2015; Peng et al., 2018a). Therefore, modern wastewater treatment plants (WWTPs) are shifting their focus from simple P removal to P recovery (Peng et al., 2018b).

Various methods have been established and applied to recover P at WRRFs. These include acid leaching of sludge incineration ash (Li et al., 2017; Chakraborty et al., 2020; Liang et al., 2021), acidogenic co-fermentation of P rich sludge (Li et al., 2019; Li et al., 2020), adsorption/desorption and ion exchange technologies (Sendrowski and Boyer, 2013; Loganathan et al., 2014; Paripurnanda et al., 2014; Gray et al., 2020), and chemical precipitation using calcium and magnesium salts (Peng et al., 2018a). Among these approaches, struvite ($MgNH_4PO_4.6H_2O$)

precipitation, in plants utilizing biological phosphorus removal, is the most extensively practiced approach for P recovery as fertilizer (Ye et al., 2017); many treatment plants use chemical methods for P removal though, and it is important to investigate possible approaches to P recovery from such plants.

Chemical P removal (CPR) is widely employed for removing P from wastewater (Szabo et al., 2008). CPR plants generate iron phosphate (Fe-P) rich sludge due to the interaction of the metal cations with orthophosphate (P_{ortho}) ions in wastewater (Peng et al., 2018b; Venkiteshwaran et al., 2018). Thus, a challenging, but potentially pragmatic approach, would be to recover P directly from sludge generated by CPR plants that use iron (Fe (III)) salts for P removal.

The mechanisms through which Fe-P sludge is generated in CPR plants include direct/co-precipitation, and adsorption (Smith et al., 2008; Wilfert et al., 2015). Under aerobic conditions P interacts with Fe(III) and forms different solids, where the most likely are iron-phosphate minerals (i.e., strengite ($FePO_4 \cdot 2H_2O$)), iron-hydroxyphosphate ($Fe_nPO_4(OH)_{3n-3}$) and P_{ortho} adsorbed to hydrous ferric oxide (HFO) surfaces (Smith et al., 2008, Wilfert et al., 2015, Wu et al., 2015, Zhang et al., 2019). HFO is the solid formed via hydrolysis of added ferric cations during CPR (Smith et al, 2008, Hauduc et al., 2015, Zhang et al, 2019; Ping et al., 2022). Smith et al. (2008) reported that soluble P_{ortho} is removed from wastewater at circumneutral pH by co-precipitation into HFO structure and/or adsorption to existing HFO surfaces. Moreover, a dynamic physiochemical model developed by Hauduc et al. (2015) described two types of P that are incorporated into HFO structure during the CPR process which are internal P (P trapped inside the structure of HFO by co-precipitation) and external or exchangeable P (P adsorbed to HFO surface). Considering the different forms of how P is incorporated to HFO will lead to best understanding P release and recovery from Fe-P solids.

Previous studies of P recovery from wastewater ferric sludges have focused on releasing P from the sludge and then precipitating it as struvite (Acelas et al., 2015; Peng et al., 2018a; Chen et al., 2019). Physiochemical factors like pH, sludge aging, reducing conditions, and the presence of competing ions have been found to play an important role in P release (Wilfert et al., 2015, Li et al., 2020). For example, it has been reported that 80% of P was released from anaerobically digested sludge compared to 25% from non-digested sludge by acidifying sludge samples collected from plants that use biological phosphorus removal combined with iron dosing (Quist-Jensen et al. 2018). When acidic and anaerobic conditions were combined in an acidogenic co-fermentation process Fe(III) was reduced to Fe(II) resulting in the release of 75% of the P from fresh Fe-P sludge (Li et al., 2020).

In contrast, alkaline pH had showed P release by dissolution of Fe-P sludge or by replacement of P_{ortho} by OH^- via ligand exchange mechanism (Wilfert et al, 2015; Xu et al, 2018). Sano et al. (2012) pointed out that P extraction from raw Fe-P sludge under alkali pH 13-14 was 22% more efficient than acid extraction at pH 2. Chen et al. (2019) also reported 69% release of P from raw Fe-P sludge at pH 11 by applying an alkaline fermentation method. It is clear that acidic and basic pH showed a potential for P release from wastewater ferric sludges. In fact, previous studies have focused on pH effect on direct P release from real wastewater ferric sludge samples. Information on P release from the pure inorganic forms of Fe-P solids generated during CPR in the absence of organic and inorganic interferences and over a wide range of pH values will provide fundamental insights into the processes and mechanisms that are active.

In CPR plants the estimated retention times of Fe-P sludge ranges between 1 to 12 days. Transformations in HFOs structures can take place as solids age and later impact P release from Fe-P sludge (Wu, et al., 2015; Li et al., 2020). Aging affects HFO structure and particularly its

adsorption/desorption capacity has been found to depend on the aging time. Long time spans, extending from days to weeks, are enough for fresh HFO structures to crystalize resulting in a reduction in surface area (Smith et al. 2008; Bligh et al., 2011) and adsorptive capacity (Conidi and Parker, 2015). Moreover, short time spans of hours to days, allow in turn aggregation and flocculation to take place among HFO particles which minimize the number of HFO accessible surfaces and active sites (Gilbert et al., 2009, Bligh et al., 2011). Li et al. (2020) studied the transformation of Fe-P complexes in bioreactors under different aging periods. They found that up to 4 days, ferrihydrite was the main Fe species and after 7 days goethite was identified with 5% of the sludge composition, which was raised to 9.4% after 30 days of aging. Therefore, it is important to consider the effect of HFO structural morphology transformations on direct P release from Fe-P sludge during aging, as very limited studies addressed this effect.

In CPR plants Fe-P sludges are generated over a range of Fe/P molar ratios and solids ages. Few studies have addressed the influence of these conditions on P release from Fe-P sludge when acidic/alkaline and competing ion treatments are employed in the absence of interferences from the complex wastewater matrix. This study investigated P release from simulated ferric sludges with different Fe/P molar ratios and ages as a function of pH and NaCl dose in the absence of such interferences. Arsenate (As(V)) extraction and fluorescein dye adsorption tests were employed as independent measures to assess surface exchangeable P and the surface area of HFO particles respectively. Furthermore, to help interpret experimental data, modeling with the PHREEQC geochemical software was conducted to simulate the release of phosphorus and iron from the Fe-P sludges. The results of this detailed investigation establish the theoretical and practical potential for P release and recovery from the inorganic fraction of wastewater ferric sludges.

3.3 Materials and methods

3.3.1 Simulated sludge preparation and sampling protocol

All chemicals involved in this study were reagent grade and used without further purification. All solutions were prepared using ultrapure water (Millipore, resistance >18.2 MΩ). A modified inorganic only version (with acetate removed) of a previously reported synthetic wastewater recipe (Jung et al., 2005) that contained $MgSO_4$, $CaCl_2$, $NaHCO_3$ and Na_3PO_4 (actual concentrations are presented in supplementary information Table A1.1) was employed. The synthetic wastewater was designed to mimic the inorganic composition of secondary-treated wastewater.

An iron (III) solution with ambient pH of 2.5 was prepared by dissolving $FeCl_3.6H_2O$ (136 mg Fe/L) in the synthetic wastewater. A fresh Fe-P sludge with a molar ratio of Fe/P of 1.5 was prepared by adding the $FeCl_3$ solution to one liter of synthetic wastewater containing Na_3PO_4 with total P concentration of 50 mg P/L under fast mixing (600 RPM) for 15 minutes. Following the above procedure, the prepared sludge had a pH of 6.35±0.2 which is typical of the pH range (6-8) observed at WWTPs using CPR (Metcalf and Eddy, 2014; Wilfert et al., 2015). Samples with a volume of 20 mL were transferred from the one liter sludge suspension, while it was mixed at high rate (600 RPM) on magnetic stirrer to ensure consistent homogenous sample composition. The samples were subsequently centrifuged at 4500 RPM for 30 minutes and decanted prior to their use in batch desorption tests. The concentration (w/v) of total suspended solids (TSS) was measured by filtering 20 mL samples using 0.45 µm cellulose nitrate membrane filters (Whatman, pore size 0.45 µm, diameter 47mm). The filter paper was then dried inside a desiccator at room temperature for 24 hours and the mass of TSS was measured.

3.3.2 P release batch experiments

The effect of pH and NaCl treatment on P and Fe release from the simulated ferric sludges was conducted in batch desorption experiments that were performed at 22±1 °C. All tests were conducted in 50 mL centrifuge tubes containing equal masses of dewatered sludge (approximately 10 mg dry weight) mixed with 20 mL of synthetic wastewater that were placed on a rotary shaker for 48 hours. At different time intervals three centrifuge tubes were sacrificed and filtered through 0.45 μm cellulose nitrate filter membranes after measuring their pH values. A 0.2 mL of concentrated (37%) HNO_3 acid, were added to each 20 mL filtrate sample to ensure complete digestion before measuring the concentrations of total soluble phosphorus (TP) and total soluble iron (TFe). Each batch experiment was run in duplicate.

In CPR plants chemical P removal is performed at pH values ranging between 6 and 8 (Metcalf and Eddy, 2014; Wilfert et al., 2015). Thus, the effect of manipulating pH above (9-12) and below this range (pH 2) on P release was evaluated. Experiments assessing the impact of pH on dissolution were carried out in two ways, under controlled and non-controlled pH conditions. For the latter, the pH of the synthetic wastewater was adjusted before mixing with the sludge solids using small volumes of either NaOH (1.0 M) or H_2SO_4 (0.5 M) solutions. The target values were adjusted such that target pH values of 2, 10 or 11 were obtained after mixing with sludge. The pH was not further adjusted, but it was recorded, after the solids were mixed with the wastewater. For controlled pH experiments manual titration with NaOH (1.0 M) to maintain constant pH values at 6, 7, 8, 9, 10, 11 and 12 was performed throughout 8 hours of reaction time, where the steady state was approximately reached based on the preliminary results.

The impact of sludge age on dissolution was investigated at pH values of 2, 9, and 10 with sludges that were aged at ambient pH (6.35-7.35) for periods of 0, 5, 9, and 11 days. The sludge solids were aged in 1 L glass beakers that were kept in dark at 22±1°C.

Experiments that assessed the effect of NaCl concentration on Fe and P release from artificial sludge were performed by adding fresh sludge solids to 15 mL of synthetic wastewater that was amended to have an NaCl concentration of 0.1 M to achieve a Cl/P molar ratio of 70.5. The pH of the solution was not adjusted in these tests and ranged between 7 and 7.5.

In all experiments the initial concentrations of TP and TFe in sludge solids that were used to calculate the percent release of P and Fe were determined by acid digestion (adding 20 mL of 10% HNO_3) of the solid sludge obtained after the centrifugation step and before mixing with synthetic wastewater. The digested solution was analysed by ICP-OES (see section 3.3.5 below). For mass balance monitoring in each experiment, three centrifuge tubes after 48 hours were filtered separately and the sum of masses of TP and TFe in filtrate solution and remained solid sludge (after digestion) was determined and compared with the initial masses for each tube. A more detailed description of the mass balance methodology can be found in the supplementary information (Table A1.2; Table A1.3). The release of TP and TFe was determined as the ratio of the measured concentrations at each time interval to the initial concentrations.

3.3.3 Surface bound P determination experiments

It was deemed important to quantify the amount of exchangeable P in the Fe-P sludge using an independent measure to better understand the mechanisms of P release with alkaline treatment and the role of sludge age in this regard. Hence, the exchangeable surface P was assessed by measuring the P released into solution after arsenate (As(V)) treatment as phosphate (PO_4^{3-}) and arsenate (AsO_4^{3-}) have similar chemistry and structural properties (O`Reilly et al., 2001). Arsenate

has been demonstrated to compete with phosphate for active sites on several minerals including calcite (Sø et al., 2012) and iron oxides like goethite (Puccia et al., 2009), and ferrihydrite (Neupane et al., 2014).

Arsenic (V) extraction tests were performed in batches at pH 6 to quantify the surface bound P that is exchangeable with As in the Fe-P solid sludges with ages of 0, 5, 9, and 11 days. In 50 ml centrifuge tubes, 20 ml of 0.01M arsenate solution (prepared by dissolving 3.2 g of $Na_2HAsO_4.7H_2O$ in 1 liter of ultrapure water at 22±1 °C) were added to prewashed sludge solids (10±0.5 mg dry weight). The pH was adjusted to 6 with diluted H_2SO_4 solution and tubes were placed in a shaker. The concentration of arsenate solution was chosen to attain a molar ratio of total P to total As(V) of 1:7. The pH value of 6 was selected to eliminate the effect of hydroxyl molecules on P release and to mimic the pH at which the Fe-P sludge was generated.

After 24 hours of extraction, the solution was filtered through 0.45 µm cellulose nitrate membrane syringe filters (Whatman, pore size 0.45 µm, diameter 47mm) and the concentrations of P, Fe, and As in solution were determined by ICP-OES (see section 3.3.5).

3.3.4 HFOs preparation and surface area determination

Samples of HFO were prepared following the forced hydrolysis method (Zelmanov and Semiat, 2008) by dissolving 1.3 g of $FeCl_3.6H_2O$ into 1 liter synthetic wastewater at 22±1 °C and ambient pH 2. A 1.0 M NaOH solution was gradually added to adjust the pH to the range of 6.0-6.5 under vigorous magnetic stirring. The generated HFO suspension was then subjected to the same sampling and aging procedures employed for the Fe-P sludges.

The surface area (SA) of the HFOs was determined using a fluorescein dye ($C_{20}H_{10}Na_2O_5$) adsorption method (Vafakish and Wilson, 2019) to avoid possible phase transformation of the HFOs particles that can occur in methods that involve drying of the solids. The adsorption tests

were performed at pH 6.5 which is in the pH range where HFOs have a positive surface charge (Kosmulski, 2020). The pK_a values for fluoresceine cationic, neutral, and anionic forms are 2.27, 4.32, and 6.50 respectively (Pirillo et al., 2008) and hence the fluorescein existed in its anionic form in the tests to facilitate adsorption.

Adsorption isotherms for fluorescein on fresh and aged HFOs were determined from a series of batch tests. A 4 mM fluorescein stock solution was prepared by dissolving 1.5 g fluorescein in 1 liter ultrapure water and diluted accordingly. A volume of 10 mL of fluorescein solution (concentrations ranging from 0.4-4 mM) were added to a fixed mass of HFOs (10±0.5 mg dry weight) in a 50 mL centrifuge tube and placed on a shaker to equilibrate for two hours at 22±1°C. The pH was adjusted to 6.5 using dilute solutions of NaOH or HCl as necessary. After two hours, the suspensions were filtered through 0.45 µm cellulose nitrate membrane filters and fluorescein filtrates were diluted. Their concentrations were determined spectrophotometrically (see section 2.5). The amount of adsorbed fluorescein Q_{eq} (mM) in each sample was calculated using equation (3-1) where C_o (mM) is fluorescein known initial concentration, C_{eq} (mM) is the measured fluorescein equilibrium concentration, V is volume (L) of fluorescein solution, and m is HFOs mass (g).

$$Q_{eq} = \frac{(C_o - C_{eq}).V}{m} \quad (3\text{-}1)$$

The maximum adsorption capacity Q_m (mol/g) of fluorescein onto the HFOs was determined by fitting a Langmuir adsorption model using nonlinear regression analysis to the measured data (Hang and Brindley, 1970) (Fig. A1.1). Since fluorescein molecules aggregate at concentrations larger than 5 µM, a coverage factor (F_c) of 2 (Inel and Tumsek, 2000) was employed and the surface area was calculated using equation (3-2).

$$SA = \frac{Q_m \times N \times A}{F_c} \quad (3\text{-}2)$$

Where N is Avogadro's number 6.022×10^{23} (molecule/mol), A is cross sectional surface area for one fluorescein molecule 7.31×10^{-19} (m^2/molecule) in a co-planner orientation (Vafakish and Wilson, 2019).

3.3.5 Chemical analysis

The solution pH was measured using pH analyzer (Orion Star™ A211, Thermo Scientific™, USA). Concentrations of total P and Fe were measured using Inductively Coupled Plasma Optical Emission Spectroscopy (ICP-OES) (PerkinElmer Optima 7300 DV, Waltham, MA, USA). Intensities were measured in axial mode at a wavelength of 213.6 nm for P and 238.2 nm for Fe with the viewing height set to 15 mm above the induction coil; the flow rate of the sample pump was set to 2 mL/min, argon was used as the plasma and auxiliary gas, set to 15 and 0.5 L/min, respectively. The concentration of fluorescein was determined at pH 6.5 by measuring the absorbance at a wavelength of 478 nm using a Duetta fluorescence and absorbance spectrometer (HORIBA Instruments Inc.).

3.3.6 Modeling approach

Equilibrium modeling was employed to obtain insights into the nature of the interactions between phosphorus and the other soluble/solid species in the various tests (Solon et al., 2019). In this study, the PHREEQC geochemical modeling software version 3.0 (US Geological Survey, 2013) was utilized. It has the capability of simulating dissolution/precipitation equilibria and surface complexation reactions and also allows modifications of the thermodynamic databases (Parkhurst and Appelo, 2013).

The PHREEQC default data base (PHREEQC.DAT) was selected for Fe-P solids simulations with some modification to the data file. For example, equilibrium reaction constant (K_{eq}) values for PO_4^{-3} protonation reactions and solubility products (K_{sp}) values for solids involved

in the system such as HFO and strengite ($FePO_{4(s)}$), were determined from NIST (2001). These values were corrected for 0.02 M ionic strength using the extended Debye-Huckel equation (Morel and Hering, 1993) as the ionic strength of the wastewater was approximately 0.02 M. Moreover, some solid phases such as struvite are not included in PHREEQC data file. Table S4 shows the list of soluble species and solid phases, along with their logK values that were modified and/or added to PHREEQC database file. For simulations, the input data was based on experimental conditions including pH values, initial total concentrations for each element (Fe, P, Ca, Mg, Na, Cl, and S), and log K values for soluble/solid species. An example of a PHREEQC simulation input file is provided in Table A1.5.

3.4 Results and discussion

3.4.1 The effect of pH on P and Fe release

Batch tests were conducted under different pH values with freshly prepared Fe-P sludge to quantify the extent to which pH impacted P release. Figure 3.1 presents the release of P and Fe as a function of time when initial pH values of 2, 10, and 11 were employed. It should be noted that the pH values were not controlled through the tests, and pH was measured at each time point until the equilibrium was achieved. The indicated values of 2, 10 and 11 represent the target values. As shown in Fig.3.1a P release was highest at pH 11 (92±3%) and this was followed by pH 10 (66±4%) while the lowest release was observed at pH 2 (23±1%). The final measured pH values at the end of 48 hours were 11, 9.2 and 2 respectively. The decrease in pH values with time for tests that had an initial pH of 10 possibly indicates the occurrence of dissolution and desorption processes in the system at intermediate pH values.

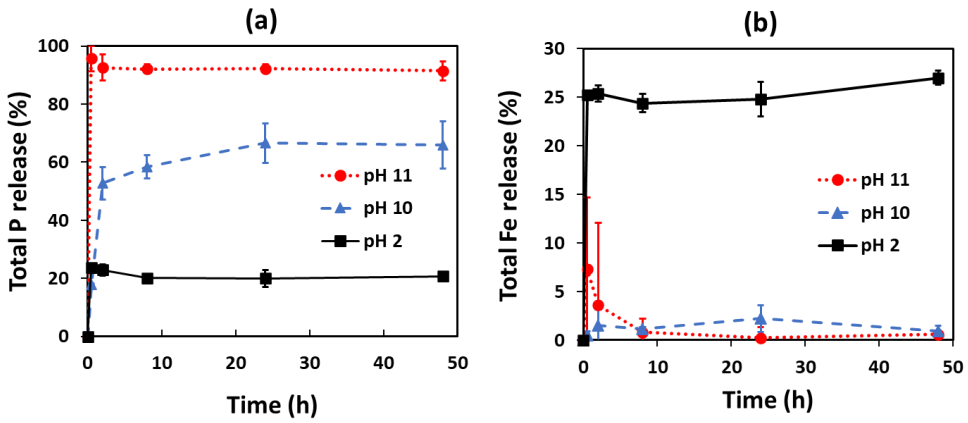

Figure 3.1 Percent release of (a) total phosphorus and (b) total iron from fresh Fe-P sludge as a function of time at initial pH values of 2, 10, and 11. Final equilibrated pH values of 2.0, 9.2 and 11.0. Error bars correspond to 95% confidence level.

The phosphorus release rates were fast in the initial 2 hours for all pH values (Fig. 3.1). However, for pH 11 and pH 2 the pH was stable, and the equilibrium (steady-state) was reached after the initial 2 hours, with P release remaining constant during the reaction time for both pH values. For pH 10, the initial pH decreased to 9.2 and phosphorus release was stable after 24 hours and onward. These results indicate a fast transformation of Fe-P sludge structure to other forms under pH 11 and 2. However, at pH 10 P desorption is likely through slower diffusion as hydroxide displace phosphate at oxygen sites on the HFO surface, and this results in slow P release until a plateau is reached, indicating equilibrium (Lu et al., 2016).

In general, P release from sludge can occur via either solubilization of P containing solids or by desorption of HFO surface complexed phosphate. The high release of P at alkaline pH values is likely explained by the competition between the hydroxyl ions and phosphate ions bound to Fe atom on the surface of the hydrous ferric oxide (HFO), via ligand exchange mechanism (Nriagu, 1984; Cornell and Schwertmann, 2003). For example, at pH 11 the concentration of OH^- is high enough to substantially replace P in the Fe-P sludge resulting in formation of ferric hydroxide

$Fe(OH)_{3(s)}$ and liberating P leading to a higher percent P release (Sano et.al., 2012) compared with pH 10 where the concentration of OH^- is ten fold less in magnitude. Furthermore, the positive surface charge of HFO is decreased as pH increases leading to electrostatic repulsion between phosphate anions and the evolving negative surface charge resulting in increase of P desorption (Yoon et al., 2014). Similar trends of increasing P release from iron-phosphate co-precipitants as solution pH increased were reported by others (Sano et al., 2012; Lu et al., 2016).

For experiments conducted at pH 2 solids transformation was observed as the color of the solids changed from orange to light yellow. The average content of total P and Fe present in the final solids were (81±3%) and (72±4%) respectively. Smith et al. (2008) reported possible strengite formation at acidic solutions below pH 5. Considering the high concentrations of total Fe (125±3 mg/L) and P (44±2 mg/L) compared to other species in the system, strengite was expected to comprise the highest fraction of the solids. PHREEQC simulations revealed the saturation index (SI) of strengite had a value of 1.52 indicating that strengite formation was likely responsible for the low percent release of P at pH 2.

Solubilization of HFO solids is not a likely mechanism for P release because P was released in substantially greater proportion than Fe. Fig. 3.1b shows the percent release of Fe versus time at acidic and basic pH values. In contrast to P release, the release of Fe was low; $\leq$ 5% at pH 11 and 10 and 25±3% at pH 2. The key factor for Fe release is the solubility of HFO which decreases as pH elevates and increases again at very high pH values (Cornell and Schwertmann, 2003). The low release of Fe is due to the different solid forms in which it can be present over the range of pH values. For pH 10 and 11 experiments, 98% of total Fe contained in the system was included the solids after 48 hours. This indicates that dissolution of HFO solids is very low and P in Fe-P sludge is replaced by OH^-. At pH 2 HFO dissolves to release Fe and P to solution where a reaction to

form strengite is possible (Smith et al., 2008). In summary, Fe remains in the solid phase as $Fe(OH)_{3(s)}$ at alkaline pH and as strengite at low pH.

To obtain a better understanding of how pH impacts P and Fe release from Fe-P sludge their release was monitored under controlled pH values. As illustrated in Fig. 3.2a at pH 6, 7, and 8 the P release was low and did not exceed 10% while the solubilization of P was most sensitive between pH 8 and 10 where the P release at pH 9 (40±3%) was half that at pH 10. In contrast, the highest release was observed at pH values between 10 (90±2%) and 12 (99±5%). The low release below pH 8 is attributed to the equilibrium between soluble P and P bound to HFO. However, the results indicate an increase of P release as solution pH increased suggesting that the increased concentration of hydroxyl ions displaces phosphate ions (Wilfert et al., 2015).

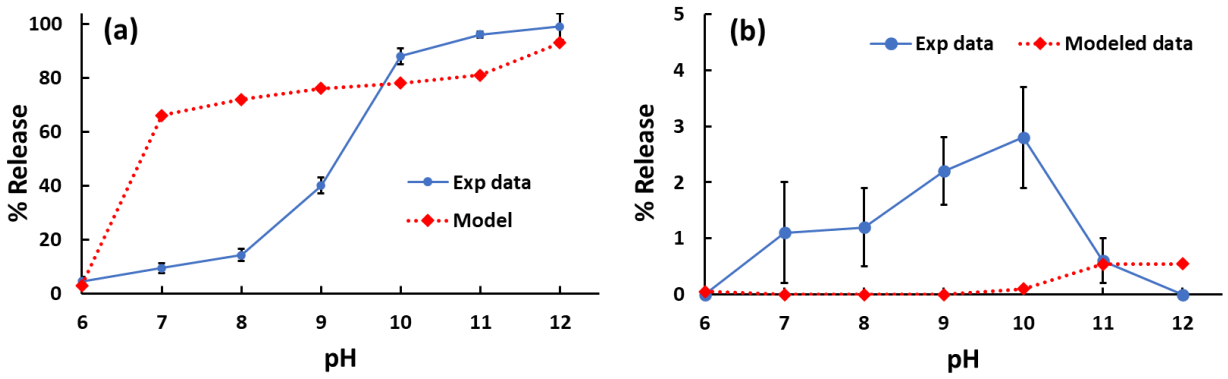

Figure 3.2 Release of (a) phosphorus and (b) iron from fresh Fe-P sludge after titration with 1.0 M NaOH for 8 hours at pH 6, 7, 8, 9, 10, 11 and 12 with predicted % release based on PHREEQC simulations.

PHREEQC simulations were employed to assess how solution chemical equilibrium speciation and the surface complexation reactions involved in the system affect P and Fe release. Results for modeled Fe and P release are shown in Fig. 3.2. The modeled values for Fe release were very low and consistent with the experimental values (Fig. 3.2b). For P release, the

experimental values at pH 6, 10, 11 and 12 were in agreement with the model while for other pH values the model over predicts the P release. The higher model predicted release at pH values in the range from 7 to 9 was likely due to the absence of relationships to describe differential partitioning of phosphorus between the surface and core of the particles in PHREEQC. Hauduc et al. (2015) reported a conceptual model for Fe/HFO dynamics where phosphorus can exist on the surface of particles (exchangeable phosphorus) and can be occluded inside the particles during the initial co-precipitation step, where phosphorus is trapped inside the HFO particle as it grows. In PHREEQC the total element concentrations are specified and the phosphorus binding sites are limited only to the final surfaces that form, and in this model such sites are not sufficient to remove phosphorus and much of the phosphate is predicted to be in solution. In reality, it seems that P trapped inside particles is not available for release at intermediate pH values. However, at higher pH values the hydroxide concentrations are high enough to drive phosphate release to solution.

3.4.2 Effect of Fe/P molar ratio on P and Fe release

In CPR plants the Fe/P molar ratio in generated Fe-P solids could vary due to the excess Fe dosage required to achieve the desired residual P concentration. Full-scale plant and laboratory data reported by Szabó et al. (2008) illustrated the reduction of residual P by increasing the molar ratio of Fe added to P removed. To understand the impact of Fe/P molar ratio on P release from Fe-P solids, batch tests were conducted at pH values 9 and 10 on freshly prepared Fe-P sludge that had an Fe/P molar ratio of 2.4 for comparison with the previously described experiments that had a Fe/P molar ratio around 1.5. However, the data presented in section 3.4.1 (Fig. 3.2a) revealed only a modest increase in P release when increasing pH from 10 to 11. Hence, it was concluded that the additional chemical requirements needed to achieve pH 11 would not justify the modest increment in P release. Therefore, pH 11 was not tested in the experiments that focused on the

impact of Fe/P ratio. As shown in Fig. 3.3a, for a Fe/P molar ratio of 1.5 the P release at basic pH values of 9 and 10 was higher than that from the solids created with molar ratio of 2.4. P release is decreased as Fe/P molar ratio increased in Fe-P solids. For higher iron dosages, the excess iron is precipitated as HFO a long with Fe-P solids (Ping et al., 2022). Therefore, it appears that a greater fraction of P was occluded in the core of the HFO particles (assuming particles are the same size for both dosages) and buried in excess HFO; thus, at higher Fe/P molar ratios less phosphate was available on the surface for exchange with the solution as the pH increased. From a practical perspective, adding an excess of Fe would be beneficial in increasing the removal efficiency of P from wastewater, but this would reduce the potential for P release and recovery from the resultant sludge.

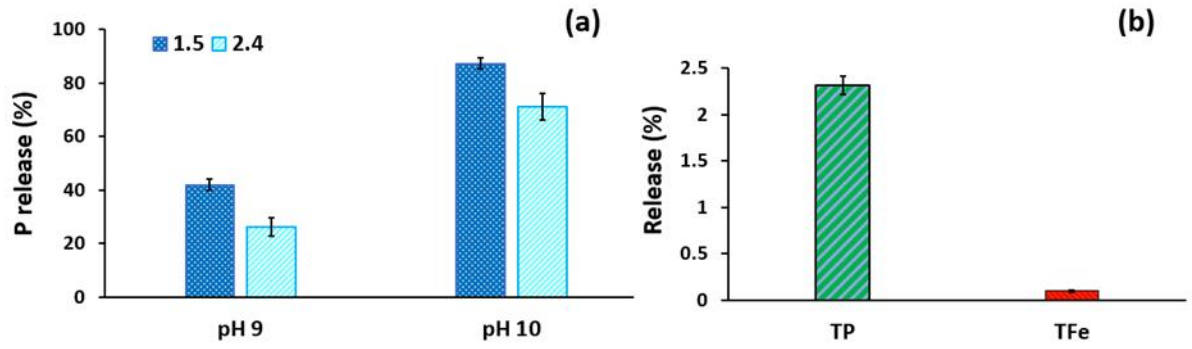

Figure 3.3 (a) Effects of Fe/P molar ratio on P release from fresh Fe-P sludge (b) effects of 0.1 M NaCl with Cl/P molar ratio of 70 and pH of 7 on P release from fresh Fe-P sludge.

3.4.3 Effect of NaCl on P and Fe release

Different inorganic anions have been reported to adsorb and compete for sites on a positively charged HFO surface (Dzombak and Morel, 1990; Afridi et al., 2019). Chloride ion was selected in this study as it is a common ion that is readily available, cost effective, and unlikely to be influenced by other reactions such as precipitation with other cations that were present in the

synthetic wastewater matrix. The effect of chloride (Cl^-) on P and Fe release from freshly prepared Fe-P solids was investigated under neutral pH and with a Cl/P molar ratio of 70. As shown in Fig. 3.3b very low release of $P < 2.5\%$ and almost no release for Fe were observed. Similar to phosphate, chloride can adsorb on metal-(hydr)oxide surface and form complexes via ligand exchange mechanism by exchanging with H_2O or/and OH^- molecules depending on solution pH (Acelas and Flórez, 2018). However, the negligible P release by competition with the Cl^- anion, even at a high chloride molar dosage, was attributed to the relatively weak chloride binding at the surface adsorption sites on HFO (Afridi et al., 2019). Therefore, the effect of Cl^- on P release is considered to be negligible and reflects that chloride complexes are weaker than phosphate complexes.

3.4.4 Influence of solids age on P and Fe release after pH adjustment

The influence of sludge age on pH induced P and Fe release, in time frames that reflect the residence times of Fe-P sludge in CPR plants, was assessed under alkaline conditions where higher P release was observed for fresh Fe-P sludge (section 3.4.1). Aging of HFOs has been reported to facilitates a transition from an amorphous to a more crystalline structure and can influence surface area and adsorptive capacity (Smith et al., 2008; Hauduc et al., 2015; Li et al., 2020). It was anticipated that these structural changes could affect P release. Batch tests were carried out to measure the release of P from aged (1, 5, 9, and 11 days) Fe-P solids (Fe/P molar ratio 1.5) after 8 hours reaction under controlled extraction pH values of 9 and 10 (sludge was aged at their ambient pH prior to treatment to release phosphorus). Table A1.6 summarizes the results for P release from the Fe-P sludge for different residence times at pH 9 and 10. Fig. 3.4 illustrates the same P release data (as Table A1.7) normalized to day 1 measured values. Normalization was performed to compare trends with other measurements that were conducted on the same samples (surface area,

As extractable P, see below). There was substantial P release at pH 10 for solids ages of 1 day and 5 days (0.96±0.02) and lower P release for solids ages of 9 (0.59±0.04) and 11 (0.63±0.06) days. The P release for solids ages of 1 and 5 days and for 9 and 11 days were not significantly different ($p < 0.001$ and $p = 0.04$ respectively). The trend in P release with solids age was also observed at pH 9 however the magnitude of the P release values was lower than pH 10. The results consistently demonstrated that solids aging reduces alkaline pH-induced P release from Fe-P sludge.

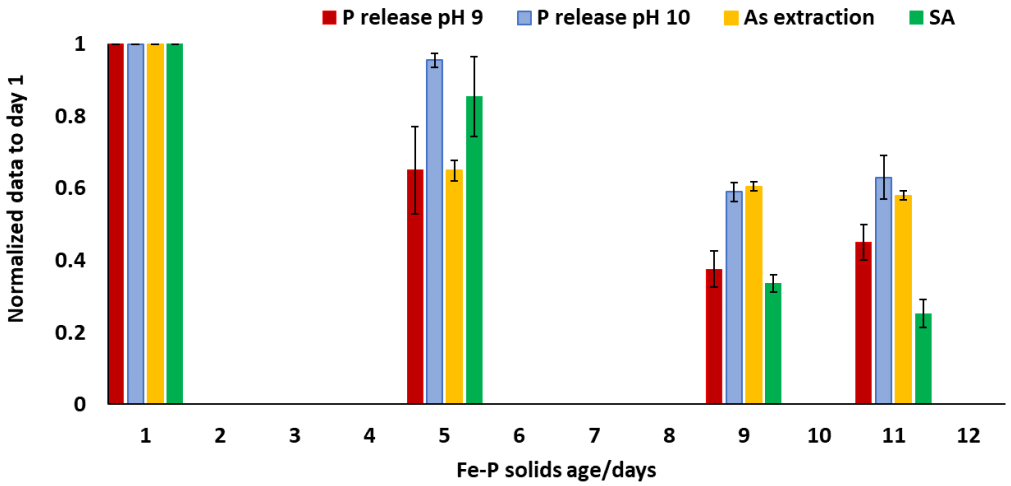

Figure 3.4 Normalized data for P release under pH 9, pH 10, and arsenic extraction, combined with surface area of HFO under different aging times.

Fig. 3.5 shows for the impact of sludge age on Fe release. For all sludge ages, Fe release was low (<5%) at pH 9 and 10. This indicates that solids age has no effect on Fe release from Fe-P sludge, and that P release is not due to solubilization of Fe-P solids but rather selective partitioning of phosphorus alone from the solid sludge to the aqueous phase.

The reduction in P release at alkaline pH for aged sludge, could be explained as the initial fresh HFO has a less dense amorphous structure with high surface area. This open structure allows

phosphate ions to initially be removed from solution by diffusion into the active sites where iron and phosphorus can share an oxygen atom in an Fe-O-P binding arrangement (Dzombak and Morel, 1990; Smith et al., 2008). Similarly at higher pH, the diffusion of hydroxyl ions from bulk solution can occur into the same active sites and exchange with phosphate ions and release P into solution, as was observed for fresh Fe-P sludge at pH 9 and 10. As the solids age the HFO structure becomes more compact and transforms from amorphous to more crystalline (e.g., goethite, and hematite, or even what Hudauc et al. (2015) call "old" HFO). This results in a reduction in surface area and phosphorus would be occluded (trapped) inside the particle. As the solids age, the surface bound P may be incorporated into the bulk structure of HFO and removed from the exchangeable surface. (Smith et al., 2008, Bligh et al., 2017). With reference to Hauduc's model it is hypothesized that during the slow process of HFO crystallization, the external or exchangeable P (P adsorbed to HFO surface) is being internalized into HFO bulk structure which gets more organized and compact with aging, causing reduction in the amount of surface exchangeable P. However, to test this hypothesis exchangeable P should be quantified by independent measures. Here we look at arsenate extractable surface-bound phosphate, and also surface area as the HFO particles age. XRD analysis to characterize structural transformations of the aged Fe-P sludge samples was attempted but was unsuccessful as all samples were amorphous and did not show crystalline phases, although this was not unexpected as HFO does not have sufficient long-range order to be detectable by XRD analysis.

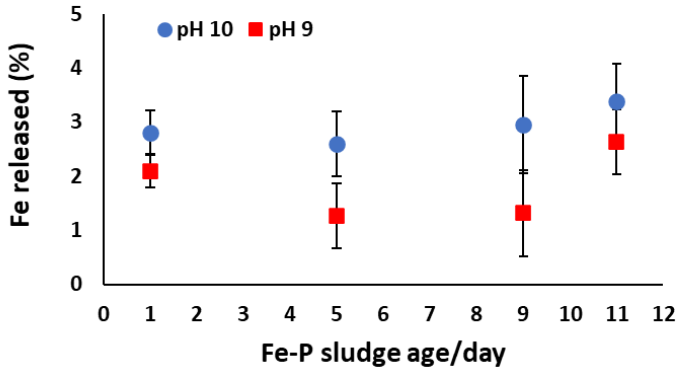

Figure 3.5 Fe release (%) from Fe-P sludge at different aging times and controlled pH values of 9 and 10.

3.4.4.1 Competitive adsorption experiments

To quantify the amount of exchangeable P in Fe-P sludges that were aged for 1, 5, 9, and 11 days, batch desorption tests were conducted where an arsenate solution was added to wet Fe-P solids. To facilitate comparison with the previously described trends in phosphate release, the As extraction data was normalized by comparing results for different sludge ages to those of the sludge with an age of 1 day (Fig. 3.4). The trends in exchangeable P were consistent with the trends in alkaline-induced P release. Surface-bound P was highest with a sludge age of 1 day and decreased to essentially a constant value for sludge ages of 5 days and older as the values for days 5, 9, and 11 could not be differentiated due to overlapping 95% CIs.

At pH 6 AsO_4^{3-} (and protonated forms) is the anion most capable to exchange with PO_4^{3-} (and protonated forms) on HFO surface as the competing effect of OH^- is minimal at this pH. Although it was expected based on PHREEQC modeling that 81% of P incorporated into HFO would be exchanged by As(V) for fresh Fe-P solids, the actual amount observed was 43% (Table

A1.7). This overprediction could be attributed to the fact that the PHREEQC considers all P as adsorbed onto the HFO surface and ignores the hypothesized internalized fraction which was not accessible to As(V).

While the normalized data in Fig. 3.4 showed a similar trend in exchangeable P by As(V) extraction and alkaline-induced P release with aging of solids, quantitatively 30% more P was released at pH 10 than through As(V) addition for the 5 days aged solids. It is clear that at alkaline conditions the competing effect of high concentrations of OH^- with phosphate for adsorption on HFO surface is higher and more thermodynamically favoured than AsO_4^{3-} exchange at pH 6. Thus, the As-extractable P represents a lower bound on the available surface phosphate, and more aggressive reagents at higher concentrations (OH^-) are able to release more P from the surface, and layers adjacent to the surface. Moreover, solution pH could impact the electrostatic interactions between HFO flocculants and thus affect the amount of exchangeable P. For example, at pH 6, under which the As extractions were performed, the HFO flocs tend to be more adjoining in the absence of the electrostatic repulsive forces that arise due to developing of negative charge on their surfaces at pH 10. The typical zero point of charge for HFO is near 7 (Smith and Ferris, 2003). The association of particles at the lower pH, at which As extraction was conducted, minimizes the available surface area of HFO flocs and reduce the availability of the surface bound P that would exchange with As(V) leading to less exchangeable P release compared to pH 10.

Generally speaking, the decrease in the amount of surface exchangeable P for sludge aged greater than 5 days with either As(V) or OH^- extraction implies P internalization during sludge aging and supports qualitatively the above mentioned hypothesis that phosphorus can partition to outer (available) and inner (unavailable) binding sites, and migrate from the outer-most sites to interior sites. Also, this decrease indicates transformations in HFO structure with age, towards

more dense particles, with a corresponding reduction in surface area and reactivity. The subsequently described dye adsorption experiments were conducted to evaluate the hypothesis that HFO particles decrease in surface area as they age.

3.4.4.2 Fluorescein adsorption tests

Changes in HFO surface area during aging of Fe-P sludge was examined to obtain further insight into structural transformations in HFO particles. Although BET analysis is the acknowledged technique for determining surface area of iron oxides, it was not implemented in this study. It requires drying of HFO particles which could alter their nature and structural properties (Wei et al., 2017). To avoid the drying process, a liquid phase dye adsorption method was adopted (Hang and Brindley, 1970). In the literature, cationic methylene blue has been regularly reported for surface area determination of soil, natural solids, and minerals including clays, activated carbon, silica, and iron oxides (Cenens and Schoonheydt, 1988; Smith et al., 2008; Hegyesi et al., 2017). However, to be more consistent and to mimic the same conditions of electrostatic interactions between HFO and PO_4^{-3} (and protonated forms), an anionic fluorescein dye was used in this study.

Batch adsorption tests using different concentrations of fluorescein dye and specific mass (10±0.5 mg dry weight) of HFO were conducted at pH 6 on HFO samples that were aged to 0, 5, 9, and 11 days. The surface areas, normalized to the sludge samples with an age of 1 day, are illustrated in Fig. 3.4 (actual values are summarized at Table A1.8). For sludge ages less than 5 days no substantial change in HFO surface area was observed as the measured values had overlapping 95% CIs. However, an obvious decrease in the surface area was observed for the elevated sludge ages of 9 and 11 days. These results suggest a transformation in HFO structure leading to a reduction in surface area, and likely a decrease in surface active sites with age,

consistent with the As-exchangeable P data and the decreased P release at alkaline pH. This observation qualitatively supports the hypothesis of surface bound P internalization during aging and also explains the decrease in exchangeable P release from aged Fe-P sludge.

3.4.5 Kinetic modeling

Zero and first order kinetic models were evaluated with respect to their ability to describe the impact of sludge age on P release at pH 10, such empirical models could help in predicting and monitoring the behaviour of P release with aging time of the sludge. The diagnostic plot for zero order kinetics is the fraction of P released versus time (Fig. 3.6a) and for first order the natural logarithm of the total concentration of released P in solution is plotted versus aging time (Fig. 3.6b). The parameters for the two models are summarized in Table 3.1. It can be seen clearly from Fig. 3.6 that both models fit the kinetic data similarly. The values of the intercept and R^2 for the two models are similar and could not be differentiated due to overlapping of standard errors. The fit by a zero-order model implies that the rate of P release with time does not depend on the initial concentration of total P. The zero order model provides a reasonable description of P release from aged sludge and is simpler than a first order model. It should be noted that the dependence of P release rate on initial concentration of P was not assessed. The use of a first order model might be considered in the future if data describing a greater range of initial P concentrations were to become available.

Table 3.1 Zero and First order kinetic models parameters.

Model	Intercept	Slope	R^2
Zero order	1.00 ± 0.03	-0.042 ± 0.004	0.870 ± 0.068
First order	0.029 ± 0.047	-0.057 ± 0.006	0.843 ± 0.104

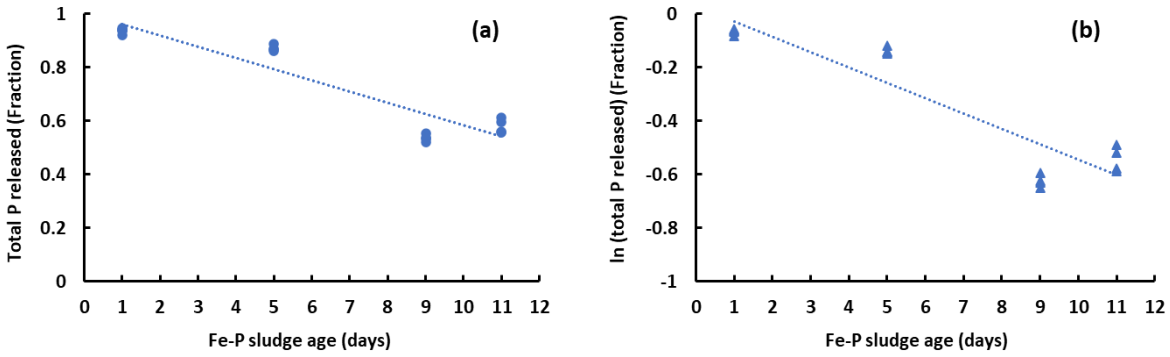

Figure 3.6 Fit of zero order model (a) and first order model (b) for P release kinetic data at pH 10 and initial P concentration of 1.420 mM at 22±1 °C.

3.5 Conclusions and practical implications

Alkaline treatment of Fe-P sludge was effective in releasing P particularly at pH value of 10 where the %P release was (90±2%). Fe:P molar ratio affects P release. As the molar ratio increased the P release decreased. Thus, high doses of Fe to achieve low residual P could result in increased difficulty in recovering phosphorus. Chloride was not effective as a competing ion to release P from Fe-P sludge. Sludge aging decreases the release of phosphorus from Fe-P sludge significantly for sludge ages greater than 5 days. Therefore, solids residence time of Fe-P sludge should be minimized for the purpose of P recovery. When considered collectively, the data on P release from different solids ages, estimated surface-bound P (by As(V) exchange), and HFO surface areas supports the hypothesis of exchangeable P internalization during aging because of structural transformation of HFO. The reduction in P release by aging of sludges was most simply described by a zero-order kinetic model. Overall, the findings in this study provides insights into the chemistry of P release in the absence of interferences from other wastewater components (organic matter, bacteria). Further work will be necessary to assess the role, if any, of these other wastewater components in modifying P release during recovery trials.

3.6 References

Acelas, N.Y., Elizabeth Flórez, E., López, D., **2015**. Phosphorus recovery through struvite precipitation from wastewater: effect of the competitive ions. Desalination and Water Treatment, 54(9): 2468-2479. doi:10.1080/19443994.2014.902337.

Afridi, M.N., Lee, W.-.H., Kim, L.-.O., **2019**. Effect of phosphate concentration, anions, heavy metals, and organic matter on phosphate adsorption from wastewater using anodized iron oxide nanoflakes. Environmental Research, 171, 428-436. doi:10.1016/j.envres.2019.01.055.

Bligh, M.W., David Waite, T.D., **2011**. Formation, reactivity, and aging of ferric oxide particles formed from Fe(II) and Fe(III) sources: Implications for iron bioavailability in the marine environment. Geochimica et Cosmochimica Acta 75 (24), 7741-7758.

Bligh, M. W., Maheshwari, P., Waite, T. D., **2017**. Formation, reactivity and aging of amorphous ferric oxides in the presence of model and membrane bioreactor derived organics. Water Research, 124, 341-352. doi:10.1016/j.watres.2017.07.076.

Cenens, J., and Schoonheydt, R.A., **1988**. Visible Spectroscopy of Methylene Blue on Hectorite, Laponite B, and Barasym in Aqueous Suspension. Clays Clay Miner. 36, 214–224. doi:10.1346/CCMN.1988.0360302.

Chakraborty, T., Balusani, D., Smith, D.S., Walton, S.J., Nakhla, G., Ray, M.B., **2020**. Reusability of recovered iron coagulant from primary municipal sludge and its impact on chemically enhanced primary treatment. Separation and Purification Technology 231:115894. doi:10.1016/j.seppur.2019.115894.

Chen, Y., Lin, H., Shen, N., Yan, W., Wang, J., Wang, G., **2019**. Phosphorus release and recovery from Fe-enhanced primary sedimentation sludge via alkaline fermentation. Bioresource technology, 278, 266–271. doi:10.1016/j.biortech.2019.01.09.

Conidi, D., Parker, W.J., **2015**. The Effect of Solids Residence Time on Phosphorus Adsorption to Hydrous Ferric Oxide Floc. Water Research 84: 323–32. doi:10.1016/j.watres.2015.07.046.

Cordell, D., Drangert, D.-.J.O., Stuart White. S., **2009**. The Story of Phosphorus: Global Food Security and Food for Thought. Global Environmental Change 19 (2): 292–305. doi:10.1016/j.gloenvcha.2008.10.009.

Cordell, D., White, S., **2014**. Life's Bottleneck: Sustaining the World's Phosphorus for a Food Secure Future. Annu Rev Environ Resour 39:161–188. doi:10.1146/annurev-environ-010213-113300.

Cornell, R. M., Schwertmann, U., **2003**. The Iron Oxides : Structure, Properties, Reactions, Occurrences, and Uses. 2nd ed. Weinheim : Wiley-VCH.

Dzombak, D.A., Morel, F.M.M., **1990**. Surface complexation modelling: hydrous ferric oxide. John Wiley and Sons, Inc., New York.

Gilbert, B., Ono, R.K., Ching, K.A., Kim, C.S., **2009**. The effects of nanoparticle aggregation processes on aggregate structure and metal uptake. Journal of Colloid and Interface Science, 339: 285-295.

Gray, H.E., Powell, T., Choi, S., Smith, D.S., Parker, W.J., **2020**. Organic phosphorus removal using an integrated advanced oxidation-ultrafiltration process. Water Research 182, 115968. doi:10.1016/j.watres.2020.115968.

Hang, P.T., Brindley, G.W., **1970**. Methylene Blue Absorption by Clay Minerals: Determination of Surface Areas and Cation Exchange Capacities (Clay-Organic Studies XVIII). Clays and Clay Minerals, 18, 203-212. doi:10.1346/CCMN.1970.0180404.

Hauduc, H., Takács, I., Smith, S., Szabo, A., Murthy, S., Daigger, G. T., Spérandio, M., **2015**. A dynamic physicochemical model for chemical phosphorus removal. Water research, 73, 157–170. doi:10.1016/j.watres.2014.12.053.

Hegyesi, N., Vad, R., Pukanszky, B., **2017**. Determination of the specific surface area of layered silicates by methylene blue adsorption: The role of structure, pH and layer charge. Applied Clay Science. 146. 50-55. Doi:10.1016/j.clay.2017.05.007.

Inel, O., Tumsek, F., The Measurement of Surface Areas of Some Silicates by Solution Adsorption. **2000**. Turkish Journal of Chemistry, 24, 9–19.

Jung, Y., Koh, H., Shin, W., Sung, N., **2005**. Wastewater treatment using combination of MBR equipped with non-woven fabric filter and oyster-zeolite column. Environmental Engineering Research, 10, 247-256. doi.org/10.4491/eer.2005.10.5.247.

Kok, D.D., van Lier, J.B., Uhlenbrook, S., Ortigara, A.R.C., Pande, S., Hubert Savenije. H., **2018**. Global Phosphorus Recovery for Agricultural Reuse. Hydrology and Earth System Sciences Discussions, 1–18. doi:10.5194/hess-2018-176.

Kosmulski, M., **2020**. The pH dependent surface charging and points of zero charge. VIII. Update., Advances in colloid and interface science, 275, 102064. doi:10.1016/j.cis.2019.102064.

Li, R., Teng, W., Li, Y., Wang, W., Cui, R., Yang. T., **2017**. Potential Recovery of Phosphorus during the Fluidized Bed Incineration of Sewage Sludge. Journal of Cleaner Production 140: 964–70. doi:10.1016/j.jclepro.2016.06.177.

Li, R.-.H., Wang, W.J., Li, B., Zhang, J.-.Y., Liu, J., Zhang, G.-.J., Guo, X.-.C., Zhang, X.-.H., Li, X.-.Y., **2019**. Acidogenic phosphorus recovery from the wastewater sludge of the membrane bioreactor systems with different iron-dosing modes. Bioresource Technology 280:360-370. doi:10.1016/j.biortech.2019.02.060.

Li, R.-.H., Cui, J.-.L., Hu, J.-.H., Wang, W.-.J., Li, B., Li, X.-.D., Li, X.-.Y., **2020**. Transformation of Fe–P Complexes in Bioreactors and P Recovery from Sludge: Investigation by XANES Spectroscopy. Environmental Science and Technology 54 (7), 4641-4650. doi: 10.1021/acs.est.9b07138.

Liang, S., Yang, L., Chen, H., Yu, W., Tao, S., Yuan, S., Xiao, K., Hu, J., Hou, H., Liu, B., Yang, J., **2021**. Phosphorus recovery from incinerated sewage sludge ash (ISSA) and reutilization of residues for sludge pretreated by different conditioners. Resources, Conservation and Recycling (169) 105524. doi:10.1016/j.resconrec.2021.105524.

Loganathan, P., Vigneswaran, S., Kandasamy, J., Bolan, N. S., **2014**. "Removal and Recovery of Phosphate From Water Using Sorption." Critical Reviews in Environmental Science and Technology 44 (8): 847–907. doi:10.1080/10643389.2012.741311.

Lu, J., Yang, J., Xu, K., Hao, J., Li. Y.Y., **2016**. Phosphorus Release from Coprecipitants Formed during Orthophosphate Removal with Fe(III) Salt Coagulation: Effects of PH, Eh, Temperature and Aging Time. Journal of Environmental Chemical Engineering 4 (3): 3322–29. doi:10.1016/j.jece.2016.07.005.

Metcalf and Eddy Inc., Tchobanoglous G., **2014**. Wastewater engineering : treatment and reuse, 5th Edition. McGraw Hill, New York.

Morel, F. M. M., Hering, J. G., **1993**. Principles and Applications of Aquatic Chemistry. John Wiley and Sons: New York. ISBN: 978-0-471-54896-6.

National Institute of Standards and Technology, **2001**. NIST Standard Reference Database 46. National Institute of Standards and Technology: Gaithersburg, Maryland.

Neupane, G., Donahoe, R. J., Arai, Y., **2014**. Kinetics of competitive adsorption/desorption of arsenate and phosphate at the ferrihydrite-water interface. Chemical Geology, 368, 31-38. doi:10.1016/j.chemgeo.2013.12.020.

Nriagu, J.O., **1984**. Phosphate Minerals: Their Properties and General Modes of Occurrence. In: Nriagu, J.O., Moore, P.B. (eds) Phosphate Minerals. Springer, Berlin, Heidelberg. doi.org/10.1007/978-3-642-61736-2_1.

O'Reilly, S.E., Strawn, D.G., Sparks, D.L., **2001**. Residence time effects on arsenate adsorption/ desorption mechanisms on goethite. Soil Science Society of America Journal, 65, 67–77.

Paripurnanda, L., Vigneswaran, S., Kandasamy, J., Bolan, N.S., **2014**. Removal and Recovery of Phosphate From Water Using Sorption. Critical Reviews in Environmental Science and Technology 44 (8) 847–907. doi:10.1080/10643389.2012.741311.

Parkhurst, D.L., Appelo, C.A.J., **2013**. Description of input and examples for PHREEQC version 3—A computer program for speciation, batch-reaction, one-dimensional transport, and inverse geochemical calculations: U.S. Geological Survey Techniques and Methods, book 6. A43, 497 p., available only at https://pubs.usgs.gov/tm/06/a43/.

Peng, L., Dai, H., Wu, Y., Peng, Y., Lu. X., **2018a**. A Comprehensive Review of Phosphorus Recovery from Wastewater by Crystallization Processes. Chemosphere. 197:768–81. doi:10.1016/j.chemosphere.2018.01.098.

Peng, L., Dai, H., Wu, Y., Peng, Y., Lu. X., **2018b**. A Comprehensive Review of the Available Media and Approaches for Phosphorus Recovery from Wastewater. Water, Air, & Soil Pollution 229: 115. doi:10.1007/s11270-018-3706-4.

Ping, Q., Zhang, B., Zhang, Z., Lu, K., Li, Y., **2022**. Speciation analysis and formation mechanisism of iron-phosphrous compounds during chemical phosphorus removal process. Chemosphere 310. 136852–136852. doi.org/10.1016/j.chemosphere.2022.136852.

Pirillo, S., Cornaglia, L., Ferreira, M.L., Elsa H. Rueda, E.H., **2008**. Removal of Fluorescein using different iron oxides as adsorbents: Effect of Ph. Spectrochimica Acta Part A: Molecular and Biomolecular Spectroscopy, (71), 2, 636-643. doi:/10.1016/j.saa.2008.01.018.

Puccia, V., Luengo, C., Avena, M., **2009**. Phosphate desorption kinetics from goethite as induced by arsenate. Colloids and Surfaces A: Physicochemical and Engineering Aspects, 348, (1–3), 221-227. doi:10.1016/j.colsurfa.2009.07.026.

Quist-Jensen, C. A., Wybrandt, L., Løkkegaard, H., Antonsen, S. B., Jensen, H. C., Nielsen, A. H., Christensen, M. L., **2018**. Acidification and recovery of phosphorus from digested and non-digested sludge. Water research, 146, 307–317. doi:10.1016/j.watres.2018.09.035.

Sano, A., Kanomata, M., Inoue, H., Sugiura, N., Xu, K. Q., Inamori, Y., **2012**. Extraction of Raw Sewage Sludge Containing Iron Phosphate for Phosphorus Recovery. Chemosphere. 89 (10): 1243–47. doi:10.1016/j.chemosphere.2012.07.043.

Sendrowski, A., Boyer, T.H., **2013**. Phosphate Removal from Urine Using Hybrid Anion Exchange Resin. Desalination 322, Elsevier: 104–12. doi:10.1016/j.desal.2013.05.014.

Smith, D. S., Ferris, F. G., **2003**. Specific surface chemical interactions between hydrous ferric oxide and iron-reducing bacteria determined using pK(a) spectra. J Colloid Interface Science 266 (1): 60-67. doi:10.1016/s0021-9797(03)00667-2.

Smith, D. S., Takacs, I., Murthy, S., Daigger, G. T., Szabo, A., **2008**. Phosphate Complexation Model and Its Implications for Chemical Phosphorus Removal. Water Environ. Res. 80 (5): 428−438.

Sø, H. U., **2011**. Adsorption of arsenic and phosphate onto the surface of calcite as revealed by batch experiments and surface complexation modelling. Technical University of Denmark.

Solon, K., Volcke, E.I.P., Sperando, M., and van Loosdercht, M., **2019**. Resource Recovery and Wastewater Treatment Modelling. Environmental Science :Water Research Technology 5, 631-642.

Szabo, A., Takács, I., Murthy, S., Daigger, G.T., Licsko, I., Smith, S., **2008**. Significance of design and operational variables in chemical phosphorus removal. Water Environ. Res., 80, 407-416.

US Geological Survey, **2013**. PHREEQC (Version 3) – A computer program for speciation, batch-reaction, one-dimensional transport, and inverse geochemical calculations, (https://wwwbrr.cr.usgs.gov/projects/GWC_coupled/phreeqc/) (accessed on December 5th, 2021).

Vafakish, B.; Wilson, L.D., **2019**. Surface-Modified Chitosan: An Adsorption Study of a “Tweezer-Like” Biopolymer with Fluorescein. Surfaces, 2(3), 468–484. doi:10.3390/surfaces2030035.

Venkiteshwaran, K., McNamara, P.J., Mayer., B.K., **2018**. Meta-Analysis of Non-Reactive Phosphorus in Water, Wastewater, and Sludge, and Strategies to Convert It for Enhanced Phosphorus Removal and Recovery. Science of the Total Environment 644: 661–74. doi:10.1016/j.scitotenv.2018.06.369.

Wei, Z., Luo, S., Xiao, R., Khalfin, R., Semiat, R., **2017**. Characterization and quantification of chromate adsorption by layered porous iron oxyhydroxide: an experimental and theoretical study. Journal of Hazardous Materials 338, 472–481. doi:10.1016/j.jhazmat.2017.06.001.

Wilfert, P., Kumar, P.S., Korving, L., Witkamp, G.-J., van Loosdrecht, M.C.M., **2015**. The relevance of phosphorus and iron chemistry to the recovery of phosphorus from wastewater: a review. Environ. Sci. Technol. 49 (16), 9400–9414. doi: 10. 1021/acs.est.5b00150.

Wu, H., Ikeda-Ohno, A., Wang, Y., Waite, T. D., **2015**. Iron and phosphorus speciation in Fe-conditioned membrane bioreactor activated sludge. Water research, 76, 213–226. doi:10.1016/j.watres.2015.02.020.

Xu, D., Zhong, C., Yin, K., Peng, S., Zhu, T., Cheng, G., **2018**. Alkaline solubilization of excess mixed sludge and the recovery of released phosphorus as magnesium ammonium phosphate. Bioresource Technology , 249, 783-790.

Ye, Y., Ngo, H. H., Guo, W., Liu, Y., Li, J., Liu, Y., Zhang, X., Jia, H. **2017**. Insight into chemical phosphate recovery from municipal wastewater. Science of the total environment, 576, 159–171. doi:10.1016/j.scitotenv.2016.10.078.

Yoon, S. Y., Lee, C. G., Park, J. A., Kim, J. H., Kim, S. B., Lee, S. H., Choi, J. W., **2014**. Kinetic, equilibrium and thermodynamic studies for phosphate adsorption to magnetic iron oxide nanoparticles. Chemical Engineering Journal, 236, 341-347. doi:10.1016/j.cej.2013.09.053.

Zelmanov, G., Semiat, R., **2008**. Phenol oxidation kinetics in water solution using iron(3)-oxide-based nano-catalysts, Water Research, (42), 14:848-3856. doi:10.1016/j.watres.2008.05.009.

Zhang, B., Wang, L., Li, Y., **2019**. Fractionation and identification of iron-phosphorus compounds in sewage sludge. Chemosphere, 223, 250–256. doi:10.1016/j.chemosphere.2019.02.052

Chapter 4 - Phosphorus Release and Recovery by Reductive Dissolution of Chemically Precipitated Phosphorus from Simulated Wastewater

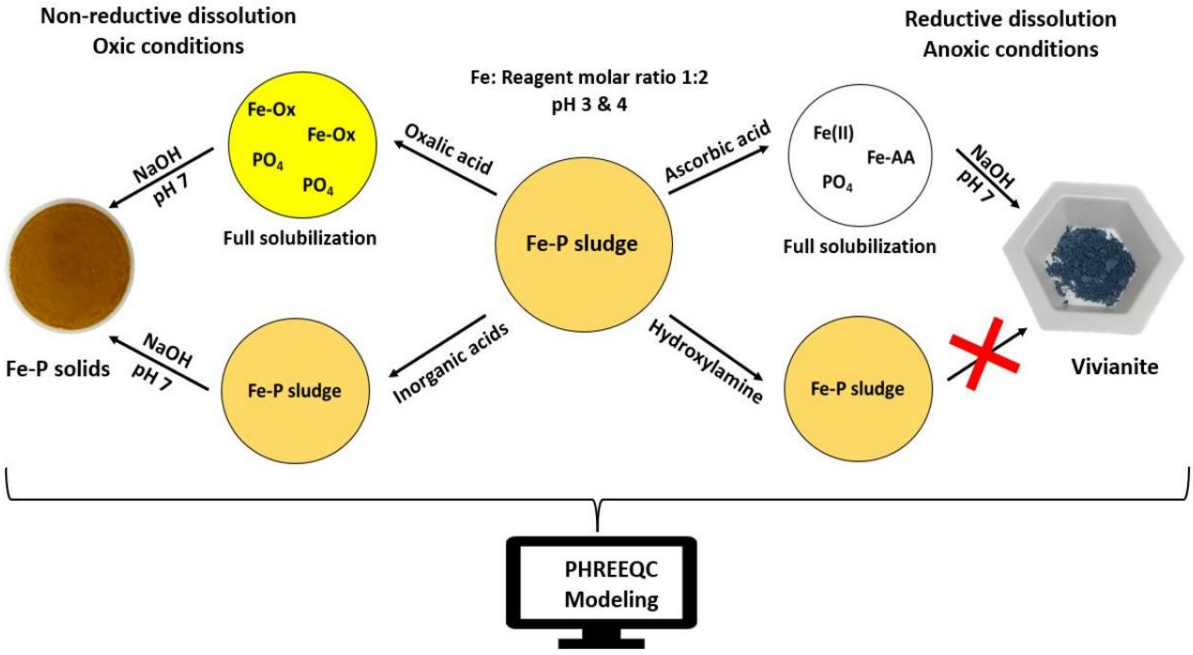

4.1 Abstract

Chemically mediated recovery of phosphorus (P) as vivianite from the sludges generated by chemical phosphorus removal (CPR) is a potential means of enhancing sustainability of wastewater treatment. This study marks an initial attempt to explore direct P release and recovery from lab synthetic Fe-P sludge via reductive dissolution using ascorbic acid (AA) under acidic conditions. The effects of AA/Fe molar ratio, age of Fe-P sludge and pH were examined to find the optimum conditions for Fe-P reductive solubilization and vivianite precipitation. The performance of the reductive, chelating, and acidic effects of AA toward Fe-P sludge were evaluated by comparison with hydroxylamine (reducing agent), oxalic acid (chelating agent), and inorganic acids (pH effect) including HNO_3, HCl, and H_2SO_4. Full solubilization of Fe-P sludge

and reduction of Fe^{3+} were observed at pH values 3 and 4 for two Fe/AA molar ratios of 1:2 and 1:4. Sludge age (up to 11 days) did not affect the reductive solubilization of Fe-P with AA addition. The reductive dissolution of Fe-P sludge with hydroxylamine was negligible, while both P (95±2%) and Fe^{3+} (90±1%) were solubilized through non-reductive dissolution by oxalic acid treatment at an Fe/oxalic acid molar ratio 1:2 and a pH 3. With sludge treatment with inorganic acids at pH 3, P and Fe release was very low (<10%) compared to AA and oxalic acid treatment. After full solubilization of Fe-P sludge by AA treatment at pH 3 it was possible to recover the phosphorus and iron as vivianite by simple pH adjustment to pH 7; P and Fe recoveries of 88±2% and 90±1% respectively were achieved in this manner. XRD analysis, Fe/P molar ratio measurements, and magnetic attraction confirmed vivianite formation. PHREEQC modeling showed a reasonable agreement with the measured release of P and Fe from Fe-P sludge and vivianite formation.

4.2 Introduction

Municipal wastewater treatment plants (WWTPs) have the potential to be a renewable resource of phosphorus (P) (Peng et al., 2018a). Approximately 1.3 Mt P/year is removed globally from wastewater streams using either chemical P removal (CPR) or enhanced biological P removal (EBPR) (Li et al., 2017). The increasing demand for P by the fertilizer industry has led to an interest in developing and integrating P recovery techniques with existing approaches that remove P from wastewater. This is consistent with the upgrading of WWTPs to function as wastewater resource recovery facilities (WRRFs) (Solon et al., 2019).

At present, struvite ($MgNH_4PO_4.6H_2O$) precipitation in EBPR plants is the most widely employed method for P recovery as fertilizer. It has been commercialised and operated at full scale

at a number of WRRFs around the world (WEF, 2011; Ye et al., 2017). In CPR plants, iron (Fe (III/II)) salts are often used to convert soluble P to solid phase iron-phosphate (Fe-P) complexes/minerals similar to those found in geochemical systems (i.e., strengite ($FePO_4.2H_2O$), Fe(III)-hydroxyphosphate ($Fe_xPO_4(OH)_{3x-3}$), and P_{ortho} adsorbed to Fe(III) hydrolysis products such as hydrous ferric oxide (HFO) surfaces) that can then be separated into concentrated sludge streams (Szabó et al., 2008; Wilfert et al., 2015). However, Fe-P solids generated in wastewater more variable and influenced by anthropogenic factors that make them differ than geochemical Fe-P solids in composition, formation processes, and environmental conditions. The high stability and low mobility of iron in wastewater Fe-P sludges makes recovery of the P challenging (Wilfert et al., 2015). The high stability and low mobility of iron in Fe-P sludges makes recovery of the P challenging (Wilfert et al., 2015). Several studies had addressed P release and recovery from Fe-P rich sludge under alkaline (Sano et al., 2012; Chen et al., 2019; Alnimer et al., 2023) and acidic (Monea et al., 2020a; Chakraborty et al., 2020; Alnimer et al., 2023) conditions, by using complexing agents (i.e., tannic, citric, tartaric, and ethylenediaminetetraacetic acid (EDTA)) (Zou et al., 2017; Ping et al., 2020; Chen et al., 2022), and by sulfide reduction (Wilfert et al., 2020). In addition, the release of phosphorus from ferric sludges via redox manipulation has received attention recently (Wilfert et al., 2015; Prot et al., 2019; Wu. et al., 2021; Xu et al., 2023).

In CPR plants, biological or chemical reductive dissolution of ferric phosphate sludge can take place under low oxidation reduction potentials (ORPs) and cause Fe bound P to be released (Wilfert et al., 2015; Wu et al., 2019). For instance, during anaerobic digestion (AD) Fe^{3+} in Fe-P sludges is reduced to Fe^{2+} biologically by dissimilatory iron-reducing bacteria (DIRB), and chemically by sulfides which are generated biologically by sulfate reducing bacteria or added as a chemical reducing agents (Wilfert et al., 2015, 2020). Typically, vivianite ($Fe_3(PO_4)_2.8H_2O$) has

been indicated to be the final form of Fe and P resulting from anerobic reductive dissolution of Fe-P sludges (Ghassemi and Recht, 1971; Fredrickson et al., 1998; Wilfert et al., 2016). Vivianite is a potential P recovery product that can be applied as slow-release fertilizer particularly for soils with Fe deficiency (Cabeza et al., 2011).

At present, AD is the most common bio-reduction technique used to release Fe and P by stimulating reductive dissolution of Fe-P solids through the activity of DIRB (Wu et al., 2019, 2020; Wu Y., et al., 2021). However, AD has drawbacks such as extended hydraulic residence times (i.e., up to 30 days) and varying digestive performance, which affect P release efficiency. Consequently, chemical reduction appears to be a possible more appealing alternative. However, earlier studies on P release from Fe-P rich sludge using chemical reducing agents were limited to sulfides (Kato et al., 2006; Likosova et al., 2013; Wilfert et al., 2020). Sulfides can mobilize P from Fe-P sludges by reducing Fe^{3+} and forming iron sulfide (FeS_n) precipitates (Nielsen et al., 2005; Kato et al., 2006). Despite sulfides having been shown to provide effective and fast release of P from Fe-P sludges, applying this approach has constraints, including reduced sludge dewaterability, difficult separation of FeS_n solids from sludge liquor, and low net release of P (Likosova et al., 2013; Wilfert et al., 2020).

A potential chemical reducing agent is ascorbic acid (AA), also known as vitamin C. It shows high reactivity toward reactive oxygen species and redox active transition metals like Co^{3+}, Cu^{2+}, and Fe^{3+} (Mahata et al., 2019; Njus et al., 2020). Effectively, AA can reduce species by donating two protons and two electrons, but normally donates only one electron at a time (Njus et al., 2020) and can form metal chelates in the pH range 2.0-12.5 (Shen et al., 2021). Of particular relevance in wastewater, especially for plants using iron salt additions, AA is recognised to be

effective in reducing Fe^{3+} in iron oxyhydroxides to the more soluble Fe(II) form (Conrad & Schade, 1968; Martinez and Uribe, 1982; Hsieh and Hsieh, 1997, 2000; Shen et al., 2021).

Although the interaction between AA and Fe^{3+} has been widely studied in terms of kinetics, complexation, and pH effects in different systems, studies on using AA for releasing P from Fe-P sludge are limited. Xu et al, (2023) recently reported a P recovery as vivianite upon release of 67.1% of total P contained in waste activated sludge using AA and pH adjustment. In principle it should be possible to utilize the iron reducing activity of AA at acidic pH as a novel route for P (and iron) recovery, potentially as vivianite, from Fe-P rich sludge.

This study investigates, for the first time, the potential of direct P release and recovery from lab synthetic Fe-P by reductive dissolution using AA. The use of lab synthetic sludge would provide better experimental control and safety, enhance the repeatability of the experiment, and avoid influence of interferences (organics and microorganisms) present in real wastewater sludge matrices. Ascorbic acid is an effective and environmentally friendly reducing agent that triggers a chemical reduction of Fe^{3+} to Fe^{2+}. Batch tests were conducted under reducing conditions to initialize reductive dissolution of Fe-P sludge by dosing AA under acidic pH. The effects of AA/Fe molar ratio, age of Fe-P sludge and pH were examined to find the optimum conditions for Fe-P solubilization. Then after solubilization of Fe-P sludge both soluble Fe and P were recovered as vivianite by increasing the pH of the solution to 7. AA can act as both reductant and chelating agent. Hence, to assess its reductive and chelating effects, tests using hydroxylamine (NH_3OH^+, reducing agent) and oxalic acid ($C_2H_2O_4$, chelating agent), as reference compounds, were performed at the same conditions for comparison. Moreover, to differentiate pH effects from redox and chelating effects, the use of inorganic acids including HNO_3, HCl, and H_2SO_4 was evaluated. Finally, modeling with the PHREEQC geochemical model was carried out to simulate Fe-P

solubilization and vivianite formation to help interpret and predict experimental data. The results of this study will help to set the basis for a potential new approach for P recovery as vivianite from raw and activated Fe-P sludge in CPR plants.

4.3 Methodology

4.3.1 Synthesis of Iron-phosphate (Fe-P) sludge

All chemicals used in experiments were reagent grade or better. All glassware were acid washed. All solutions were prepared using ultrapure water (Millipore, 18.2 MΩ.cm resistance) that was purged with nitrogen gas for 15 minutes, to eliminate dissolved oxygen. A synthetic wastewater was prepared according to the recipe by Jung et al. (2005) with adjustments to simulate only the inorganic composition ($MgSO_4$, $CaCl_2$, $NaHCO_3$ and Na_3PO_4 see Table A2.1) of secondary-treated wastewater. The iron-phosphate sludge used in this study was prepared with a molar Fe/P ratio of 1.5 according to the synthesis method previously reported (Alnimer et al. 2023). Briefly, a solution of $FeCl_3.6H_2O$ (2.4 mM Fe) was added to 1 L of synthetic wastewater containing Na_3PO_4 (1.6 mM P) under fast mixing using magnetic bar for 15 min until the pH of the solution reached 6.35±0.2. The resulting Fe-P solids were separated from solution by centrifuging at 4500 RCF for 30 minutes and washed with ultrapure water. For experiments investigating the effect of Fe-P sludge age on reductive dissolution the sludge solids were aged in 1 L glass beakers that were kept in dark at 22±1°C at ambient pH (6.35-7.35) for periods of 5 and 11 days.

4.3.2 Batch reactions

4.3.2.1 Dissolution of Fe-P sludge

The effects of ascorbic acid, hydroxylamine, oxalic acid and inorganic acid treatment on dissolution of Fe-P sludge were carried out in batch experiments that were performed under oxic

and anoxic conditions at 22±1 ℃. All tests were conducted in 150 mL 3 necked round bottom flasks covered with the rubber septum into which dewatered Fe-P sludge (wet Fe-P solids equivalent to approximately 44 mg when dried) had been mixed with 100 mL of the synthetic wastewater. Ascorbic acid and hydroxylamine tests were conducted inside an anaerobic chamber (built in-house) with argon flushing. All Fe-P sludge suspensions were deoxygenated by nitrogen purging for 15 minutes prior to chemical reagent addition.

The reductive dissolution of Fe-P sludge by ascorbic acid treatment was investigated under fixed pH values of 3 and 4 for two different Fe/AA molar ratios of 1:2 and 1:4. These conditions were selected to ensure that complete dissolution of Fe-P sludge would occur and AA will maintained in its protonated form (Fig S1) although the reaction stoichiometry shows 1 mole of ascorbic acid (H_2A) is required to reduce 2 moles of Fe^{3+} to produce Fe^{2+} and dehydroascorbic acid (D) as in Eq (1) (Hsieh and Hsieh, 1997; Tu et al, 2017):

$$H_2A + 2Fe^{3+} \rightarrow D + 2Fe^{2+} + 2H^{+} \quad (4\text{-}1)$$

Moreover, metal solubility is enhanced under acidic conditions (Cornell and Schwertmann, 2003). Therefore, the pH was fixed at 3 and 4 during AA treatment to maintain Fe^{2+} in the soluble phase and enhance P release.

Freshly prepared solutions containing either 4.48 mM or 8.96 mM of ascorbic acid were added to the Fe-P sludge suspensions and stirred for 2 hours. The pH of the mixtures was kept constant by manual titration with HCl (1.0 M) and redox potentials were monitored during the test using ORP electrode which was immersed in the reaction solution. Samples were collected at regular time intervals and filtered through 0.45 μm cellulose nitrate filter membranes for analysis. The filtrates were collected in glass vials to which 0.1 mL of 0.5 M HCl had been added to quench

the autooxidation of Fe^{3+} (Deng, 1997) before analysis for total soluble phosphorus (TP), total soluble iron (TFe) and total soluble Fe^{3+}. Each batch experiment was run in duplicate.

Experiments assessing the impact of hydroxylamine and oxalic acid (Ox) treatment on Fe-P sludge dissolution were similarly conducted at pH 3 and a molar ratio of 1:2 for Fe/HA (anoxic conditions) and Fe/Ox (oxic conditions), using freshly prepared 4.48 mM solutions of both reagents at 22±1°C for 2 hours reaction time. For inorganic acid experiments, the pH of the reaction solution was adjusted at 3. However, as pH drifts were observed it was fixed at 3 by manual titration with (1.0 M) solutions of either H_2SO_4, HNO_3, or HCl under oxic conditions for 8 h reaction time. P and Fe release were calculated using equation (4-2):

$$\%R\ release = \frac{R_e}{R_o} \times 100 \quad (4\text{-}2)$$

where (R_o) and (R_e) represent the total measured concentrations (mg/L) of Fe or P in solid and liquid phases respectively.

4.3.3 Vivianite formation

Vivianite precipitation tests were performed in batches following the ascorbic acid and hydroxylamine treatments inside an anaerobic chamber with argon flushing at room temperature. The pH of the reaction solution was adjusted to 7 by adding NaOH (1.0 M) and the corresponding ORP value was measured (-352±5 mV/Ag/AgCl). After 30 minutes of rapid mixing (600 RPM) the suspension was filtered using 0.45 µm cellulose nitrate membrane filters (Whatman, pore size 0.45 µm, diameter 47mm). Concentrations of TP, TFe, and Fe^{+2} were measured in the filtrate and the solids were collected and vacuum-dried for 24 hours to avoid oxidation of Fe^{2+} and kept in a sealed glass vials placed inside the anaerobic glove box for further characterization by XRD. For

comparison, a pure vivianite sample was synthesized in the lab from 0.2 M $K_2HPO_4 \cdot 3H_2O$ and 0.3 M $FeCl_2 \cdot 4H_2O$ solution at pH 7 to obtain pure vivianite crystals (Procedure available in A2).

4.3.4 Vivianite characterization and quantification

4.3.4.1 XRD analysis

XRD analysis of the dried vivianite solids was determined under normal oxic conditions. The sample was added to a 0.7 mm glass capillary and tamped to settle solids. Just before measurement the capillaries were sealed with a burner and mounted in a sample holder. XRD analysis was conducted with a Bruker D8 Discover equipped with a Davinci design diffractometer employing Co-Ka radiation (15-110° 2θ, step size 0.01°). The XRD-pattern fitting was identified using Diffrac.Eva software.

4.3.4.2 Fe/P molar ratio

The Fe/P molar ratio in the generated vivianite solids was determined by acid digestion. A fresh sample of vivianite solids (30 mg wet weight) was transferred to a 50 mL tube and mixed with 20 mL of 10% HNO_3 solution. After solubilization the concentrations of P and Fe in the digested solution were measured by ICP-OES (see section 4.3.5) and the Fe/P molar ratio was calculated.

4.3.4.3 Magnetic attraction

Vivianite is a paramagnetic mineral with a magnetic susceptibility varying from 0.8 to 1.7×10^{-6} m^3/kg (Minyuk et al., 2013). The magnetic property of the dried vivianite solids was examined using a normal permanent magnet to test if the recovered solids were attracted to the magnet.

4.3.5 Chemical analysis

pH and ORP values were measured with a digital benchtop meter (Orion Star A211, Thermo Scientific, USA). Inductively Coupled Plasma Optical Emission Spectroscopy (ICP-OES) (PerkinElmer Optima 7300 DV, Waltham, MA, USA) was used to measure concentrations of TP and TFe. A modified version of the ferrozine method (Stookey, 1970) as reported by Viollier et al., (2000) was used to analyse soluble Fe^{2+}. Prior to analysis, 2 mL of each sample was filtered in an anaerobic chamber and fixed with 0.1 mL of (0.5 M) HCl. A stock solution of ferrozine was prepared by dissolving 0.25 g of 3-(2-pyridyl)-5,6-diphenyl-1,2,4-triazine- 4',4''- disulfonic acid, monosodium salt hydrate (Alfa Aesar) in 250 ml of 50 mM HEPES buffer solution at pH 7.0. A volume of 50 µL of sample was then added to 2.45 ml of ferrozine solution in a cuvette and the absorbance of the developed pink complex was measured immediately at 562 nm with a Duetta fluorescence and absorbance spectrometer (HORIBA Instruments Inc.). For soluble Fe^{3+} fraction determination, 0.2 mL of 6.25 M hydroxylamine hydrochloride was added to a filtered sample and digested with agitation for one hour to reduce Fe^{3+} to Fe^{2+}. The ferrozine procedure was then followed and the concentration of Fe^{3+} was calculated by taking the difference between the 2 measurements.

4.3.6 Modeling approach

Ion speciation and dissolution/precipitation reactions of the various solutions were modelled under equilibrium conditions using PHREEQC version 3.0 (US Geological Survey, 2013). The PHREEQC default data base (PHREEQC.DAT) was selected for the Fe-P solids, Fe-ascorbate, and Fe-oxalate complex simulations with some modification to the data file. The equilibrium reaction constants (K_{eq}) values for PO_4^{3-} protonation reactions and the solubility products (K_{sp}) values for solids such as hydrous ferric oxide (HFO) a solid formed via hydrolysis

of added ferric cations during CPR (Smith et al, 2008), and strengite, were obtained from NIST (2001). Moreover, struvite, ferrous oxalate ($FeC_2O_{4(s)}$), magnesium oxalate ($MgC_2O_{4(s)}$), and calcium oxalate ($CaC_2O_{4(s)}$) and soluble species of ascorbate and oxalate were added to the PHREEQC data file. Table A2.2 shows the list of soluble species and solid phases, along with their logK values that were modified and/or added to PHREEQC database file. For simulations, the input data was based on experimental conditions including pH values, initial total concentrations for each element (Fe, P, Ca, Mg, Na, Cl, and S) and organic ligands (ascorbate and oxalate) and logK values for soluble/solid species. An example of a PHREEQC simulation input file is provided in Table A2.3.

4.4 Results and discussion

4.4.1 Reductive dissolution of Fe-P sludge by ascorbic acid

Batch tests were conducted under anaerobic conditions at fixed pH values of 3 and 4 for two different Fe/AA molar ratios of 1:2 and 1:4 with freshly prepared Fe-P sludge to quantify the impact of ascorbic acid treatment on Fe^{3+} reduction and P release. Figure 4.1 displays plots of the fractions of solid Fe^{3+}, soluble Fe^{2+}, and TP as a function of time in the presence of ascorbic acid at pH 3 for Fe/AA molar ratios 1:2 and 1:4. Upon addition of ascorbic acid, the solution ORP value dropped from +374±5 mV to +38±5 and +35±5 mV/Ag/AgCl respectively. Fig. 4.1 shows a progressive increase in the fractions of soluble Fe^{2+} (Fig. 4.1a) and soluble TP (Fig. 4.1b) that approached unity within the 120 minutes of reaction. This occurred in parallel with the decay in the fractions of Fe^{3+} in the Fe-P solids (Fig. 4.1a) for all experiments. Despite differences in the rates of increase of Fe^{2+} and TP and Fe^{3+} decay with the different ascorbic acid doses, steady state releases of 97±1% and 98±1% were consistently attained after 60 minutes for TP and Fe^{2+} respectively indicating complete solubilization of the Fe-P sludge. Tests conducted at pH 4 for the

same Fe/AA molar ratios showed similar results as pH 3 (Fig A2.1). This suggests that a pH 4 and a molar dose of 1:2 (Fe/AA) are effective for complete solubilization of Fe-P sludge, and associated release of phosphate and iron. Moreover, from a practical perspective, adjusting to lower pH values will give the same impact on Fe-P sludge dissolution but use more resources.

Dissolution of HFO solids due to Fe^{3+} reduction by AA is apparently the mechanism responsible for P release from Fe-P sludge. The similarity in concentrations of soluble TFe that were measured during the tests and soluble Fe^{2+} (Fig A2.2) associated with the absence of Fe^{3+} ions in solution suggests complete reduction of Fe^{3+} to the more soluble Fe^{2+} form and leading to full P release from the Fe-P sludge. The mechanism for reductive dissolution of iron(III) oxides by ascorbic acid under acidic and anoxic conditions has been previously reported (Banwart et al., 1989; Suter et.al, 1991; Panies et al., 1995; Deng, 1997; Hsiesh and Hsieh, 2000; Debanth et al., 2010). The key steps include chemisorptive interactions between the iron(III) oxide surface and ascorbate anion (HA^-) yielding inner-sphere ascorbate-iron(III) surface complexes [$\equiv Fe^{III}HA$] that in turn become reactive sites for electron transfer and result in formation and release of Fe^{2+} and dehydroascorbic acid (zero charge) to the solution and thus full dissolution of iron(III) oxide.

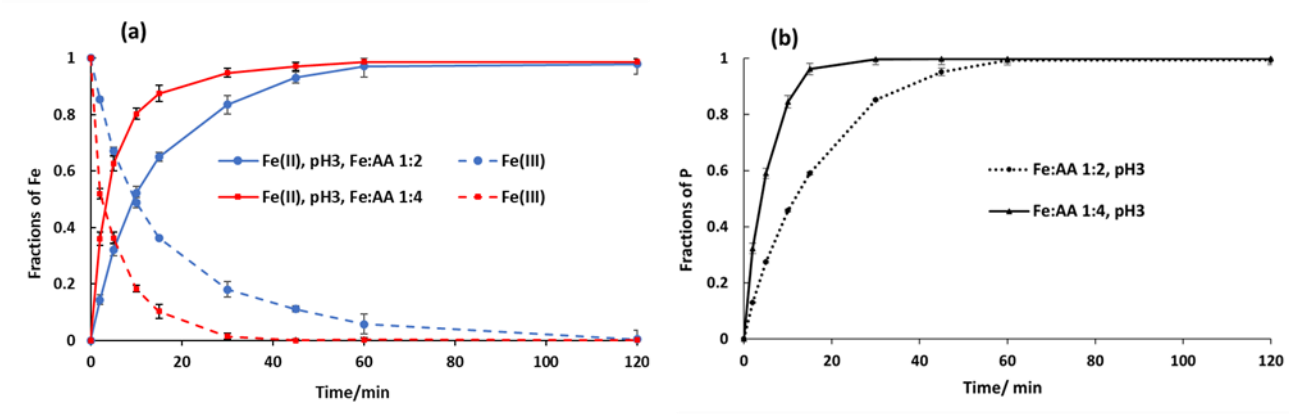

Figure. 4.1. Fractions of (a) iron(III) and iron (II), (b) total phosphorus versus time for treatment of fresh Fe-P sludge with ascorbic acid at Fe/AA molar ratios of 1:2 and 1:4 at pH 3. Error bars correspond to 95% confidence level.

In addition to being a reducing agent, AA has been found to act as a complexing agent for Fe^{2+} under anaerobic conditions and at pH values ranging between 1 and 5.5. The complexation results in formation of a stable cationic complex $[Fe(II)\text{-}HA]^{+}$($K_{\beta}=10.2\times10^{-3}$ or logK=1.99) (Wersin,1990) that has a violet color at pH values greater than 4 and is colorless at lower pH values (Plug et. al., 1984; Conrad and Schade, 1968). In the current system there was excess AA compared to iron and at the pH values used (pH 3 and 4), some of the excess AA was expected to be singly protonated. As indicated in Figure A2.3 approximately 50% of AA would be present as HA^{-} at pH 4 and 10% at pH 3 which would be available to chelate Fe^{2+} and form the $[Fe(II)\text{-}HA]^{+}$ complex. This was consistent with the light violet color that was observed in the first 30 minutes of the reaction at pH 4 and likely contributed to the full dissolution of Fe-P sludge and stabilization of soluble Fe^{2+}.

Although the formation of the ferrous ascorbate complex $[Fe(II)\text{-}HA]^{+}$ was expected, experimental measurements were not available to confirm this mechanism. Hence, PHREEQC simulations were employed to investigate the aqueous and solid phase speciation of TP, TFe, and complexes of Fe^{2+} and AA in the reaction solution at equilibrium after AA treatment at pH 3. Table 4.1 illustrates modeling results for Fe and P speciation. As shown in Table 4.1, the predicted values of TFe and TP release were in agreement with the experimental values. The simulations also demonstrated (Table 1) that three quarters of the total soluble Fe in the system is expected to exist as free Fe^{2+} while almost one quarter exists as $FeH_2PO_4^{+}$. The low predicted formation of ferrous ascorbate complex $[Fe(II)\text{-}HA]^{+}$ (1%) at pH 3 and (7%) at pH 4 (Table A2.4) was consistent with the low persistence of the light violet color. Moreover, some uncertainty might be

associated with the limited availability of thermodynamic data for ferrous ascorbate complexes used in the PHREEQC modelling.

Table 4.1. Fe and P species after AA treatment at pH 3: Observed vs model predictions

	%TP	$\%TFe^{3+}$	$\%TFe^{2+}$	$\%Free\ [Fe^{2+}]$	$\%FeH_2PO_4^{+*}$	$\%[Fe(II)\text{-}HA]^{+*}$
Modeled	100	3	97	75	22	1
Experimental	97±1	2±1	98±1	---	---	---

* Percent of Fe^{2+} in the form of a complex

Fe-P sludge in CPR plants can typically have ages as long as 12 d (Metcalf and Eddy, 2014). Therefore, the behaviour of P and Fe release from Fe-P sludges of different age under AA treatment was examined. It has been documented that HFOs undergo structural transformations with time, that can decrease their accessible reactive surfaces and affect their surface area and adsorptive capacity (Smith et al., 2008; Bligh and Waite, 2011; Hauduc et al., 2015). Further, aging of Fe-P solids has been reported to result in reduced P release upon alkaline treatment at pH 10 (Alnimer et al., 2023). As adsorption of ascorbate anion on HFO surface is the key step in reductive dissolution of Fe-P sludge by AA, it was expected that sludge age could affect (slow down) the adsorption process and thus P and Fe release. Figure 4.2 displays the percent release of TP, TFe, and Fe^{2+} from fresh, 5 and 11 day old Fe-P sludge when a Fe/AA molar ratio of 1:2 was employed at pH 3. Figure 4.2 shows releases of greater than 93% for TP, TFe, and Fe^{+2} for all sludge ages and pH values. These results indicate the negligible effect of sludge age on reductive dissolution of Fe-P solids by AA with the 1:2 Fe/AA molar dose. Practically, these results suggests that reductive dissolution by AA treatment gives a broad timespan for this treatment to be applied and could be a better approach for releasing P from chemical sludge than pH adjustment which has been shown to be impacted negatively by solids age (Alnimer et al., 2023).

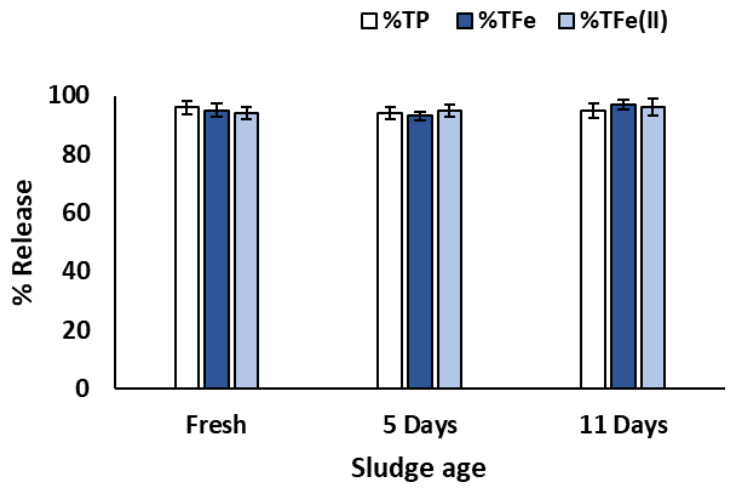

Figure. 4.2. Release of TP, TFe, and Fe^{2+} from Fe-P solids under different solids age after treatment with ascorbic acid at Fe/AA molar ratio of 1:2 at pH 3.

In principle, AA can solubilize HFO through a reductive reaction or a complexation reaction, or both. To provide a point of reference to the reductive performance of AA, tests were conducted with hydroxylamine as a "pure" reductant in that complexation of iron by hydroxylamine is expected to be negligible. Hydroxylamine is a common reducing agent used to reduce Fe^{3+} to Fe^{2+} in the analysis of aqueous solutions (Standard methods, 2005). The potential for reductive dissolution of Fe^{3+} to release P from freshly prepared Fe-P sludge with hydroxylamine was investigated at pH 3 and an Fe/hydroxylamine molar ratio of 1:2. The results (Table A2.5) showed negligible solubilization of the Fe-P sludge with (3.4±0.2%) and (1±0.1%) of the TP and TFe respectively released indicating no reductive dissolution effect of hydroxylamine on Fe-P sludge.

Previous studies have shown that both AA and hydroxylamine have similar efficiency (up to 97% match in their performance) in reducing soluble Fe^{3+} to Fe^{2+} ions in bulk solution at pH values between 1 and 4 at 25 °C (Elmagirbi et al., 2012). However, for solid phases particularly

crystalline iron(III) oxides and iron phosphate minerals, the iron(III) reducing activity of hydroxylamine is decreased. For example, Lovely and Phillips, (1987) reported that hydroxylamine was able to reduce Fe^{3+} in amorphous Fe(III) oxyhydroxides but not in Fe_2O_3, Fe_3O_4 and strengite ($FePO_4.2H_2O$) mineral phases. In fact, hydroxylamine can act as oxidant toward fairly strong reducing species like Fe^{2+} (Holleman & Wiber, 2001) and thus suppress reductive dissolution of solid iron(III) oxide. Such oxidation was also demonstrated in a study carried out by Madsen (2014) that demonstrated that hydroxylamine acted as a strong oxidant in the presence of growing iron-phosphate crystals, and was ineffective in reducing Fe^{3+} to Fe^{2+} in strengite. Therefore, hydroxylamine seems to not be an effective reductant for Fe^{3+} associated with Fe-P sludge solids compared to ascorbic acid.

4.4.2 Non-reductive dissolution of Fe-P sludge by oxalic acid

The previously described results indicate that complexation with AA is likely one of the mechanisms responsible for Fe-P sludge dissolution. For comparison, oxalic acid was selected as a complexing agent that is not redox active towards Fe^{3+}. Oxalic acid is a relatively strong diprotic organic acid (pK_{a1} =1.25, pK_{a2} = 4.28) found to be highly effective for dissolving iron oxides and chelating Fe in solution (Veglio et al 1998; Lee et al., 2007; Liang et al., 2019). Fig. 4.3 compares the release of TP and TFe from freshly prepared Fe-P sludge after oxalic acid treatment with an Fe/Ox molar ratio of 1:2 at pH 3 to that achieved with AA. It can be seen that the dissolutions of TP (95±2%) and TFe (90±1%) were only slightly less than that obtained with AA (Table A2.5).

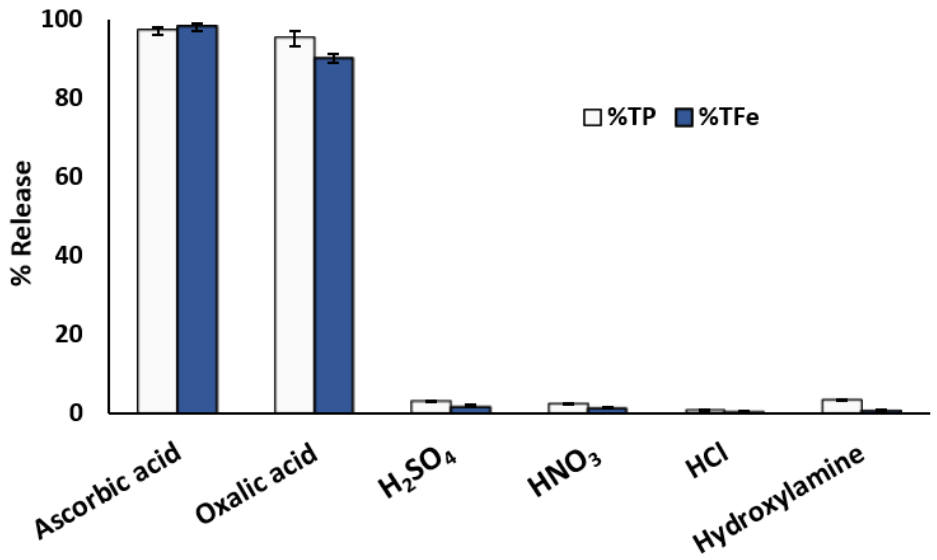

Figure. 4.3. Release of TP and TFe from fresh Fe-P sludge after treatment with ascorbic acid, oxalic acid, inorganic acids (H_2SO_4, HNO_3, and HCl), and hydroxylamine at pH 3.

The non-reductive dissolution mechanism of Fe-P sludge by oxalic acid involves adsorption of the oxalate species onto the HFO surface through surface complexation reactions which are followed by the desorption process (Panias et al., 1996). The form of adsorbed oxalate species and type of formed surface complex is pH dependent. For example, according to the distribution diagram of oxalate species (Fig. A2.4), $HC_2O_4^-$ is the predominant species at pH 3 and is most likely adsorbed onto the HFO surface forming a mononuclear monodentate [$\equiv Fe^{III}$ - HC_2O_4] surface complex. The dissolution takes place when the adsorbed surface ferric-oxalate complex ions are desorbed from HFO surface and transfer to the acidic solution as stable soluble Fe(III)-oxalate complexes (Panias et al., 1996).

To explore the speciation of Fe^{3+} and oxalic acid and obtain insight to the potentially formed Fe(III)-oxalate complexes, PHREEQC simulations were performed at pH 3. Table 4.2 summarizes the modeling results along with the experimental data for comparison. The modeled values for TFe and TP release (Table 4.2) were in agreement with the experimental values.

Moreover, the simulations (Table 4.2) showed that Fe^{3+} was primarily present in the form of Fe(III)-oxalate complexes which represented 99.7% of the Fe and hence free Fe^{3+} was less than 1% of the total TFe released from the Fe-P solids.

Table 4.2. PHREEQC simulations for Fe and P species after oxalic acid treatment at pH 3

	%TP	$\%TFe^{3+}$	$\%Fe(Ox)_3^{3-*}$	$\%Fe(Ox)_2^{-*}$	$\%Fe(HOx)^{2+*}$	$\%Fe(Ox)^{+*}$
Modeled	97.5	100	25	34.4	38	2.3
Experimental	95±2	90±1	---	---	---	---

* Percent of Fe^{3+} in the form of a complex

The observed and simulated results were consistent with the strong complexation reaction between Fe^{3+} and oxalic acid which resulted in formation of soluble mononuclear mono/bi/tridentate complexes. Further, the complexing effect of oxalic acid enhances P release from Fe-P solids by stabilizing soluble Fe^{3+} in solution via formation of the complexes (Table 4.2) which suppress regeneration of Fe-P solids (i.e., strengite at pH 3).

Oxalic acid and AA showed similar effects on solubilizing Fe-P sludge regardless of the dissolution mechanism that took place. Oxalic acid exhibited a stronger complexing effect toward Fe^{3+} in solution than AA toward Fe^{2+} whereas AA resulted in the predominant form of iron being the reduced cation; the measured value for $\%Fe^{2+}$ in the oxalic acid treatments was extremely low (1.3±0.2%). The formation of $Fe(Ox)_3^{3-}$, $Fe(Ox)_2^{-}$, $Fe(HOx)^{2+}$, and $Fe(Ox)^{+}$ complexes is more thermodynamically favoured (logK values 20.2, 15.57, 9.3, and 9.53 respectively) (NIST, 2001) than formation of $[Fe(II)\text{-}HA]^{+}$ complex (logK=1.99). Therefore, these findings suggest that the reductive dissolution effect of AA is the main driving force for solubilizing HFO while the complexation effect can to some extent stabilize Fe^{2+} in solution although it can exists as free cation and thus enhance P release. Complexation is not required for solubilization under reducing conditions because the Fe^{2+} cation is more soluble than the Fe^{3+} cation, for example, the Ksp values

of $Fe(OH)_{2(s)}$ and $Fe(OH)_{3(s)}$ are 7.9×10^{-16} and 1.6×10^{-39} at 25 ℃ respectively (Harris & Lucy, 2016).

The dissolution experiments were performed at acidic pH; to demonstrate that solubilization is due to reduction and complexation and not simply the low pH, batch tests were conducted using sulfuric, nitric, and hydrochloric acid at pH 3. As illustrated in Figure 4.3, the effect of the inorganic acids on P and Fe release was substantially less than that of either the AA or oxalic acid treatments at pH 3. This demonstrates that the redox/complexation capabilities of ascorbate and oxalate ions toward Fe^{2+} and Fe^{3+} in acidic media are necessary for dissolution of the synthetic sludge. Although acidic treatment has been employed for releasing P and Fe from Fe-P solids and sludge ash, even more acidic conditions (pH ≤1) have been needed to solubilize Fe-P and hence the demand for chemicals is high (Wilfert et al., 2015; Monea et al., 2020a; Chakraborty et al., 2020). It is clear that the redox and chelating effects associated with acidic AA treatment are more effective in solubilizing Fe-P sludge and stabilizing Fe in solution than common acidic treatments.

4.4.3 Vivianite formation and characterization

After the full solubilization of the Fe-P sludge in the AA experiments, the recovery of P and Fe as vivianite by adjusting the pH of the reaction mixture to 7 was assessed. Figure 4.4 illustrates the percentage of total P and Fe^{2+} in the solid and soluble phases after 30 minutes of vivianite precipitation at pH 7 along with PHREEQC simulation results. The recovery of the initial soluble P (0.15±0.02 mM) and Fe^{2+} (0.22±0.01 mM) as solid vivianite were 88±2% and 90±1% respectively. These results demonstrate the feasibility of recovering both elements. Further, they confirm that the chelating effect of AA which stabilizes Fe^{2+} in solution at acidic pH is not effective at neutral conditions where vivianite formation (logK=36) (Wilfert et al., 2018) is more

thermodynamically favoured over the Fe(II)-ascorbate complexes. Given that the stoichiometric ratio of iron and phosphorus in vivianite is the same as the initial synthetic sludge (Fe/P molar ratio of 1.5), it was expected that all soluble P and Fe^{2+} would be consumed, and no excess would remain in solution. However, an excess soluble P (12±2%) and Fe^{2+} (10±1%) were measured in solution after vivianite precipitation. Moreover, the measured yield of formed vivianite (0.065 ± 0.002 mmol) was lower than the modeled (0.071 mmol) value. This variation in the measured and modeled values was attributed to the short reaction duration (30 minutes) that was given for vivianite precipitation.

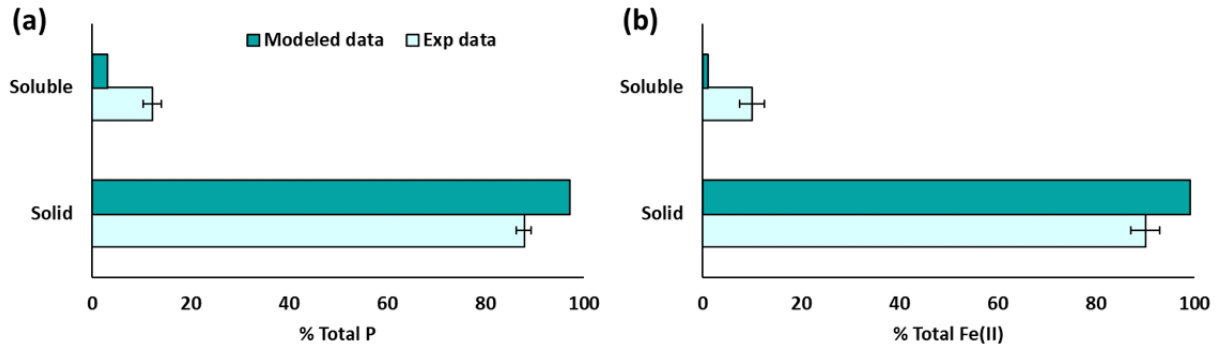

Figure 4.4. Percentage measured and modeled values of soluble and solid (a) P and (b) Fe^{2+} after vivianite precipitation at pH 7 for 30 minutes.

To confirm the precipitated solids were vivianite, XRD analysis was performed and compared with pure vivianite solids (synthesized) that were generated in the lab (for details of the synthesis method refer to A2). Both samples had the same blue color (Figure A2.5) indicating partial oxidation of Fe^{2+} in the solid (Zhang et al., 2022). Figure 4.5 shows the XRD spectra for both the precipitated sample and synthesized sample along with a standard vivianite spectrum. A very good match was observed for both samples with the reference vivianite spectrum. Moreover, the Fe/P molar ratio was measured for both the precipitated and synthesized vivianite samples to

quantify their P and Fe content. The measured Fe/P molar ratios after acid digestion were 1.53 and 1.57 respectively which were very close to the theoretical value of vivianite ($Fe_3(PO_4)_2.8H_2O$, Fe/P = 1.5) and within the values of 1.1-1.7 reported for vivianite in digested sludge (Wilfert et al., 2016). In addition, the precipitated and synthesized vivianite showed magnetic properties (Figure A2.6). Accordingly, the obtained results for XRD, Fe/P molar ratio analysis, and magnetic properties indicate that the generated solid from AA treatment to Fe-P sludge was vivianite and suggest no significant effect of the inorganic components of the synthetic wastewater on vivianite purity.

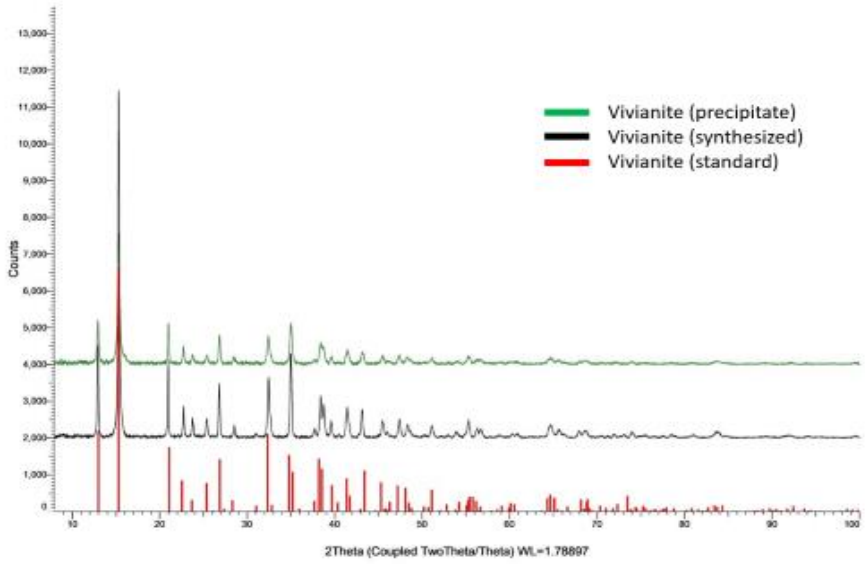

Figure 4.5. XRD spectra for vivianite precipitate, synthetic vivianite, and standard vivianite.

4.5 Discussion

In CPR plants , iron is commonly dosed since it can remove phosphorus to a very low level (Szabó et al., 2008). Around 90% of the P in the wastewater influent ends up in the sludge in the form of Fe-P solids providing a potential secondary source for phosphorus mining (Cornel & Schaum, 2009). The key process in P recovery is releasing P from Fe-P sludge. However, this

process is considered challenging as it is affected by various factors such as bonding characteristics between Fe and P, age of Fe-P solids, and the complex composition of sludge (Yu et al., 2021).

This study showed that redox manipulation of Fe-P sludge using AA at acidic pH was highly effective in releasing P from Fe-P sludge as AA can exhibit both reducing and chelating properties toward Fe ions. During AA treatment 98% of solid Fe^{3+} in Fe(III)-P sludge was reduced to Fe^{2+} followed by full dissolution and release of Fe^{2+} and PO_4^{3-} to solution. This was obtained at a minimum Fe/AA molar ratio of 1:2 and at both pH values tested of 3 and 4. In fact, employing AA treatment at acidic pH has many advantages that offer a great promise for practical applications of P recovery. These advantages include: (i) strong reducing effect of AA compared to other common reducing agents that are used to reduce Fe^{3+} to Fe^{2+} in water analysis, such as hydroxylamine which failed to reduce solid Fe^{3+} in Fe(III)-P sludge; (ii) AA can form complexes with Fe^{2+} which enhance solubilization and stabilization of Fe^{2+} in solution; (iii) the performance of the reductive dissolution effect of AA toward Fe-P sludge was not affected by solids age which practically makes AA treatment suitable for sludges with long residence time; (iv) AA is more effective for mobilization of P from Fe-P sludge compared to other pre-treatment methods (i.e., wet acidic treatment); (v) soluble Fe^{2+} and PO_4^{3-} can be recovered as vivianite mineral by adjusting the solution to pH 7.0; (vi) AA is environmentally friendly and inexpensive, improving its utility in a variety of engineering applications (i.e., dichlorination of drinking water and corrosion inhibition). However, this study generated valuable information that could be used to conduct a cost-benefit analysis in future application.

The data obtained for AA treatment in this study describe the release of Fe and P from a synthetic inorganic Fe-P sludge generated from a simple wastewater matrix (absence of inorganic

and organic interferences). The data in the simplified inorganic synthetic sludge studies here are consistent with that reported recently by Xu et al. (2023) for P and Fe ascorbic acid induced release from real Fe-P rich waste activated sludge. This suggests similar release behaviour for P and Fe from Fe-P sludge by AA treatment in the presence and absence of inorganic and organic interferences.

4.6 Conclusions

This study is the first attempt to provides insights into P release and recovery by reducing Fe(III)-P sludge using AA as reductant in the absence of interferences from other wastewater components (organic matter, bacteria). The reductive dissolution of AA on Fe-P sludge at Fe/AA molar ratio 1:2 and pH values 3 and 4 was effective where full solubilization of Fe-P sludge was achieved. Sludge aging did not affect the reductive dissolution of Fe-P sludge by AA demonstrating the suitability of AA treatment for sludges with extended residence times. The use of hydroxylamine (reducing agent) was not effective in reducing Fe^{3+} in Fe-P sludge. Oxalic acid as a chelating agent was effective in solubilizing Fe-P sludge at oxic conditions and stronger in chelating Fe than AA. Inorganic acids showed low release (<10%) of P and Fe at pH 3 compared to AA and oxalic acid. After AA treatment P and Fe were recovered from solution in the form of vivianite by increasing the solution pH to 7 with %recovery of 88±2% and 90±1% respectively. XRD, Fe/P molar ratio measurements, and magnetic attraction all conformed qualitatively and quantitively vivianite formation. Overall, this method exhibited good performance in releasing P from sludge under acidic conditions and is promising for establishing a new route for P recovery in the form of vivianite.

4.7 References

Alnimer, A. A., Smith, D.S., Parker, W. J., **2023**. Insight into direct phosphorus release from simulated wastewater ferric sludge: Influence of physiochemical factors. Journal of Environmental Chemical Engineering. 11: 3. doi.org/10.1016/j.jece.2023.110259.

Banwart, S., Davies, S., Stumm, W., **1989**. The role of oxalate in accelerating the reductive dissolution of hematite (α-Fe_2O_3) by ascorbate. Colloids and Surfaces, 39 (2), 303-309, doi.org/10.1016/0166-6622(89)80281-1.

Bligh, M.W., & Waite, T.D., **2011**. Formation, reactivity, and aging of ferric oxide particles ormed from Fe(II) and Fe(III) sources: Implications for iron bioavailability in the marine environment. Geochimica et Cosmochimica Acta 75 (24), 7741-7758.

Cabeza, R., Mazuz, Y., Stokes, J., Kragel, J. E., Woldorff, M. G., Ciaramelli, E., Olson, I. R., Moscovitch, M., **2011**. Overlapping Parietal Activity in Memory and Perception: Evidence for the Attention to Memory Model. J Cogn Neurosci 2011; 23 (11): 3209–3217. doi:10.1162/jocn_a_00065.

Celine Lippens, C., & Jo De Vrieze, J.D., **2019**. Exploiting the unwanted: Sulphate reduction enables phosphate recovery from energy-rich sludge during anaerobic digestion. Water Research. 163: 114859. doi.org/10.1016/j.watres.2019.114859.

Chakraborty, T., Balusani, D., Smith, D.S., Walton, S.J., Nakhla, G., Ray, M.B., **2020**. Reusability of recovered iron coagulant from primary municipal sludge and its impact on chemically enhanced primary treatment. Separation and Purification Technology 231:115894. doi:10.1016/j.seppur.2019.115894.

Chen, R., Dai, X., Dong, B., **2022**. Decrease the effective temperature of hydrothermal treatment for sewage sludge deep dewatering: mechanistic of tannic acid aided. Water Res. 217, 118450. doi.org/10.1016/j.watres.2022.118450.

Chen, Y., Lin, H., Shen, N., Yan, W., Wang, J., Wang, G., **2019**. Phosphorus release and recovery from Fe-enhanced primary sedimentation sludge via alkaline fermentation. Bioresource technology, 278, 266–271. doi:10.1016/j.biortech.2019.01.09.

Conrad, M. E., & Schade, S. G., **1968**. Ascorbic acid chelates in iron absorption: a role for hydrochloric acid and bile. Gastroenterology, 55(1), 35–45.

Cornel, P., & Schaum, C., **2009**. Phosphorus recovery from wastewater: needs, technologies and costs. Water Sci. Technol. 59, 1069–1076. doi.org/10.2166/WST.2009.045.

Cornell, R. M., and Schwertmann, Udo., **2003**. The Iron Oxides : Structure, Properties, Reactions, Occurrences, and Uses. 2nd ed. Weinheim : Wiley-VCH.

Debnath, S., Hausner, D. B., Strongin, D. R., Kubicki, J., **2010**. Reductive dissolution of ferrihydrite by ascorbic acid and the inhibiting effect of phospholipid. Journal of colloid and interface science, 341(2), 215–223. doi.org/10.1016/j.jcis.2009.09.035.

Deng, Y., **1997**. Effect of pH on the reductive dissolution rates of iron(III) hydroxide by ascorbate. Langmuir. 13, 1835-1839. doi.org/10.1021/la9607013.

Elmagirbi, A., Sulistyarti, H., Atikah, **2012**. Study of Ascorbic Acid as Iron(III) Reducing Agent for Spectrophotometric Iron Speciation. J. Pure App. Chem. Res., 1 (1), 11-17.

Fredrickson, J. K., Zachara, J. M., Kennedy, D. W., Dong, H., Onstott, T. C., Nancy W. Hinman, N. W., Li, S., **1998**. Biogenic iron mineralization accompanying the dissimilatory reduction of hydrous ferric oxide by a groundwater bacterium. Geochimica et Cosmochimica Acta, (62): 19–20, 3239-3257. doi.org/10.1016/S0016-7037(98)00243-9.

Ghassemi, M., & Recht, H. L., **1927**- & United States. Environmental Protection Agency. Office of Research and Monitoring. (1971). Phosphate precipitation with ferrous iron, by Masood Ghassemi [and] Howard L. Recht. Washington : [U.S. Environmental Protection Agency]; for sale by the Supt. of Docs., U.S. Govt. Print. Off.

Harris, D.C. & Lucy, C. A., **2016**. Quantitative Chemical Analysis. 9th Edition, W.H. Freeman and Company, New York.

Hauduc, H., Takács, I., Smith, S., Szabo, A., Murthy, S., Daigger, G. T., Spérandio, M., **2015**. A dynamic physicochemical model for chemical phosphorus removal. Water research, 73, 157–170. doi:10.1016/j.watres.2014.12.053.

Holleman, A.F. & Wiberg, E., **2001**. Inorganic Chemistry. Academic Press, San Francisco.

Hsieh, Y.-H. P., Hsieh, Y. P., 1997. Valence state of iron in the presence of ascorbic acid and ethylenediaminetetraacetic acid. J. Agric. Food Chem. 45, 1126–1129.

Hsieh, Y. H., & Hsieh, Y. P., **2000**. Kinetics of Fe(III) reduction by ascorbic acid in aqueous solutions. Journal of agricultural and food chemistry, 48(5), 1569–1573. doi.org/10.1021/jf9904362.

Jung, Y., Koh, H., Shin, W., Sung, N., **2005**. Wastewater treatment using combination of MBR equipped with non-woven fabric filter and oyster-zeolite column. Environmental Engineering Research, 10, 247-256.

Kato, F., Kitakoji, H., Oshita, K., Takaoka, M., Takeda, N., Matsumoto, T., **2006**. Extraction Efficiency of Phosphate from Pre-Coagulated Sludge with NaHS. Water Science & Technology 54 (5): 119. doi:10.2166/wst.2006.554.

Lee, S. O., Tran, T., Jung, B. H., Kim, S. J., Kim, M. J., **2007**. Dissolution of iron oxide using oxalic acid, Hydrometallurgy. 87, 3–4, 91-99, doi.org/10.1016/j.hydromet.2007.02.005.

Li, L., Li, R.-H., Li, Y., Xu, J., Li, X.-Y., **2017**. Recovery of organic carbon and phosphorus from wastewater by Fe-enhanced primary sedimentation and sludge fermentation, Process Biochemistry. 54, 135-139. doi.org/10.1016/j.procbio.2016.12.016.

Liang, S., Chen, H., Zeng, X., Li, Z., Yu, W., Xiao, K., Hu, J., Hou, H., Liu, B., Tao, S., Yang, J., **2019**. A comparison between sulfuric acid and oxalic acid leaching with subsequent purification and precipitation for phosphorus recovery from sewage sludge incineration ash. Water research, 159, 242–251. doi.org/10.1016/j.watres.2019.05.022.

Likosova, M. E., Keller, J., Rozendal, R. A., Poussade, Y., S. Freguia. S., **2013**. Understanding Colloidal FeSx Formation from Iron Phosphate Precipitation Sludge for Optimal Phosphorus Recovery. Journal of Colloid and Interface Science 403: 16–21. doi:10.1016/j.jcis.2013.04.001.

Lovley D. R., & Phillips, E. J., **1987**. Rapid assay for microbially reducible ferric iron in aquatic sediments. Appl Environ Microbiol. 53(7):1536-40. doi: 10.1128/aem.53.7.1536-1540.1987.

Madsen, H. E. L., **2014**. Redox process catalysed by growing crystal-strengite, $FePO_4.2H_2O$, crystallizing from solution with iron(II) and hydroxylamine. Journal of Crystal Growth, 401, 275-278. doi.org/10.1016/j.jcrysgro.2013.11.025.

Mahata, S., Mitra, I., Mukherjee, S., Venkata P., Reddy B., Ghosh, G. K., Linert, W., Sankar C. W., **2019**. Speciation Study of L-ascorbic Acid and its Chelated Cu(II) & Ni(II) Complexes: an Experimental and Theoretical Model of Complex Formation. South African Journal of Chemistry, 72, 229-236. doi.org/10.17159/0379-4350/2019/v72a30.

Martínez, P., & Uribe, D., **1982**. Study of the Complexes of the Ascorbic Acid-Iron(III) System. Zeitschrift für Naturforschung B, 37, 1446 - 1449.

Metcalf and Eddy Inc., Tchobanoglous G., 2014. Wastewater engineering : treatment and reuse, 5th Edition. McGraw Hill, New York.

Minyuk, P. S., Subbotnikova, T. V., Brown, L. L., Murdock, K. J., **2013**. High-temperature thermomagnetic properties of vivianite nodules, Lake El'gygytgyn Northeast Russia, Clim. Past. (9):1 433-446. doi.org/10.5194/cp-9-433-2013.

Monea, M.C., L¨ohr, D.K., Meyer, C., Preyl, V., Xiao, J., Steinmetz, H., Sch¨onberger, H., Drenkova-Tuhtan, A., **2020a**. Comparing the leaching behavior of phosphorus, aluminum and iron from post-precipitated tertiary sludge and anaerobically digested sewage sludge aiming at phosphorus recovery. J. Clean. Prod. 247, 119129. doi.org/10.1016/j.jclepro.2019.119129.

National Institute of Standards and Technology, **2001**. NIST Standard Reference Database 46. National Institute of Standards and Technology: Gaithersburg, Maryland.

Nielsen, A. H., Hvitved-Jacobsen, T., Vollertsen, J., **2005**. Kinetics and stoichiometry of sulfide oxidation by sewer biofilms. Water research, 39(17), 4119–4125. doi.org/10.1016/j.watres.2005.07.031.

Njus, D., Kelley, P. M., Tu, Y. J., Schlegel, H. B., **2020**. Ascorbic acid: The chemistry underlying its antioxidant properties. Free radical biology & medicine, 159, 37–43. doi.org/10.1016/j.freeradbiomed.2020.07.013.

Panias, D., Taxiarchou, M., Paspaliaris, I., Kontopoulos, A., **1996**. Mechanisms of dissolution of iron oxides in aqueous oxalic acid solutions. Hydrometallurgy, 42, 257-265. doi.org/10.1016/0304-386X(95)00104-O.

Peng, L., Dai, H., Wu, Y., Peng, Y., Lu, X., **2018a**. A Comprehensive Review of Phosphorus Recovery from Wastewater by Crystallization Processes. Chemosphere 197. Elsevier Ltd: 768–81. doi:10.1016/j.chemosphere.2018.01.098.

Ping, Q., Lu, X., Li, Y., Mannina, G., **2020**. Effect of complexing agents on phosphorus release from chemical-enhanced phosphorus removal sludge during anaerobic fermentation. Bioresource Technol 301, 122745. doi: 10.1016/j.biortech.2020.122745.

Plug, C. M., Dekker, D., Bult, A. **1984**. Complex stability of ferrous ascorbate in aqueous solution and its significance for iron absorption. Pharmaceutisch Weekblad Scientific. Edition 6, 245–248. doi.org/10.1007/BF01954553.

Prot, T., Nguyen, V. H., Wilfert, P., Dugulan, A. I., Goubitz, K., De Ridder, D. J., Korving, L., Rem, P., Bouderbala, A., Witkamp, G. J., van Loosdrecht, M. C. M., **2019**. Magnetic separation and characterization of vivianite from digested sewage sludge. Separation and Purification Technology, (224): 564-579. doi.org/10.1016/j.seppur.2019.05.057.

Sano, A., Kanomata, M., Inoue, H., Sugiura, N., Xu, K. Q., Inamori, Y., **2012**. Extraction of Raw Sewage Sludge Containing Iron Phosphate for Phosphorus Recovery. Chemosphere 89 (10): 1243–47. doi:10.1016/j.chemosphere.2012.07.043.

Shen, J., Griffiths, P. T., Campbell, S. J., Utinger, B., Kalberer, M., & Paulson, S. E., **2021**. Ascorbate oxidation by iron, copper and reactive oxygen species: review, model development, and derivation of key rate constants. Scientific reports, 11(1), 7417. doi.org/10.1038/s41598-021-86477-8.

Smith, S., Takacs, I., Murthy, S., Daigger, G. T., Szabo, A., **2008**. Phosphate Complexation Model and Its Implications for Chemical Phosphorus Removal. Water Environ. Res. 80 (5): 428−438.

Solon, K., Volcke, E.I.P., Sperando, M., van Loosdercht, M. **2019**. Resource Recovery and Wastewater Treatment Modelling. Water Res. Technol. doi.org/10.1039/C8EW00765A.

Standard Methods for the Examination of Water and Wastewater, **2005**. 21st ed., American Public

Health Association/American Water Works Association/Water Environment Federation, Washington, DC, USA.

Stookey, L. L., **1970**. Ferrozine, a new spectrophotometric reagent for iron. Anal. Chem. 42, 779–781.

Suter, D., Banwart, S., Werner Stumm, W., **1991**. Dissolution of hydrous iron(III) oxides by reductive mechanisms. Langmuir. 7 (4), 809-813. doi: 10.1021/la00052a033.

Szabó, A., Takács, I., Murthy, S., Daigger, G. T., Licskó, I., Smith, S. D., **2008**. Significance of Design and Operational Variables in Chemical Phosphorus Removal. Water Environment Research 80 (5): 407–16. doi:10.2175/106143008X268498.

Tu, Y.-J., Njus, D., Schlegel, H. B., **2017**. A theoretical study of ascorbic acid oxidation and HOO˙/O2˙− radical scavenging. Organic & Biomolecular Chemistry. (15):20, 4417-4431. doi.org/10.1039/c7ob00791d.

US Geological Survey, **2013**. PHREEQC (Version 3) – A computer program for speciation, batch-reaction, one-dimensional transport, and inverse geochemical calculations, (https://wwwbrr.cr.usgs.gov/projects/GWC_coupled/phreeqc/) (accessed on December 5th, 2021).

Veglio, F., Passariello, B., Barbaro, M., Plescia, P., Marabini, A.M., **1998**. Drum leaching tests in the iron removal from quartz using oxalic acid and sulphuric acids. Int. J. Miner. Process. 54 183–200. doi.org/10.1016/S0301-7516(98)00014-3.

Viollier, E., Inglett, P. W., Hunter, K., Roychoudhury, A. N., van Cappellen, P., **2000**. The ferrozine method revisited: Fe(II)/Fe(III) determination in natural waters, Appl. Geochem. 15: 785–790. doi.org/10.1016/S0883-2927(99)00097-9.

WEF, 2011. Nutrient removal - manual of practice. WEF Manual of Practice No. 34. (1): 72-83.

Wersin, P., **1990**. Ph.D. Thesis, No. 9230, Swiss Federal Institute of Technology (ETH Zu¨ rich).

Wilfert, P., Dugulan, A.I., Goubitz, K., Korving, L., Witkamp, G.J., Van Loosdrecht, 2018. Vivianite as the main phosphate mineral in digested sewage sludge and its role for phosphate recovery. Water Res. 144, 312–321.

Wilfert, P., Mandalidis, A., Dugulan, A. I., Goubitz, K., Korving, L., Temmink, H., **2016**. Vivianite as an Important Iron Phosphate Precipitate in Sewage Treatment Plants. Water Research 104. Elsevier Ltd: 449–60. doi:10.1016/j.watres.2016.08.032.

Wilfert, P., Meerdink, J., Degaga, B., Temmink, H., Korving, L., Witkamp, G. J., Goubitz, K., van Loosdrecht, M. C. M., **2020**. Sulfide induced phosphate release from iron phosphates and its potential for phosphate recovery. Water Research. (171): 115389, doi.org/10.1016/j.watres.2019.115389.

Wilfert, P., Prashanth S. K., Korving, L., Witkamp, G. J., van Loosdrecht, M.C.M., **2015**. The Relevance of Phosphorus and Iron Chemistry to the Recovery of Phosphorus from Wastewater: A Review. Environmental Science and Technology 49 (16): 9400–9414. doi:10.1021/acs.est.5b00150.

Wu, M., Liu, L., Gao, B., Sillanpää, M., **2021**. Phosphate substances transformation and vivianite formation in P-Fe containing sludge during the transition process of aerobic and anaerobic conditions. Bioresource Technology. 319. 124259. doi.org/10.1016/j.biortech.2020.124259.

Wu, Y., Cao, J., Zhang, Q., Xu, R., Fang, F., Feng, Q., Li, C., Xue, Z., Luo, J., **2020**. Continuous waste activated sludge and food waste co-fermentation for synchronously recovering vivianite and volatile fatty acids at different sludge retention times: performance and microbial response. Bioresource Technol 313, 123610. doi: 10.1016/j.biortech.2020.123610.

Wu, Y., Luo, J. Y., Zhang Q., Aleem, M., Fang, F., Xue, Z. X., Cao, J. S., **2019**. Potentials and challenges of phosphorus recovery as vivianite from wastewater: a review. Chemosphere. (226) 246–258. doi.org/10.1016/j.chemosphere.2019.03.138.

Wu, Y., Wang, C., Wang, S., An, J., Liang, D., Zhao, Q., Tian, L., Wu, Y., Wang, X., & Li, N., **2021**. Graphite accelerate dissimilatory iron reduction and vivianite crystal enlargement. Water research. 189, 116663. doi.org/10.1016/j.watres.2020.116663.

Xu, X., Xu, Q., Du, Z., Gu, L., Chen, C., Huangfu, X., Shi, D., **2023**. Enhanced phosphorus release from waste activated sludge using ascorbic acid reduction and acid dissolution. Water research. 229, 119476. doi.org/10.1016/j.watres.2022.119476.

Ye, Y., Ngo, H. H., Guo, W., Liu, Y., Li, J., Liu, Y., Zhang, X., Jia, H., **2017**. Insight into Chemical Phosphate Recovery from Municipal Wastewater. Science of The Total Environment 576 : 159–71. doi:10.1016/j.scitotenv.2016.10.078.

Yu, B., Luo, J., Xie, H., Yang, H., Chen, S., Liu, J., Zhang, R., Li, Y., **2021**. Species, fractions, and characterization of phosphorus in sewage sludge: a critical review from the perspective of recovery. Sci. Total Environ. 786, 147437.

Zhang. J, Chen. Z, Liu. Y, Wei. W, Ni. B-J., **2022**. Phosphorus recovery from wastewater and sewage sludge as vivianite, Journal of Cleaner Production.370: 133439. doi.org/10.1016/j.jclepro.2022.133439.

Zou, J., Zhang, L., Wang, L., Li, Y., **2017**. Enhancing phosphorus release from waste activated sludge containing ferric or aluminum phosphates by EDTA addition during anaerobic fermentation process. Chemosphere 171, 601–60.

Chapter 5 - Impact of Organic Matter on Chemical Phosphorus Removal and Recovery from a Synthetic Wastewater Matrix

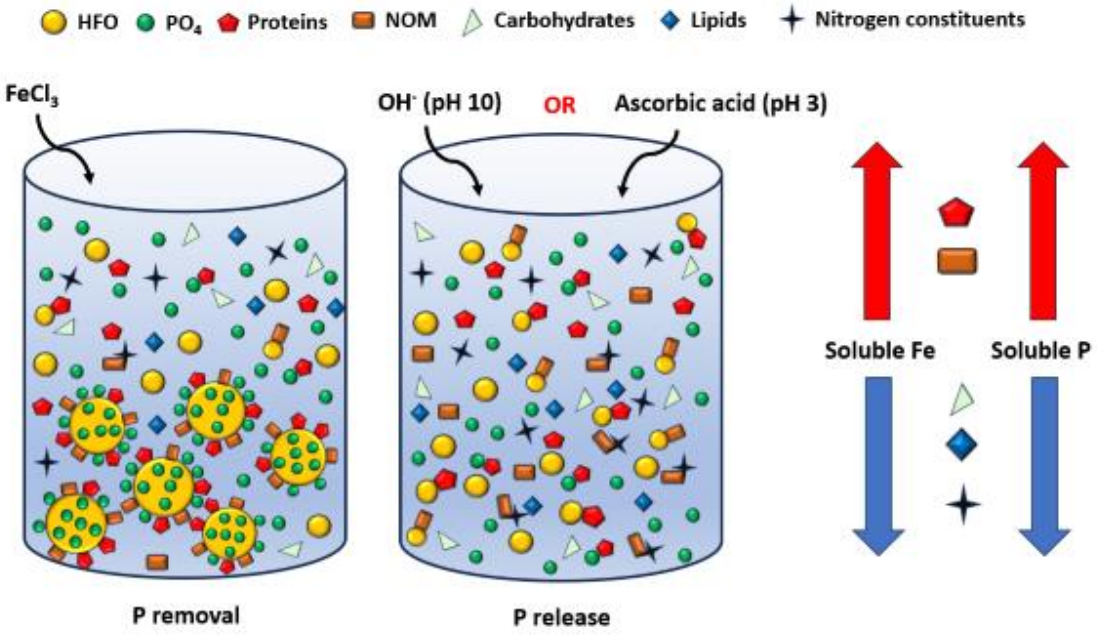

5.1 Abstract

This novel study evaluated the influence of different OM constituents (carbonaceous and nitrogenous), that are found in raw municipal wastewater, on chemically mediated P removal by $FeCl_3$. Batch tests were performed using synthetic wastewaters containing meat extract (ME), potato starch, glycerol, and Luther Marsh (LM) concentrate to represent proteins, carbohydrates, lipids, and NOM respectively while peptone, urea, and ammonium chloride represented nitrogenous constituents. Results showed insignificant effect of nitrogenous constituents, potato starch and glycerol on P removal. However, ME and LM caused a remarkable reduction in P removal (3.0±0.4% and 23±1% respectively) when compared to an inorganic control recipe

(62±2%). Elevated soluble Fe (SFe) residuals for ME (87±5%) and LM (51±1%) indicated interactions between Fe(III) cations and negatively charged functional groups like hydroxyl, carboxyl, and phenolic groups available in ME and LM. No change in P removal performance is observed for carbonaceous constituents in the presence of nitrogen source except for LM which exhibited a substantial increase by (23%). Significant negative correlations between P removal and residual SFe were observed for carbonaceous constituents in the absence and presence of nitrogen source. This suggested Fe solubilization as the mechanism responsible for reduced P removal. The presence of OM did not influence P release from Fe-P sludge in wet alkaline (pH 10) and ascorbic acid treatments. The findings of this study identify, for the first time, DOM constituents with higher impact on P removal and recovery, ultimately enabling a better understanding of P recovery from wastewaters that are treated with by Fe(III) salts.

5.2 Introduction

The discharge of phosphorus (P) to aquatic ecosystems due to anthropogenic activities can lead to eutrophication and potential severe environmental impacts for aquatic life (Huser et al., 2016; Venkiteshwaran et al., 2018). Phosphorus is also a non-renewable resource required for global agriculture, where currently the majority of P for chemical fertilizer is obtained by mining operations (Cordell and White, 2014; Kok et al., 2018). Municipal wastewater treatment plants (WWTPs) are a significant anthropogenic point sources for P entering surface waters and have the potential to be an alternative P source with reduced environmental impacts compared to mining (Bowes et al., 2015; Peng et al., 2018a). For instance, between 2002 and 2010, approximately 62% of global total anthropogenic P load to freshwater bodies originated from sewage effluents (Mekonnen & Hoekstra, 2018). Further, in 2015, sewage effluents counted for 70% of total P loadings to rivers in UK (Bunce et al., 2018). In this context either biological or chemical

technologies have the potential to be employed in WWTPs to prevent eutrophication and recover P to offset the needs for non-renewable P mining.

Chemical P removal (CPR) has been widely practiced in WWTPs for efficient and stable P removal (Wu et al., 2019). It involves dosing metal salts into wastewater to form insoluble metal-phosphate solids that can be separated by physical means. Iron(III) chloride ($FeCl_3$) is the most frequent metal salt employed (Ping et al., 2022). In a CPR process, the iron(III) cation can interact with orthophosphate (P_{ortho}) anion through different pathways including direct-precipitation, co-precipitation, and adsorption (Smith et al., 2008; Ping et al., 2022; Alnimer et al., 2023). This generates different types of Fe-P solids, where the most likely are Fe(III)-P minerals (i.e., strengite $FePO_4.2H_2O$), Fe(III)-hydroxyphosphate ($Fe_xPO_4(OH)_{3x-3}$), and P_{ortho} adsorbed to Fe(III) hydrolysis products such as hydrous ferric oxide (HFO) surfaces (Smith et al., 2008, Wilfert et al., 2015, Ping et al., 2022; Alnimer et al., 2023). The extent of P removal and the form of Fe-P solids are influenced by factors such as solution pH, Fe salt type and dose, floc age, mixing intensity, and presence of organic matter (OM) (Szabo et al., 2008; Li et al., 2018; Ping et al., 2022). However, among these factors, the effect of OM interferences on P removal and recovery from wastewater remains an active area of research (Wilfert et al., 2015; Ping et al., 2022).

OM in wastewater originates from human and food wastes, decomposition of animal and plant residues, and industrial discharges (Huang et al., 2004; Metcalf and Eddy, 2014; Chen et al., 2023). It spans a wide range of chemical structures and molar masses and exists in both particulate and dissolved (particles <0.45 μm) forms (Omoike and Vanloon, 1999; Metcalf and Eddy, 2014, Volcke et al., 2023). The dissolved organic matter (DOM) in wastewater is complex, containing a variety of carbonaceous and nitrogenous constituents that contribute to the overall chemical oxygen demand (COD) (Metcalf and Eddy, 2014; Yuan et al., 2019). Although its chemical

composition varies from source to source, the major components of domestic wastewater COD have been reported to include proteins (<60%), carbohydrates (40-90%), lipids (<40%), and natural organic matter (NOM)) (Levine et al., 1985; Raunkjaer et al., 1994; Sophonsiri & Morgenroth, 2004; Huang et al., 2010; Le et al., 2016; Yuan et al., 2019). Generally, DOM comprises a variety of functional groups (i.e., hydroxyl, phenolic, carbonyl, carboxylic, aromatic, amino, and amido groups) capable of interacting with Fe(III) cationic species and thus have significant implications for the effectiveness of CPR processes (He et al., 2014; Sundman et al., 2016; Chen et al., 2019).

When DOM associate with Fe(III) through complexation, co-precipitation or adsorption reactions it can influence the hydrolysis and solubility of Fe(III) (Gaffney et al., 2008; Karlsson and Persson, 2012; Zhao et al., 2016). It has been reported that DOM-bearing carboxylic functional groups can complex Fe(III) and form stable soluble mononuclear Fe(III)-DOM complexes capable of supressing Fe(III) hydrolysis and polymerization (Sharma et al., 2010; Karlsson and Persson, 2012). However, DOM with high aromatic content showed a higher tendency toward co-precipitation with Fe(III) hydrolysis products (Du et al., 2018; Chen et al. 2014; Riedel et al. 2013). In addition, DOM rich with negatively charged functional groups like carboxyl, hydroxyl and phenolic groups can adsorb to positively charged HFO surfaces through electrostatic interactions, ligand exchange, and hydrophobic interactions (Zhang et al., 2015, Taujale et al., 2016). The reactive sites at the HFO surface that are capable of interacting with anionic DOM also have the potential to interact with phosphate anions. Viewed collectively, Fe(III) and DOM interactions can impact the efficiency of CPR process by hindering Fe(III) hydrolysis and polymerization processes (Karlsson and Persson, 2012; Zhou et al., 2015) or by competing with P for active sites on Fe(III) hydrolysis products (Wilfert et al., 2015; Kida and Fujitake, 2020).

Ping et al, (2022) studied the effect of OM on P removal from wastewater by Fe salts and demonstrated that humic acids inhibited the P removal rate but only marginally affected the extent of removal. Other studies have looked at the impact of natural dissolved organic carbon (DOC) on P removal from wetland waters by iron and aluminium salts. Qualls et al, (2009) found that high concentrations of natural DOC inhibited both the short-term removal of phosphate, and the longer-term removal of total P from the water column. Hashim et al, (2021) showed that during electrocoagulation treatment of wastewater using iron-based electrodes, OM reacted rapidly with Fe cations and inhibited their coagulation and floc formation. In addition, the influence of DOM on P removal from wastewater streams by precipitation as recovery products such as struvite (Zhou et al., 2015), vivianite (Li et al., 2021), and calcium phosphate (Sindelar et al., 2015) have been addressed. While previous work (Qualls et al., 2009; Zhou et al., 2015; Sindelar et al., 2015; Hashim et al., 2021; Li et al., 2021; Ping et al., 2022) has focused on the impact of bulk natural DOM on P removal and recovery by Fe salts from wastewater, limited work has examined the impact of the individual carbonaceous and nitrogenous constituents comprising DOM, like proteins, carbohydrates, and lipids.

This novel study aims to evaluate the impact of individual and combinations of municipal wastewater carbonaceous and nitrogenous constituents on P removal with $FeCl_3$ and subsequent recovery of P from the generated solids. Batch precipitation tests were initially performed using a synthetic wastewater containing typical concentrations of proteins, carbohydrates, lipids and NOM. Subsequently, P release and recovery batch tests were conducted using wet alkaline and ascorbic acid treatments (Alnimer et al., 2023a, 2023b) to assess the impact of OM on P recovery. The results obtained in this study, for the first time, identify DOM constituents with higher impact on P removal and recovery, thus enabling a better understanding of P recovery from wastewater

that is treated with Fe(III) salts. The results will help improve approaches for CPR beyond those currently employed.

5.3 Materials and methods

5.3.1 Preparation of synthetic wastewater

Unless otherwise specified, all chemicals used in this study were of reagent grade and commercially available. All glassware were acid washed. Ultrapure water (Millipore, resistance >18.2 MΩ) was used for preparation of all solutions. A modified version of the synthetic wastewater recipe (Table A3.1 and A3.2) reported by Boeije et al. (1999) was employed as a model for domestic sewage mimicking "household" (grey water) and "sanitary" (black water) fractions. From this recipe and for simplicity and consistency, carbonaceous constituents including meat extract (ME), potato starch, glycerol, were selected to represent proteins, carbohydrates, and lipids respectively. Peptone, urea, and ammonium chloride were selected to represent nitrogenous constituents. In addition, Luther Marsh (LM) reverse osmosis concentrate was employed as a carbonaceous constituent representing natural organic matter (NOM). Luther Marsh was collected as described in Al-Reasi et al. (2012). The inorganic constituents followed a recipe for artificial wastewater Jung et al., (2005) (Table A3.3) and included $MgSO_4$, $CaCl_2$, and $NaHCO_3$ and Na_3PO_4. The "full recipe" included all components while simplified matrices were employed in some tests to investigate the roles of specific components. Table 5.1 summarizes concentrations and descriptions of the key components in the full recipe, and Table 5.2 describes the specific "simplified matrix" experiments that were performed. The concentrations of the carbonaceous constituents used here were selected such that the total concentrations of proteins, carbohydrates and lipids were similar to the original synthetic wastewater recipe (Table A3.4).

The wastewater recipes were prepared by dissolving the components (Table 5.1 and Table 5.2) in one litre of ultrapure water. As potato starch is inherently insoluble under normal conditions, a stock solution was prepared by adding 1 g of potato starch powder to about 70 mL of ultrapure water that was subsequently heated to 300 °C with occasional stirring until the powder completely dissolved (Jaber, 2020). The solution was then poured into a volumetric flask and topped to a volume of 1 L. The full recipe had a measured chemical oxygen demand (COD) value of 405±5 mg-O_2/L, total organic carbon (TOC) of 120±3 mg-C/L, total nitrogen (TN) of 54±2 mg-N/L, and a pH of 8.2. These values fit into the ranges reported by Volcke et al, (2023) for raw municipal wastewater (Table A3.5).

Table 5.1 Components in recipe simulating domestic wastewater.

Component	Concentration (mg/L)	Description	Supplier
Carbon source			
Meat extract*	189	Mostly proteins	Millipore
Potato starch	103	Carbohydrates	Sigma Aldrich
Glycerol	44.5	Lipids	Sigma Aldrich
Luther Marsh	5	Natural organic matter	Grand River Watershed, ON Canada
Nitrogen source			
Peptone	15	Water-soluble product of partial hydrolysis of proteins	Sigma Aldrich
Urea	75	Carbamide	Sigma Aldrich
NH_4Cl	11	Ammonium chloride	VWR
Phosphorus source			
$Na_3PO_4 \cdot 12H_2O$	61	Tribasic sodium orthophosphate	Sigma Aldrich
Inorganic source			
$NaHCO_3$	300	Sodium bicarbonate	Sigma Aldrich
$MgSO_4 \cdot 7H_2O$	24	Magnesium sulphate	Sigma Aldrich
$CaCl_2 \cdot 2H_2O$	2.5	Calcium chloride	Fisher Scientific

*Note: Meat extract is mostly proteinaceous and includes both carbon and nitrogen and here was arbitrarily labeled as a carbon source, with the realization that it also includes nitrogen.

Table 5.2 Composition and characteristics of matrices employed to assess the effect of carbonaceous and nitrogenous constituents on P removal.

Recipe Name	Recipe Composition[a]	TOC[b] (mg C/L)	TN (mg N/L)	pH (±0.03)
Full	All constituents from Table 5.1	120±3	54±2	8.18
Control	Inorganic constituents only (Table 1).	0	0	8.9
All carbon (all-C)	All carbon sources (Table 5.1)	114±2	22±1	8.22
All nitrogen (all-N)	All nitrogen sources (Table 5.1)	18±1	39±2	8.63
Peptone	Peptone	8±1	2	8.87
Urea	Urea	16±2	37±1	8.81
Ammonium Chloride	NH_4Cl	0	4	8.85
Meat extract (ME)	Meat extract	74±4	21±1	8.33
Starch	Starch	26±3	0	9.01
Glycerol	Glycerol	18±4	0	8.99
Luther Marsh (LM)	Luther Marsh	10±1	0.23±0.02	8.67
Meat extract-N (ME-N)	Meat extract + all nitrogen sources (Table 5.1)	98±5	64±3	8.36
Starch-N	Starch + all nitrogen sources (Table 5.1)	43±2	40±1	8.78
Glycerol-N	Glycerol + all nitrogen sources (Table 5.1)	39±3	39±1	8.80
Luther Marsh (LM-N)	Luther Marsh + all nitrogen sources (Table 5.1)	27±3	41±2	8.53

[a]Concentrations and descriptions of all components are the same as those listed in Table 1. All recipes were prepared in 1 L solution of inorganic "Control". Measured values of the characteristics of each recipe are reported.

[b] TOC is measured instead of COD to monitor carbon content of the recipe in the absence of nitrogen.

5.3.2 P removal batch experiments

Batch experiments were conducted in triplicate at 22±1 ℃ to investigate the effect of carbonaceous and nitrogenous constituents on P removal. Experiments that assessed the effect of each single carbonaceous and nitrogenous constituent, and/or combination, on P removal were conducted using different formulations of the full recipe as illustrated in Table 5.2. Each formulation was designed to highlight different components to assess how the organic matter composition influences the interactions between Fe and P. For starch and glycerol recipes, further tests were conducted using higher concentrations for both constituents (400 mg/L and 260 mg/L respectively) with equivalent TOC values of 100 mg C/L. The inorganic constituents (excluding NH_4Cl) were included in all formulations.

An Fe(III) solution with pH of 2.5 was used as coagulant in all tests and was prepared by dissolving $FeCl_3 \cdot 6H_2O$ (13.6 mg Fe/L) in ultrapure water. All P removal tests were performed in 1 L glass beakers using an Fe/P molar ratio of 1.5 that was achieved by adding the $FeCl_3$ solution to 1 L of synthetic wastewater under fast stirring (600 RPM) conditions for 15 minutes. The resulting suspensions had a pH ranged between 7.2 and 7.3. Samples were collected from the one litre sludge suspension while it was mixed for TP and TFe measurement to ensure consistent sample composition. The initial concentrations of TP and TFe were determined by acid digestion using (37%) HNO_3. In addition, samples were collected and filtered using 0.45 µm cellulose nitrate membrane filters (Whatman, pore size 0.45 µm, diameter 47 mm). Concentrations of total phosphorus (TP) and total iron (TFe) in the filtrate were measured and the P removal was calculated using equation (5-1):

$$\%P\ removal = \frac{(P_o - P_e)}{P_o} \times 100 \qquad (5\text{-}1)$$

where P_o and P_e represent the initial and residual P concentrations (mg P/L) in the liquid phase respectively.

5.3.3 P release batch experiments

5.3.3.1 Iron(III) phosphate (Fe-P) sludge preparation

Fe-P sludges were generated from both the full and control recipes to assess whether the presence of OM during coagulation impacts the subsequent release of P for recovery. Fresh Fe-P sludges with an Fe/P molar ratio of 3.5 were prepared by dosing $FeCl_3.6H_2O$ (40 mg Fe/L) solution into one litre of synthetic wastewater containing Na_3PO_4 (5 mg P/L) under high stirring (600 RPM) for 15 minutes. The Fe/P ratio in these tests was increased relative to the P removal experiments such that sufficient solids were generated for the subsequent desorption experiments. Hence, the pH of the synthetic wastewater solutions was adjusted to 9 by NaOH (1.0 M) before Fe addition to obtain a final pH of 7.1-7.2. Samples (50 mL) were transferred from the one litre sludge suspension, while it was mixed at high rate (600 RPM) on a magnetic stirrer for use in the batch tests. The samples were centrifuged at 4500 RCF for 30 minutes and decanted prior to their use in batch desorption tests.

5.3.3.2 P release from Fe-P sludge

Batch desorption tests were carried out to study the effect of alkaline (pH 10) and ascorbic acid (AA) treatment on P and Fe release from the control and full recipe Fe-P sludges. In order to produce sufficient solids for recovery experiments, the Fe-P solids were generated using the full and control recipes at pH values of (7.22±0.01) and (7.24±0.01) and had higher Fe/P molar ratios of (3.51±0.02 and 3.47±0.03 respectively) than the 1.5 molar ratio used in the removal experiments. The initial concentration ($X_\circ$) of TP and TFe was measured in the sludge solids

obtained after the centrifugation step but before mixing with synthetic wastewater. The methods employed for alkaline and AA treatment to solubilize P and Fe are presented in Alnimer et al. (2023a and 2023b) respectively. All tests were conducted in 50 mL centrifuge tubes containing equal masses of dewatered sludge (amount equivalent to approximately 5 mg dry weight) that were placed on a rotary shaker. For tests assessing the effect of alkaline treatment on P release, sludge samples were mixed with 20 mL of synthetic wastewater and the pH was adjusted to 10 where it was maintained by manual titration with (0.5 M) NaOH over the 8 hour reaction time.

Ascorbic acid tests were conducted inside an anaerobic chamber that was flushed with argon gas (Ar) and consisted of contacting sludge samples with 20 mL of freshly prepared ascorbic acid solution. The Fe/AA molar ratio was set to 1:2 and the solution pH was maintained at 3 by manual titration with (0.5 M) HCl for 2 hours reaction time while monitoring oxidation-reduction potential (ORP). At the end of each test samples were filtered through 0.45 µm cellulose nitrate filter membranes (Whatman, pore size 0.45 µm, diameter 47 mm) and the filtrate concentrations of TP, TFe, and Fe^{2+} were measured. Each batch experiment was run in triplicate. The release of P and Fe was calculated using equation (5-2):

$$\%X\,release = \frac{X_e}{X_o} \times 100 \qquad (5\text{-}2)$$

where X_e and X_o represent the concentration (mg/L) of P or Fe in liquid phase and in initial solid phase respectively.

5.3.4 Chemical analysis

The concentration (w/v) of total suspended solids (TSS) was measured by filtering 150 mL samples using 0.45 µm cellulose nitrate membrane filters (Whatman, pore size 0.45 µm, diameter

47 mm). The filter paper was then dried inside a desiccator at room temperature for 24 hours and the mass of TSS was measured.

The solution pH and ORP values were measured with a digital benchtop meter (Orion Star A211, Thermo Scientific, USA). Inductively Coupled Plasma Optical Emission Spectroscopy (ICP-OES) (PerkinElmer Optima 7300 DV, Waltham, MA, USA) was used to measure concentrations of soluble TP and TFe. Intensities were measured in axial mode at a wavelength of 213.6 nm for P and 238.2 nm for Fe with the viewing height set to 15 mm above the induction coil; the flow rate of the sample pump was set to 2 mL/min, Ar was used as the plasma and auxiliary gas, set to 15 and 0.5 L/min, respectively. Ferrozine method (Viollier et al., 2000) was used for Fe^{2+} determination. TOC and TN were measured using a Total Organic Carbon and Nitrogen Analyzer (TOC-LCPH, Shimadzu, Japan). COD was determined by the US EPA approved dichromate method 410.4 using COD medium range reagent vials - HI93754B-25 (Hanna Instruments, Woonsocket, RI, USA). In these analyses 2 mL of sample were transferred to a ready-to-use vial containing 2 mL of pre-dosed dichromate reagent. The vial then was directly placed in a COD digester (DRB 200, HACH, USA) for 2 hours at 150 °C. Following digestion the absorbance was measured at 600 nm using a DR6000 Benchtop Spectrophotometer (HACH, USA). The COD calibration curve was prepared using known additions of potassium hydrogen phthalate (KHP), dried overnight at 120 °C.

5.3.5 Statistical analysis

Statistical analysis was conducted using either ANOVA or t-tests as appropriate, slope difference, and 95% confidence level overlap analysis. Results of ANOVA and t-tests are indicated by reporting the result of the F or t value, respectively, as well as the corresponding p value; degrees of freedom of the statistical test are reported in brackets.

5.4 Results and discussion

5.4.1 Effect of various formulations on P removal

Phosphorus removal batch tests were conducted with an initial P concentration of 5 mg/L and Fe dose of 13.6 mg /L (Fe/P molar ratio 1.5). To quantify the extent to which matrix composition impacted P removal by Fe(III) salt, these tests were performed using different synthetic wastewater recipes. Figure 5.1 presents the values of P removal and soluble Fe (SFe) residual for each synthetic wastewater formula. It should be noted that the pH for P removal for all tests ranged between 7.1 and 7.3 (Table A3.5) which is typical of the pH range (6-8) observed at WWTPs using CPR (Metcalf and Eddy, 2014; Wilfert et al., 2015). Fig. 5.1a shows P removal for the full (19±1%), all-C (14±1%), all-N (62±1%), and control (62±2%) recipes. The observed P removal was 3 and 4 times higher in the control and all-N recipes than the full and all-C recipes respectively. In contrast to P removal, the full and all-C recipes exhibited notably higher SFe residual values of (63±2%) and (66±1%), respectively compared to the all-N (8±3%) and control (11±2%) recipes. These results indicate that the presence of organic carbon in wastewater can significantly affect P removal and SFe residual while the nitrogenous components have a negligible effect on these responses.

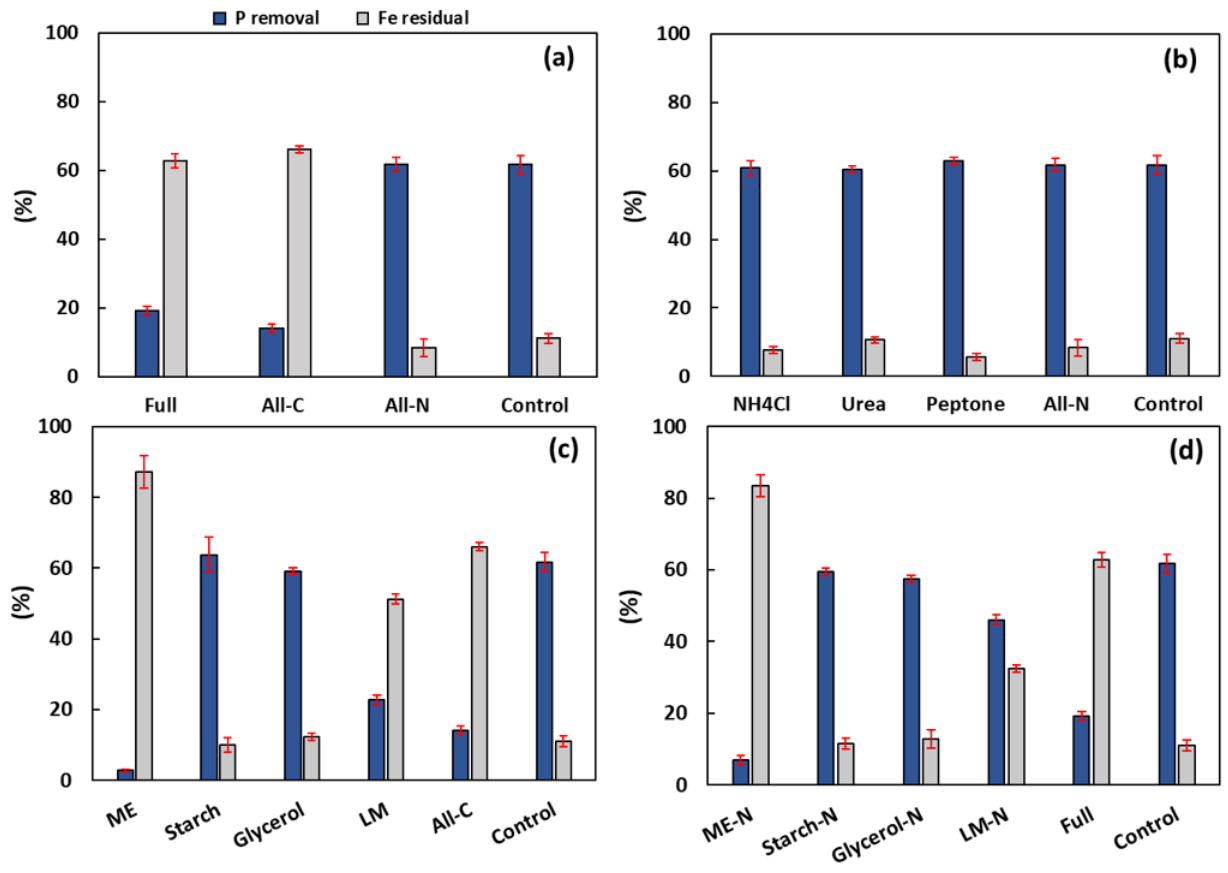

Figure 5.1 P removal and soluble Fe residual (%) using different wastewater formulations. (a) full, carbon sources, nitrogen sources and inorganic control formulations, (b) nitrogenous formulations individually and in combination, (c) carbonaceous formulations individually and in combination, and (d) carbonaceous constituents plus all-N recipe. Note: some bars are repeated across graphs to assist with visual comparisons within each subset of results.

In general, P removal from wastewater by Fe salts at circumneutral pH can occur via either co-precipitation with Fe hydrolysis products (i.e., hydrous ferric oxide, HFO) or by adsorption onto precipitated HFO surfaces (Smith et al., 2008; Wilfert et al., 2015; Ping et al., 2023). However, the presence of organic matter in wastewater could potentially perturb the P removal process, as organic matter can bind Fe cations and solubilize HFO and/or compete with phosphate for adsorption onto surfaces of Fe hydrolysis products (Duan & Gregory, 2003). The elevated

residual soluble Fe for cases where P removal was reduced is consistent the interaction of organic carbon with Fe to reduce P uptake and is subsequently discussed in detail.

The low P removal performance observed for the full and all-C recipes is attributed to the solubilization of a high fraction of the HFO by the carbon constituents as evidenced by the high SFe residual values for both recipes (Fig 5.1a). Further, the high TOC concentrations (Table 5.2) for the full and all-C recipes compared to all-N and core recipes suggest that it is the carbon constituents playing a role in enhancing the solubilization of HFO. Solubilization of a high fraction of HFO will in turn minimize the number of available surfaces and active sites for phosphate to bind to HFO, and thus lowered the P removal. Ome carbon constituents have negatively charged functional groups (i.e., carboxylic, phenolic, and alcoholic) capable of interacting with Fe^{3+} cations and thus suppress the formation and polymerisation of HFO responsible for P removal. Although blocking of existing HFO surface sites is possible by organic matter, the observed solubilization of iron implies the significant pathway was complexation of iron in solution rather than physical-chemical blocking of surface HFO phosphate binding sites. To obtain a better understanding of how the different carbonaceous and nitrogenous constituents impacted P removal by Fe^{3+}, additional batch tests were conducted with single and/or combinations of the carbon and nitrogen sources.

5.4.1.1 Impact of nitrogenous constituents

Nitrogen (N) is a primary nutrient that exists in wastewater in the form of organic and inorganic compounds. In raw municipal wastewater, urea contributes 80% of total organic nitrogen while ammonia nitrogen (NH_4^+-N) accounts for 70%-82% of total inorganic nitrogen (Hanson & Lee, 1971; Li et al., 2017). In this study, urea and peptone were selected to represent organic components, and NH_4Cl was employed for the inorganic component of TN.

The effect of each individual nitrogen component on P removal was evaluated. As illustrated in Fig. 5.1b the NH_4Cl, urea, and peptone recipes exhibited similar P removal performance that were similar to the all-N and control recipes in that there were minimal effects of the components on removal. The P removal values for these recipes were not statistically different (one-way ANOVA, $F(4,25) = 1.74$, $p = 0.173$). It was anticipated that nitrogenous compounds could interact with the Fe^{3+} cation through the amino groups and reduce HFO formation via complexation (similar to the mechanism for carbon compounds discussed above). For example, peptone is a product of partial hydrolysis of proteins and includes amino functional groups (Franek et al., 2000). Urea ($CO(NH_2)_2$) also contains two amino groups ($-NH_2$), which can potentially coordinate with metals through the lone pairs of electrons on the N atom. The formation of an $[Fe(urea)_6]^{3+}$ complex with coordination occurring via oxygen rather than nitrogen atom of urea has been reported (Penland et al., 1957; Charle, 1966; Eltayeb, 2000). However, the observed low SFe residuals (<12%) for all N constituents, similar to the inorganic controls, indicate no significant interactions occurred between Fe^{3+} and N atoms in amino groups for the pH and concentrations used in this study. This suggests no influence of nitrogenous components on either formation of HFO or competing P for active sites. Moreover, the complexation of Fe^{3+} with nitrogen compounds are weaker and thermodynamically less favoured (i.e., no thermodynamic data available at NIST) than the formation of iron phosphate precipitates. Viewed collectively, the results indicate that the availability of Fe^{3+} for phosphorus removal is not significantly affected by the presence of common nitrogen compounds.

5.4.1.2 Impact of carbonaceous constituents

The organic carbon in municipal wastewater originates primarily from human activities such as food waste, washing, and excretion (Huang et al., 2010; Tang et al., 2010). Proteins, carbohydrates, lipids and NOM are considered to be the major carbonaceous components in municipal wastewater (Liu and Liptak, 2000; O'Flaherty & Gray, 2013). For simplicity, in this study ME, potato starch, glycerol, and LM concentrate were selected to represent proteins, carbohydrates, lipids and NOM organic matter components respectively. The influence of each carbonaceous constituent employed in the full and all-C recipes on P removal by Fe^{3+} was explored. Fig. 5.1c demonstrates similar P removal for the control (62±2%), starch (64±5%) and glycerol (61±2%) recipes, and a remarkable reduction in P removal performance for the ME (3±0.4%) and LM (23±1%) recipes. The results suggest no impact of starch and glycerol on P removal, while ME and LM had a significant impact on this response.

Relatively low residual SFe values (Fig. 5.1c) were observed for starch (10±2%) and glycerol (12±1%) indicating minimal impact on formation of HFO flocs although these constituents bear hydroxyl groups (Figure A3.1) capable of complexing Fe^{3+} cations. Moreover, the P removal results indicate that starch and glycerol do not compete with P for adsorption on HFO surface surfaces. This could be attributed to the weak ionization of the hydroxyl groups on the components at the neutral pH that the P removal tests were conducted (Table A3.6). For example, glycerol is considered as a weak acid with pK_a value of 14.15 (Ketchie et al., 2007) and can form soluble complexes with Fe^{3+} at pH > 9 (More & Yokoi, 1994).

To obtain further insight into the impact of starch and glycerol on P removal, batch removal tests were performed with higher concentrations of starch (400 mg/L) and glycerol (260 mg/L) with equivalent TOC values of 100 mg C/L. Fig. 5.2 shows P removal and SFe residual values for the inorganic control, starch and glycerol recipes. Similar results were obtained for control and glycerol recipes, while for starch, P removal was reduced by approximately 50% and the SFe residual increased by 5 fold. The impact of starch at high concentrations is attributed to the starch molecule physically blocking sorption sites on HFO. At high concentrations the weak Van der Waals forces are likely sufficient that the starch molecule coats the surface of HFO to some extent.

The increased solubilization of Fe suggests that there is some soluble phase association between the starch molecules and iron at these elevated concentrations. Singh et al, (2014) demonstrated that when iron oxide nanoparticles are formed by neutralization of acidic ferric solutions in the presence of starch that starch functionalized iron oxide nanoparticles will form; such particles would be measured as dissolved iron in the experiments performed here, and any associated P would also be measured as soluble. The formation of starch-HFO nanocomposites would hinder the formation of HFO flocs and keep P in soluble phase. In summary, the results indicate that carbohydrates and lipids having similar structural properties to starch and glycerol will likely only impact P removal with Fe(III) salts under extreme concentrations. In typical domestic wastewaters the role of carbohydrates and lipids on modifying phosphate removal appears to be negligible.

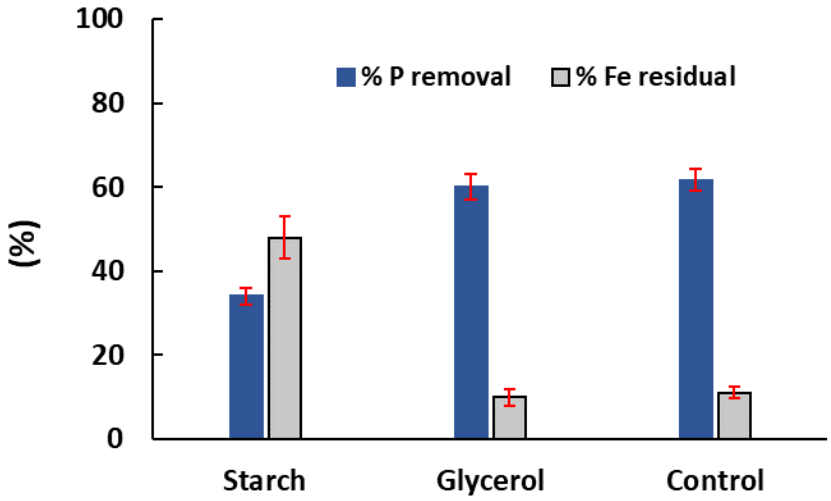

Figure 5.2 P removal and soluble Fe residual (%) for starch and glycerol recipes at elevated concentrations (400 mg/L and 260 mg/L). TOC equivalent to 100 mg C/L for both recipes. Inorganic control results shown for comparison.

The ME and LM recipes exhibited high residual SFe values of (87±5%) and (51±1%) respectively indicating significant interactions between these two components and Fe^{3+} cations. ME appeared to maintain a high fraction of Fe^{3+} in solubilized form by suppressing its hydrolysis and polymerization and subsequently the formation of HFO flocs responsible for P removal. Considering the relative concentrations of TOC (74±4) and TN (21±1) for the ME recipe (Table 5.2) ME was deemed to be a proteinaceous constituent with negatively charged functional groups (i.e., OH^-, $RCOO^-$) and amino groups that were capable of complexing $Fe^{3+}$and hydroxy Fe(III) cations (Tucker et al., 1975;). In addition, proteins can suppress P removal by interacting with phosphates and forming soluble protein-phosphate complexes. It has been reported that many proteins originating from animal sources can interact with phosphates in solution through amino groups that have positively charged nitrogen sites (Parca et al., 2011; Audette et al., 2017). Therefore, it is noteworthy that proteinaceous constituents can negatively impact P removal through interacting with both the Fe^{3+}cation and PO_4^{3-} anion.

The organic matter in the LM concentrate has been previously characterized and consists of terrigenous (allochthonous) materials that are almost exclusively considered as humic acid (Al-Reasi, 2011). The 3.3 fold increase in residual SFe with the LM recipe as compared to the control recipe (Fig. 5.1c), indicates the capability of the LM constituents to form soluble Fe(III) complexes and thus reduce the generation of HFO floc and associated P removal. This was attributed to the presence of carboxyl, benzoic, and phenolic functional groups in the humic acid structure (Figure A3.2) that are able to form stable complexes with hydroxy Fe^{3+}cations (Gu et al., 1994; Sundman et al., 2016). Moreover, LM can reduce P removal by competing with phosphates for active sites on HFO surfaces (Gu et al., 1994; Cui et al., 2014; Alsherbi, 2022). However, the TOC concentrations before and after P removal were 10±1 and 9±1 mg/L respectively. This suggested limited adsorption of humic acids and hence Fe^{3+} solubilization was the main mechanism responsible for reducing P removal.

While both the ME and LM constituents reduced P removal by iron solubilization, the residual SFe with LM was 1.7 fold lower than that with ME (Fig. 5.1c). This could be attributed to the low TOC value for LM compared to ME (Table 5.2) and the lack of amino groups in LM (measured TN=0.23±0.02) which can increase complexation with Fe. Further, the all-C recipe (Fig. 5.1c), had P removal (14±1) and residual SFe (66±1) values between those corresponding to ME and LM alone. Taking into account the negligible effects of starch and glycerol on P removal, the impacts of the all-C recipe could be considered to represent the mixing of the ME and LM recipes. The intermediate performance for the all-C recipe compared to ME alone could be attributed to the interactions between proteins in ME and humic acids in LM. Proteins have positively charged amino groups that can be attracted to negatively charged hydroxyl, carboxyl, and phenolic groups on humic acid and decrease their reactivity; thus, affording the opportunity

for more production of HFO flocs which reduce Fe solubilization and increase P removal. The results are consistent with those of Tan et al, (2008), where formation of stable complexes between humic acids and proteins at pH 7 was observed. Therefore, the interactions between different organics in wastewater could potentially impact P removal by either decreasing or increasing Fe solubilization.

5.4.1.3 Impact of combination of carbonaceous and nitrogenous constituents

In municipal wastewaters OM includes nitrogenous constituents with amino functional groups that are capable of interacting with negatively charged species like phosphates and thus decrease P removal (Audette et al., 2017). The previously described results with ME indicated that the presence of nitrogen in OM reduced P removal. Therefore, the influence of adding the mixed nitrogen source (peptone, urea, and NH_4Cl as in Table 5.1) to each carbonaceous constituent recipe on P removal was investigated. The impact of nitrogen source on starch and glycerol recipes was negligible as the 95% confidence intervals overlapped for P removal and residual SFe values in the presence (Fig. 5.1d) and absence of nitrogen source (Fig. 5.1c). The same effect was also observed for residual SFe values for ME with a no significant increase in P removal in the presence of nitrogen source (p = 3.18). However, the LM recipe exhibited a substantial increase by (23%) in P removal performance in the presence of nitrogen source indicating a positive effect. The observed enhancement in P removal for LM in the presence of nitrogen source was consistent with an interaction between negatively charged groups in LM (carboxyl, hydroxyl, and phenolic groups) and positively charged amino groups available in nitrogen source recipe. This in turn would allow more Fe^{3+} to hydrolyze and generate HFO flocs as reflected by the (18%) decrease in residual SFe.

A reduction in HFO surfaces available for phosphate binding is a proposed mechanism of how organic matter might decrease phosphate removal efficiencies. Such a decrease in binding can either be caused by solubilizing HFO or by organic matter functional groups competing for phosphate adsorption sites on the HFO surface. To gain more insight into the mechanism responsible for reduction in P removal, the relationship between P removal and residual SFe was assessed for carbonaceous constituents in the absence (C) and presence of nitrogen source (C+N). Fig. 5.3 reveals significant negative correlations ($p<0.05$, $R^2 \geq 0.996$) and ($p<0.05$, $R^2 \geq 0.985$) between P removal and residual SFe for both the C+N and C only recipe clusters. Although the presence of nitrogen source enhanced P removal for carbonaceous constituents, both recipe clusters shared the same intercept value and slopes (difference in slope analysis, $p = 0.369$). It can be inferred that carbon sources rich with proteinaceous constituents and humic acids such as ME and LM lower P removal efficiency mainly via solubilizing Fe and suppressing its hydrolysis and HFO floc formation. Carbon sources rich with carbohydrates like starch and lipids like glycerol will have negligible impacts on CPR.

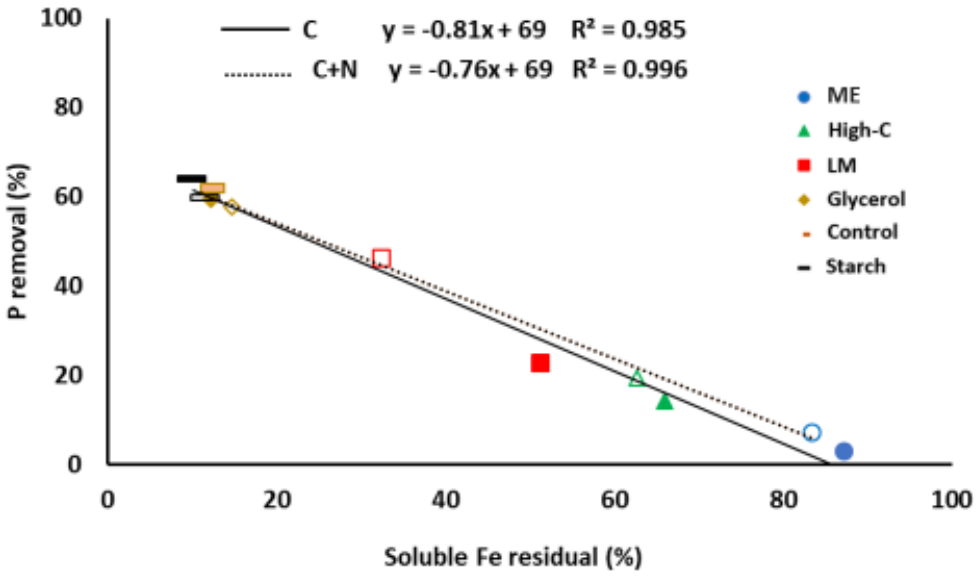

Figure 5.3 Relation between soluble Fe residuals and P removal for carbonaceous recipes (C) (filled marker) and carbonaceous plus nitrogenous recipes (C+N) (unfilled marker).

5.4.2 Effect of OM on P release

Modern wastewater treatment has evolved to the point where resource recovery is becoming a significant priority; especially as phosphorus is a non-renewable resource (Alnimer et al. 2023b). As it was found that the presence of OM affects P removal it was anticipated that it could impact P release from Fe-P sludge, as the organic composite sludge material may have different reactivity compared to inorganic sludge alone. It should be noted that, with the exception of the starch recipe, the TOC concentrations did not change through the P removal test (Table A3.7) indicating negligible OM was co-precipitated in the Fe-P sludge particles. This suggests that the presence of OM could only affect P release from Fe-P sludge through reactions in the bulk solution. For example, the presence of Lewis acid sites on OM might consume OH^- anions if high pH manipulation is utilized for P recovery, or OM might be reduced and consume reducing agent if low pe manipulation is utilized for P recovery. To investigate these possibilities, batch tests were

conducted under (i) wet alkaline (increase pH to 10) treatment and (ii) ascorbic acid treatment (pe decrease) with freshly prepared Fe-P sludge to quantify the extent to which the release of P by these treatments is impacted by OM.

Figure 5.4 presents the release of P and Fe when the solids were generated from the full and control recipes. As shown in Fig. 5.4, P and Fe release from the Fe-P solids that were produced from control and full recipes were similar (95% confidence intervals overlapped) for both treatments. These results were consistent with previously published results for similar treatments of Fe-P sludge (Fe/P molar ratio 1.5) in the absence of OM (Alnimer et al., 2023a and 2023b). The lower P release value for pH 10 treatment in this study (67±3%) when compared to Alnimer et al, (2023) work (90±2%) was consistent with the effect of the Fe/P molar ratio used during sludge production on P release which decreases as the Fe/P molar ratio increases. Moreover, the AA treatment achieved full dissolution of the Fe-P solids with almost all Fe^{3+} reduced to Fe^{2+}. These results suggests that OM had no direct impact on P recovery. However, when the reduction in P removal in the presence of OM is considered this could lead to the net production of lower quality Fe-P solids and/or solids with a higher Fe/P molar ratio as a result of the need to increase Fe doses to achieve P removal targets. This would particularly impact P recovery if the wet alkaline treatment is employed where recovery is not as efficient.

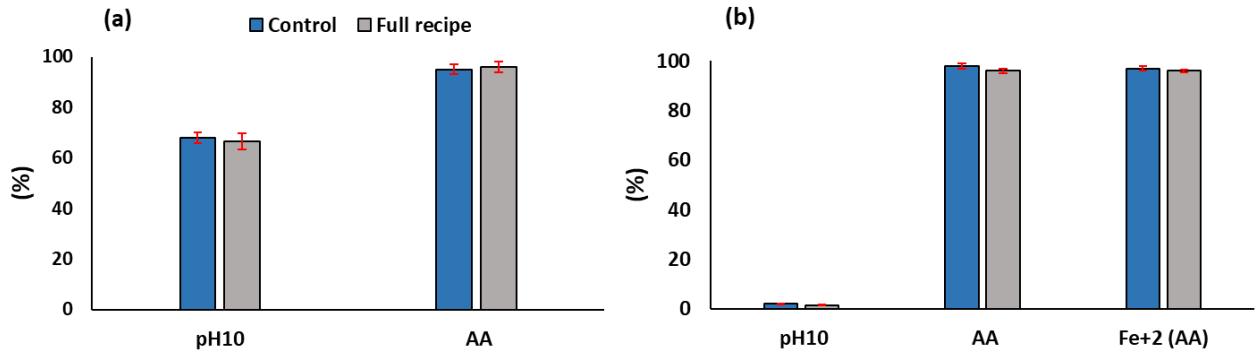

Figure 5.4 Release of (a) TP and (b) TFe from Fe-P solids after wet alkaline (pH 10) and AA treatments.

5.5 Conclusions

The influence of OM on P removal by $FeCl_3$ and on P release from Fe-P sludge by alkaline (pH 10) and ascorbic acid treatments was investigated using synthetic wastewater recipes. The presence of an OM mixture (carbonaceous and nitrogenous constituents) reduced P removal performance 3 fold when compared to an inorganic control. The use of nitrogenous-based recipes including peptone, urea, and ammonium chloride, and carbonaceous recipes including starch and glycerol had no effect on P removal. Low P removal values were observed for ME and LM recipes (3.0±0.4% and 23±1% respectively) when compared to the control recipe (62±2%). No change in P removal performance observed for carbonaceous constituents in the presence of nitrogen source except for LM which exhibited a substantial increase by (23%). Iron(III) solubilization is accountable for the reduction in P removal by ME and LM where high residual SFe values (87±5% and 51±1% respectively) were observed. A significant negative correlation between P removal and residual SFe were observed for carbonaceous constituents in the absence and presence of nitrogen source. Under alkaline (pH 10) and ascorbic acid treatment the presence of OM during sludge generation did not influence P release from the Fe-P sludge. Overall, the finding of this study

provides novel insights into how the presence of different carbonaceous and nitrogenous DOM constituents affect chemical P removal and recovery from wastewater by $FeCl_3$.

5.6 References

Alnimer, A. A., Smith, D.S., Parker, W. J., **2023**. Insight into direct phosphorus release from simulated wastewater ferric sludge: Influence of physiochemical factors. Journal of Environmental Chemical Engineering. 11: 3. doi.org/10.1016/j.jece.2023.110259.

Al-Reasi, H. A., Smith, D. S., Wood, C. M., **2012**. Evaluating the ameliorative effect of natural dissolved organic matter (DOM) quality on copper toxicity to Daphnia magna: improving the BLM. Ecotoxicology, 21(2), 524-537.

Al-Reasi, H. A., Wood, C. M., & Smith, D. S., **2011**. Physicochemical and spectroscopic properties of natural organic matter (NOM) from various sources and implications for ameliorative effects on metal toxicity to aquatic biota. Aquatic Toxicology, 103(3-4), 179-190.

Alsherbi, A. H., **2022**, Influence of Dissolved Organic Matter on Phosphate Interactions with Hydrous Ferric Oxides. Theses and Dissertations. 2457. https://scholars.wlu.ca/etd/2457.

Audette, Y., Smith, D. S., Parsons, C. T., Chen, W., Rezanezhad, F., & Van Cappellen, P., 2020. Phosphorus binding to soil organic matter via ternary complexes with calcium. Chemosphere. 260, 127624.

Béres, K.A., Homonnay, Z., Barta Holló, B., **2023**. Synthesis, structure, and Mössbauer spectroscopic studies on the heat-induced solid-phase redox reactions of hexakis(urea-O)iron(III) peroxodisulfate. Journal of Materials Research. 38, 1102–1118. doi.org/10.1557/s43578-022-00794-w.

Boeije, G., Corstanje, R., Rottiers, A., Schowanek, D., **1999**. Adaptation of the CAS test system and synthetic sewage for biological nutrient removal: Part I: development of a new synthetic sewage. Chemosphere. 38(4):699–709. doi:10.1016/s0045-6535(98)00311-7.

Bowes, M. J., Jarvie, H. P., Halliday, S. J., Skeffington, R. A., Wade, A. J., Loewenthal, M., Gozzard, E., Newman, J. R., Palmer-Felgate, E. J., **2015**. Characterising phosphorus and nitrate inputs to a rural river using high-frequency concentration-flow relationships. The Science of the total environment. 511, 608–620. doi.org/10.1016/j.scitotenv.2014.12.086.

Bunce, J. T., Ndam E., Ofiteru, I. D., Moore, A., Graham, D. W., **2018**. A Review of Phosphorus Removal Technologies and Their Applicability to Small-Scale Domestic Wastewater Treatment Systems. Front. Environ. Sci. doi: 10.3389/fenvs.2018.00008.

Charle, B. C., **1966**. Development in Inorganic nitrogen Chemistry. Elsevier Scientific Publishin Company; Amesterdam, London. Newyork. P296.

Chen, C., Dynes, J. J., Wang, J., and Sparks, D. L., **2014**. Properties of Fe-Organic Matter Associations via Coprecipitation versus Adsorption. Environ. Sci. Technol. 48, 13751–13759. doi:10.1021/es503669u.

Chen, W., Teng, C., Qian, C. & Yu, H., **2019**. Characterizing properties and environmental behaviors of dissolved organic matter using two-dimensional correlation spectroscopic analysis. Environmental Science and Technology. 53, 4683–4694.

Cordell, D., White, S., **2014**. Life's Bottleneck: Sustaining the World's Phosphorus for a Food Secure Future. Annu Rev Environ Resour 39:161–188. doi:10.1146/annurev-environ-010213-113300.

Cui. X., & Choo, K. H., **2014**. Natural orgnic matter removal and fouling control in laow-pressure membrane filtration for water treatment. Environmental Engineering Research, 19 (1), 1-8.

Dai, J., Zhang, Q., Liu, J., Wen. S., Zhang, Y., He, D., Du, Y., **2022**. Coprecipitation of Organic Matter, Phosphate With Iron: Implications for Internal Loadings of Phosphorus in Algae-Dominated and Macrophyte-Dominated Lakes. Front. Environ. Sci. 10:953509. doi: 10.3389/fenvs.2022.953509.

Du, Y., Ramirez, C. E. & Jaffé, R., **2018**. Fractionation of Dissolved Organic Matter by Co-Precipitation with Iron: Effects of Composition. Environ. Process. 5, 5–21. doi.org/10.1007/s40710-017-0281-4.

Duan, J., & Gregory, J., **2003**. Coagulation by hydrolysing metal salts. Advances in colloid and interface science, 100, 475-502.

Eltayeb, A., **2000**. Reaction of urea thiourea and their derivatives with Tertiary phosphine transition Metal halides, MSc., Thesis, University of Khartoun, Sudan.

Franek, F., Hohenwarter, O., Katinger, H. P., **2000**. Plant protein hydrolysates: Preparation of defined peptide fractions promoting growth and production in animal cells cultures. Biotechnol Prog. 16: 688–692.

Ghunmi, L. A., Zeeman, G., van Lier, J., Fayyed, M., **2008**. Quantitative and qualitative characteristics of grey water for reuse requirements and treatment alternatives: the case of Jordan. Water science and technology : a journal of the International Association on Water Pollution Research, 58(7), 1385–1396. doi.org/10.2166/wst.2008.444.

Gu, B., Schmitt, J., Chen, Z., Liang, L., & McCarthy, J. F., **1994**. Adsorption and desorption of natural organic matter on iron oxide: mechanisms and models. Environmental science & technology, 28(1), 38-46.

Hanson, A. M., & Lee, G. F., **1971**. Forms of organic nitrogen in domestic wastewater. Journal - Water Pollution Control Federation, 43(11), 2271–2279.

Hashim, K., Saad, W. I, Safaa, K., Al-Janabi, A., **2021**. Effects of organic matter on the performance

of water and wastewater treatment: Electrocoagulation a case study. IOP Conf. Ser.: Mater. Sci. Eng. doi:10.1088/1757-899X/1184/1/012018.

He, X., Xi, B., Zhang, Z., **2014**. Insight into the evolution, redox, and metal binding properties of dissolved organic matter from municipal solid wastes using two-dimensional correlation spectroscopy. Chemosphere 117, 701–707.

Huang, M. H., Li, Y. M., Gu, G. W., **2010**. Chemical composition of organic matters in domestic wastewater. Desalination, 262:36-42.

Huang, W., Chen, L., Peng, H., **2004**. Effect of NOM characteristics on brominated organics formation by ozonation. Environ. Int. 29 (8), 1049-1055.

Huser, B. J., Egemose, S., Harper, H., Hupfer, M., Jensen, H., Pilgrim, K. M., Reitzel, K., Rydin, E., Futter, M., **2016**. Longevity and effectiveness of aluminum addition to reduce sediment phosphorus release and restore lake water quality. Water Research. 97, 122-132. doi.org/10.1016/j.watres.2015.06.051.

Jung, Y., Koh, H., Shin, W., Sung, N., **2005**. Wastewater treatment using combination of MBR equipped with non-woven fabric filter and oyster-zeolite column. Environmental Engineering Research, 10, 247-256.

Karlsson, T., & Persson, P., **2012**. Complexes with aquatic organic matter suppress hydrolysis and precipitation of Fe(III). Chem. Geol. 322−323, 19−27. doi:10.1016/j.chemgeo.2012.06.003.

Ketchie, W. C., Murayama, M., Davis, R. J., **2007**. Promotional Effect of Hydroxyl on the Aqueous Phase Oxidation of Carbon Monoxide and Glycerol over Supported Au Catalysts. Top. Catal. 44, 307−317.

Kida, M., Fujitake, N., **2020**. Organic carbon stabilization mechanisms in mangrove soils: a review. Forests 11, 981.

Kok, D.D., van Lier, J.B., Uhlenbrook, S., Ortigara, A.R.C., Pande, S., Hubert Savenije. H., **2018**. Global Phosphorus Recovery for Agricultural Reuse. Hydrology and Earth System Sciences Discussions, 1–18. doi:10.5194/hess-2018-176.

Le, C., Kunacheva, C., Stuckey, D. C., **2016**. Protein Measurement in Biological Wastewater Treatment Systems: A Critical Evaluation. Environmental Science & Technology. 50 (6), 3074-3081. doi: 10.1021/acs.est.5b0526.

Li, C., & Sheng, Y., **2021**. Organic matter affects phosphorus recovery during vivianite

crystallization. Water science and technology : a journal of the International Association on Water Pollution Research, 83(8), 2038–2050. doi.org/10.2166/wst.2021.112.

Li, R.H., Cui, J.L., Li, X.D., Li, X.Y., **2018**. Phosphorus removal and recovery from wastewater using Fe-dosing bioreactor and cofermentation: investigation by X-ray absorption near-edge structure spectroscopy. Environ. Sci. Technol. 52 (24), 14119–14128.

Li, Y., Hai-bo Li, H., Xu, X., Xiao, S., Wang, S, Xu, S., **2017**. Fate of nitrogen in subsurface infiltration system for treating secondary effluent. Water Science and Engineering. 10, 3, 217-224. doi.org/10.1016/j.wse.2017.10.002.

Liu, D. H. F., & Liptak, B. G. (Eds.), **1999**. Wastewater Treatment (1st ed.). CRC Press. doi.org/10.1201/9781003075752.

Mekonnen, M., & Hoekstra, A. Y., **2018**. Global Anthropogenic Phosphorus Loads to Freshwater and Associated Grey Water Footprints and Water Pollution Levels: A High-Resolution Global Study. Daugherty Water for Food Global Institute: Faculty Publications. 71. https://digitalcommons.unl.edu/wffdocs/71.

Metcalf and Eddy Inc., Tchobanoglous G., **2014**. Wastewater engineering : treatment and reuse, 5th Edition. McGraw Hill, New York.

Mikutta, C., **2011**. X-ray absorption spectroscopy study on the effect of hydroxybenzoic acids on the formation and structure of ferrihydrite. Geochim. Cosmochim. Acta. 75, 5122–5139. doi.org/10.1016/j.gca.2011.06.002.

Mori, Y., & Yokoi, H., **1994**. Studies on the Interaction between Iron(III) and Glycerol or Related Polyols over a Wide pH Range. Bulletin of the Chemical Society of Japan. 76, 10, 2724-2730. doi.org/10.1246/bcsj.67.2724.

Omoike, A. I., vanLoon, G. W., **1999**. Removal of phosphorus and organic matter removal by alum during wastewater treatment. Water Research. 33, 17, 3617-3627. doi.org/10.1016/S0043-1354(99)00075-5.

Parca, L., Gherardini, P. F., Helmer-Citterich, M., & Ausiello, G., **2011**. Phosphate binding sites identification in protein structures. Nucleic acids research, 39(4), 1231–1242. doi.org/10.1093/nar/gkq987.

Peng, L., Dai, H., Wu, Y., Peng, Y., Lu. X., **2018a**. A Comprehensive Review of Phosphorus Recovery from Wastewater by Crystallization Processes. Chemosphere. 197: 768–81. doi:10.1016/j.chemosphere.2018.01.098.

Penland, R. B., Muushima, S., Curran, C., Quagliano, J. V., **1957**. Infrared absorption spectra of inorganic co-ordination complexes. X. Studies of some metal-urea complexes. J. Am. Chem. Soc. 79:1575-1578.

Ping, Q., Zhang, B., Zhang, Z., Lu, K., Li, Y., **2022**. Speciation analysis and formation mechanisism of iron-phosphrous compounds during chemical phosphorus removal process. Chemosphere 310. 136852–136852. doi.org/10.1016/j.chemosphere.2022.136852.

O'Flaherty, E. & Gray, N. F., **2013**. A comparative analysis of the characteristics of a range of real and synthetic wastewaters. Environ Sci Pollut Res. 20: 8813–8830. doi:10.1007/s11356-013-1863-y.

Qualls, R. G., Sherwood, L. J., Richardson., C. J., **2009**. Effect of natural dissolved organic carbon on phosphate removal by ferric chloride and aluminum sulfate treatment of wetland waters. Water Resources Research. (45): W09414, doi:10.1029/2008WR007287.

Raunkjaer, K., Hvitvedjacobsen, T., Nielsen, P. H., **1994**. Measurement of pools of protein, carbohydrate and lipid in domestic waste-water. Water Research. 28: 251-262.

Riedel, T., Zak, D., Biester, H., Dittmar T., **2013**. Iron traps terrestrially derived dissolved organic matter at redox interfaces. Proc Natl Acad Sci 110:10101–10105. doi.org/10.1073/pnas.1221487110.

Sundman, A., Karlsson, T., Sjöberg, S., Persson, P., **2016**. Impact of iron–organic matter complexes on aqueous phosphate concentrations. Chemical Geology. 426, 109-117. doi.org/10.1016/j.chemgeo.2016.02.008.

Smith, S., Takacs, I., Murthy, S., Daigger, G. T., Szabo, A., **2008**. Phosphate Complexation Model and Its Implications for Chemical Phosphorus Removal. Water Environ. Res. 80 (5): 428−438.

Singh, P. N., Tiwary, D., Sinha, I., **2014**. Improved removal of Cr(VI) by starch functionalized iron oxide nanoparticles. Journal of Environmental Chemical Engineering. 2 (4) 2252-2258. doi.org/10.1016/j.jece.2014.10.003.

Szabó, A., Takács, I., Murthy, S., Daigger, G. T., Licskó, I., Smith, S. D., **2008**. Significance of Design and Operational Variables in Chemical Phosphorus Removal. Water Environment Research 80 (5): 407–16. doi:10.2175/106143008X268498.

Sharma, P.; Ofner, J.; Kappler, A., **2010**. Formation of binary and ternary colloids and dissolved complexes of organic matter, Fe and As. Environ. Sci. Technol. 2010, 44, 4479–4485.

Shon, H. K., Vigneswaran, S., & Snyder, S. A., **2006**. Effluent Organic Matter (EfOM) in Wastewater: Constituents, Effects, and Treatment. Critical Reviews in Environmental Science and Technology, 36(4), 327–374. doi.org/10.1080/10643380600580011.

Shon, H. K., Vigneswaran, S., Ben Aim, R., Ngo, H.H., Kim, I.S., Cho, J., **2005b**. Influence of flocculation and adsorption as pretreatment on the fouling of ultrafiltration and nanofiltration

membranes: application with biologically treated sewage effluent. Environ. Sci. Technol. 39(10), 3864–3871.

Sophonsiri, C., & Morgenroth, E., **2004**. Chemical composition associated with different particle size fractions in municipal, industrial, and agricultural wastewaters. Chemosphere. 55: 691-703.

Sindelar, H. R., Brown, M. T., & Boyer, T. H., **2015**. Effects of natural organic matter on calcium and phosphorus co-precipitation. Chemosphere, 138, 218–224. doi.org/10.1016/j.chemosphere.2015.05.008.

Tan, W. F., Koopal, L. K., Weng, L. P., van Riemsdijk, W. H., Norde, W., **2008**. Humic acid protein complexation. Geochim. Cosmochim. Acta. 72: 2090-2099.

Tang, S., Wang, Z., Wu, Z. and Zhou, Q., **2010**. Role of dissolved organic matters (DOM) in membrane fouling of membrane bioreactors for municipal wastewater treatment. Journal of Hazardous materials 178(1-3), 377-384.

Taujale, S., Baratta, L. R., Huang, J., Zhang, H., **2016**. Interactions in Ternary Mixtures of MnO_2, Al_2O_3, and Natural Organic Matter (NOM) and the Impact on MnO_2 Oxidative Reactivity. Environ. Sci. Technol. 50, 2345−2353.

Tucker, W. F., Asplund, R. O., Holt, S. L., **1975**. Preparation and properties of Fe^{3+}-amino acid complexes: Crystalline complexes with aliphatic amino acids. Archives of Biochemistry and Biophysics. 166, 2, 433-438. doi.org/10.1016/0003-9861(75)90406-3.

Venkiteshwaran, K., McNamara, P.J., Mayer., B.K., **2018**. Meta-Analysis of Non-Reactive Phosphorus in Water, Wastewater, and Sludge, and Strategies to Convert It for Enhanced Phosphorus Removal and Recovery. Science of the Total Environment. 644: 661–74. doi:10.1016/j.scitotenv.2018.06.369.

Volcke, E. I. P., Solon, K., Comeau, Y., Henze, M., **2023**. Wastewater Characteristics. Edited by Guanghao Chen; Mark C.M. van Loosdrecht; George A. Ekama; Damir Brdjanovic., Biological Wastewater Treatment: Principles, Modelling and Design. Chapter 3 (77-110). IWA Publishing. doi.org/10.2166/9781789060362_0077.

Viollier, E., Inglett, P. W., Hunter, K., Roychoudhury, A. N., van Cappellen, P., **2000**. The ferrozine method revisited: Fe(II)/Fe(III) determination in natural waters, Appl. Geochem. 15: 785–790. doi.org/10.1016/S0883-2927(99)00097-9.

Wilfert, P., Prashanth S. K., Korving, L., Witkamp, G. J., van Loosdrecht, M.C.M., **2015**. The Relevance of Phosphorus and Iron Chemistry to the Recovery of Phosphorus from Wastewater: A Review. Environmental Science and Technology 49 (16): 9400–9414. doi:10.1021/acs.est.5b00150.

Wu, Y., Luo, J. Y., Zhang Q., Aleem, M., Fang, F., Xue, Z. X., Cao, J. S., **2019**. Potentials and challenges of phosphorus recovery as vivianite from wastewater: a review. Chemosphere. (226) 246–258. doi.org/10.1016/j.chemosphere.2019.03.138.

Yuan, R., Shen, Y., Zhu, N., Yin, C., Yuan, H. & Dai, X., **2019**. Pretreatment-promoted sludge fermentation liquor improves biological nitrogen removal: molecular insight into the role of dissolved organic matter. Bioresource Technology. 293, 122082.

Zhang, H., Taujale, S., Huang, J., Lee, G.-J., **2015**. Effects of NOM on Oxidative Reactivity of Manganese Dioxide in Binary Oxide Mixtures with Goethite or Hematite. Langmuir 2015, 31, 2790−2799.

Zhao, Q., Poulson, S.R., Obrist, D., Sumaila, S., Dynes, J.J., McBeth, J.M., Yang, Y., **2016**. Ironbound organic carbon in forest soils: quantification and characterization. Biogeosciences. 13, 4777–4788.

Zhou, Z., Hu, D., Ren, W., Zhao, Y., Jiang, L. M., & Wang, L., **2015**. Effect of humic substances on phosphorus removal by struvite precipitation. Chemosphere, 141, 94-9.

Chapter 6 Conclusions & Future Work

6.1 Conclusions

In wastewater treatment, chemically mediated P removal using iron(III) salts generates iron-phosphate (Fe-P) sludge. P release and recovery from Fe-P sludge represents a potential sustainable source of phosphorus for use in fertilizer but is potentially challenging. To attempt to identify and resolve these challenges, this study provides clear knowledge about the performance of direct P release and recovery from the inorganic fraction of Fe-P sludge in the absence of potentially confounding organic matter and microorganisms. In lab bench scale, simulated Fe-P sludge that mimicked the inorganic composition of actual Fe-P sludge in CPR plants was utilized for different treatments including wet acidic/basic, competing anions, and reducing agent treatments. As a step towards more complex, realistic water chemistries, the influence of organic matter on CPR was addressed. Based on this research the following conclusions can be made:

1. Alkaline treatment (pH≥10) was effective in releasing P from Fe-P sludge. At pH≥10 the concentration of OH^- is high enough to substantially replace P in the Fe-P sludge resulting in formation of ferric hydroxide $Fe(OH)_{3(s)}$ and liberating P (P release 90±2%). Further, the positive surface charge of HFO is decreased as pH increases leading to electrostatic repulsion between phosphate anions and the evolving negative surface charge which also results in an increase in P desorption.

1.1 Fe:P molar ratio affects P release. Under alkaline treatment, the amount of P released was found to decrease as Fe:P molar ratio increased. From a practical perspective, higher Fe:P ratios would be beneficial in increasing the removal efficiency of P from wastewater, but this would reduce the potential for P release and recovery from the resultant sludge.

1.2 P release was affected by Fe-P sludge age. Solids aging reduces alkaline pH-induced P release from Fe-P sludge significantly after 5 days. Aging during time frames that reflect the residence times of Fe-P sludge in CPR plants (i.e., 1 to 12 days), cause HFOs structures to become more compact and transform from amorphous to more crystalline. This results in a reduction in surface area and P would be occluded (trapped) inside HFOs particles. Moreover, as the solids age, the surface bound P may be incorporated into the bulk structure of HFO and removed from the exchangeable surface. This was qualitatively supported by arsenic extraction and HFO surface area determination. Therefore, solids residence time of Fe-P sludge should be minimized to five days or less for the purpose of P recovery.

1.3 The reduction in P release by aging was most simply described by Zero-order kinetic model . The zero order model provides a reasonable description of P release from aged sludge and is simpler than a first order model. However, the dependence of P release rate on initial concentration of P was not assessed. The use of a first order model might be considered in the future if data describing a greater range of initial P concentrations were to become available.

2- P release was not affected by chloride anion. The relatively weak chloride binding at the surface adsorption sites on HFO made the effect of chloride insignificant on P release and reflected weaker chloride complexes compared to phosphates.

3- Ascorbic acid treatment was highly effective in releasing P form Fe-P sludge. The reductive dissolution by AA on Fe-P sludge at Fe/AA molar ratio 1:2 and pH values 3 and 4 was effective and full solubilization of Fe-P sludge was achieved. Sludge aging (up to 11 days) did not affect the reductive dissolution of Fe-P sludge by AA, demonstrating the suitability of AA treatment for sludges with extended residence times. The use of hydroxylamine (reducing agent) was not

effective in reducing Fe^{3+} in Fe-P sludge. Oxalic acid as a chelating agent was effective in solubilizing Fe-P sludge at oxic conditions and stronger in chelating Fe than AA. Inorganic acids showed low effect (<10%) on releasing P and Fe at pH 3 compared to AA and oxalic acid.

4- P recovery as vivianite after AA treatment was feasible. Reductive dissolution has an advantage over simple chelation to solubilize the iron in that the reduced Fe-P mineral vivianite can be formed directly after dissolution by simple pH adjustment. After acidic AA treatment P and Fe were recovered from solution in the form of vivianite by increasing the solution pH to 7 with %recovery of 88±2% and 90±1% respectively. XRD, Fe/P molar ratio measurements, and magnetic attraction all conformed qualitatively and quantitively vivianite formation.

5- PHREEQC showed reasonable simulations. For wet alkaline treatment, modeling with the PHREEQC geochemical software did not always agree with the measured release of phosphorus from the Fe-P sludge. PHREEQC assumes all surface sites for phosphorus are exchangeable and has no mechanism to represent phosphorus trapped within HFO particles. However, for ascorbic acid treatment, PHREEQC modeling showed a reasonable agreement with the measured release of P and Fe from Fe-P sludge and vivianite formation suggesting it as a good tool for interpreting and predicting P and Fe release and recovery systems.

6- Organic matter particularly proteinaceous constituents and NOM modify CPR by Fe(III) salts. P removal performance showed significant decrease in the presence of protein-like constituents (meat extract) and NOM (Luther Marsh) where %P removal was (3±0.4%) and (23±1%) respectively compared to (62±2%) release for inorganic control (no organic matter) experiments. Results for soluble Fe measurements conformed that HFO solubilization is the mechanism responsible for the reduction in P removal due to the interactions between Fe(III) and negatively charged functional groups (i.e., hydroxyl, carboxyl, and phenolic groups) on NOM and

proteinaceous materials. However, nitrogenous (peptone, urea, and NH_4Cl) and carbonaceous (starch and glycerol) constituents showed negligible effect on P removal. Further, no change in P removal performance observed for carbonaceous constituents in the presence of nitrogen source except for LM which exhibited a substantial increase by 23%.

7- P release from Fe-P sludge was not affected by organic matter. Both wet alkaline (pH 10) and ascorbic acid treatments for P release from Fe-P sludge were not influenced by the presence of organic matter during Fe-P sludge formation. However, considering the negative effect of OM on P removal, the presence of organic matter (NOM and proteinaceous materials) during sludge formation could lead to production of lower quantity Fe-P solids and/or solids with high Fe/P molar ratio as a result of increasing Fe doses to achieve desired P removal. This could impact P recovery indirectly, particularly if the less efficient (compared to redox manipulation) wet alkaline treatment is employed.

6.2 Recommendations for Future Work

Phosphorus recovery as vivianite by AA treatment for Fe-P sludge at pH values 3 and 4 is a promising route for P recovery from wastewater sludge. It was achieved in the absence (this study) and in the presence (Xu et al., 2023) of organic matter. Therefore, it is recommended that further studies should be focus the following:

1. Investigate the influencing factors of vivianite formation in depth, particularly the crystallization mechanism (i.e., addition of seed crystals to increase vivianite size and purity) and the impact of organic matter in order to optimize the operating conditions precisely.

2. Develop different separation and purification procedures of vivianite to enhance the recovery efficiency and product purity.

Appendices

Appendix 1 (Chapter 3 appendix)

Table A1.1. Inorganic components of synthetic wastewater adapted from Jung *et al.* (2005).

Chemical Reagent	Concentration (mg/L)
Magnesium sulfate ($MgSO_4.7H_2O$)	24.0
Calcium chloride ($CaCl_2.2H_2O$)	2.40
Sodium bicarbonate ($NaHCO_3$)	300.0
Sodium phosphate tribasic ($Na_3PO_4.12H_2O$) (mg P/L)	50.00

Mass balance sample calculations

a) Fe-P solids precipitation (P removal process)

Prior to the batch recovery tests Fe-P sludge solids with Fe/P molar ratio 1.5 were prepared by removal (precipitation) of 50 mg/L soluble phosphorus by suitable Fe dose according to the following formula:

Fe(III) dose (mg/L) = *(Fe/P molar ratio)* × *P conc. (mg/L)* × $(\frac{Fe\ atomic\ mass}{P\ atomic\ mass})$ (Metcalf and Eddy, 2014; WEF, 2011)

Fe dose required for removal of 50 mg P/L = $1.5 \times 50 \frac{mg}{L} \times \frac{55.85}{30.97}$ = 135.25 mg Fe/L.

Mass balance formula : Input = output + build up, where,

Input = initial Fe and P concentrations mg/L, (theoretically calculated)

Output= residual Fe and P concentrations mg/L in solution, (measured)

Build up= Fe and P concentrations mg/L in solid Fe-P sludge, (measured)

Table A1.2. Mass balance tests (Fe-P solids precipitation)

Element	Input (mg/L)	Output (mg/L)	Build up (mg/L)	Output + build up (mg/L)	% Error
P	50	5.74±0.41	46.62±0.51	52.4±0.7	4.8±1.4%
Fe	136.25	1.54±0.26	130.3±3.3	131.9±3.3	3.2±2.4%

b) Mass balance tests (P recovery batch experiments)

Recovery batch tests involved releasing P and Fe from Fe-P solids. The initial P and Fe concentrations in Fe-P solids were determined by acidic digestion of Fe-P solids and ICP-OES.

Mass balance formula : Input = output + build up, where,

Input = initial Fe and P concentrations mg/L, in Fe-P solids before reaction starts (measured)

Output= Fe and P concentrations mg/L in solution after reaction completion, (measured)

Build up= Fe and P concentrations mg/L in solid Fe-P sludge remined after reaction completion, (measured)

Table A1.3. Mass balance tests (P recovery batch experiments)

Element	Input (mg/L)	Output (mg/L)	Build up (mg/L)	Output + build up (mg/L)	% Error
P	47.67±1.12	20.37±0.61	29.03±0.56	49.4±0.8	3.62±2.89%
Fe	129.2±2.1	6.016±0.20	120.03±1.5	135.2±2.1	4.64±2.32%

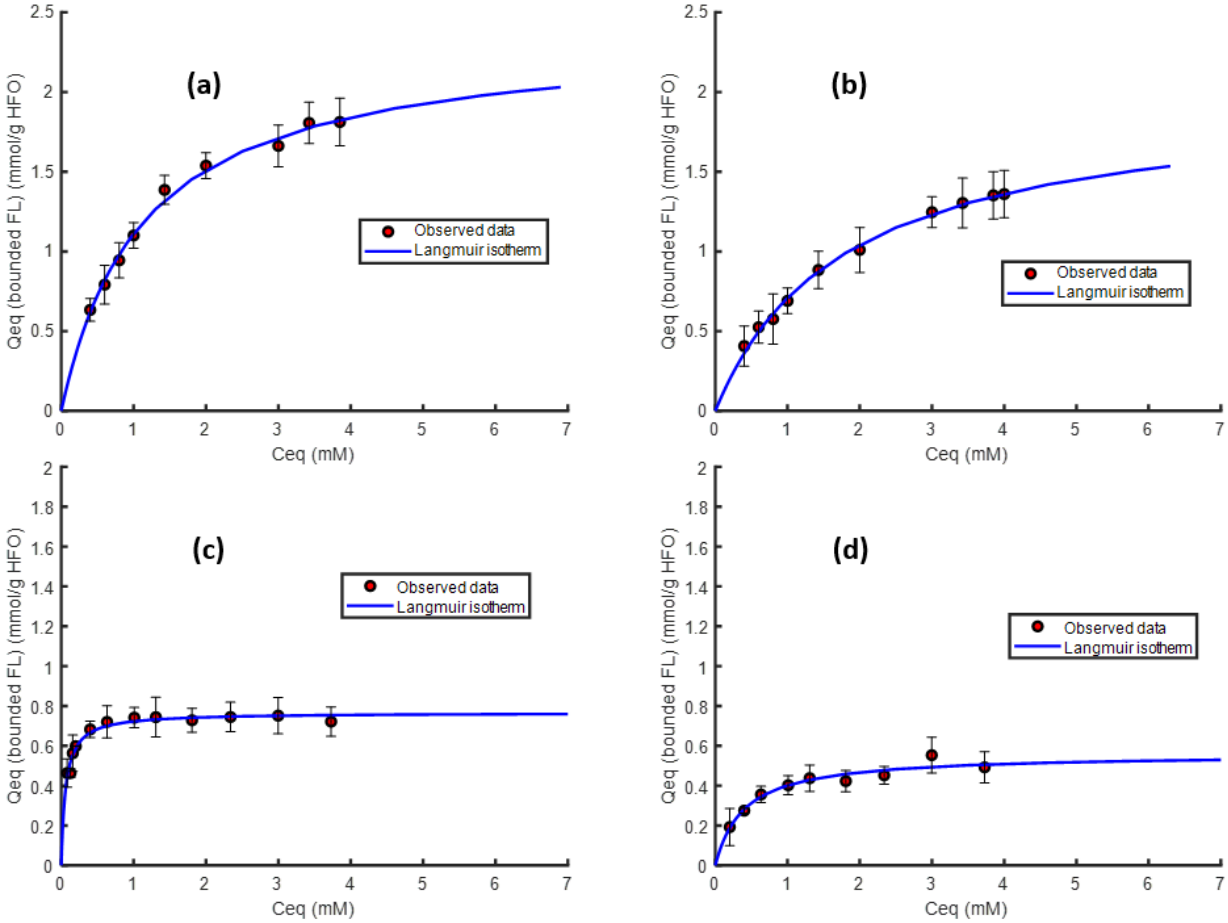

Figure A1.1. Adsorption isotherms for fluorescein (FL) uptake with HFO at different aging times and pH 6.5 fitted with Langmuir model (a) fresh HFO, (b) 5 days aged HFO, (c) 9 days aged HFO, and (d) 11 days aged HFO.

Table A1.4. List of soluble species, solid phases, and surface complexation reactions added or/and modified to PHREEQC database with their corresponding logK values.

Soluble species	Reaction	Log K_{eq} at 25℃	Reference
HPO_4^{2-}	$PO_4^{3-} + H^+ \rightleftharpoons HPO_4^{2-}$	11.66	(Smith et al., 2008)
$H_2PO_4^-$	$PO_4^{3-} + 2H^+ \rightleftharpoons H_2PO_4^-$	18.64	(Smith et al., 2008)
H_3PO_4	$PO_4^{3-} + 3H^+ \rightleftharpoons H_3PO_4$	20.65	(Smith et al., 2008)
$FeOH^{2+}$	$Fe^{3+} + H_2O \rightleftharpoons FeOH^{2+} + H^+$	-2.77	(Smith et al., 2008)
$Fe(OH)_2^+$	$Fe^{3+} + 2H_2O \rightleftharpoons Fe(OH)_2^+ + 2H^+$	-6.29	(Smith et al., 2008)
$Fe(OH)_4^-$	$Fe^{3+} + 4H_2O \rightleftharpoons Fe(OH)_4^- + 4H^+$	-21.77	(Smith et al., 2008)
$FeHPO_4^+$	$Fe^{3+} + HPO_4^{2-} \rightleftharpoons FeHPO_4^+$	19.96	(Smith et al., 2008)
$FeH_2PO_4^{2+}$	$Fe^{3+} + H_2PO_4^- \rightleftharpoons FeH_2PO_4^{2+}$	22.11	(Smith et al., 2008)
Eq. Phases (solids, fix pH and pe)	Reaction	Log K_{sp} at 25℃	Reference
Strengite	$FePO_4.2H_2O \rightleftharpoons Fe^{3+} + PO_4^{3-} + 2H_2O$	-25*	(NIST, 2001; Smith et al., 2008)
Struvite	$MgNH_4PO_4.6H_2O \rightleftharpoons Mg^{2+} + NH_4^+ + PO_4^{3-} + 6H_2O$	-13.26	(Taylor et al., 1963)
Scorodite	$FeAsO_4.2H_2O \rightleftharpoons Fe^{3+} + AsO_4^{3-} + 2H_2O$	-20.429	(Nordstrom and Archer 2003)
pH_Fix	H+ = H+	0.0	Define pH fixing mineral
pe_Fix	e- = e-	0.0	Define pe fixing mineral
HFO surface complexation	Reaction	LogK at 25℃	Reference
$\equiv FeH_2PO_4$	$\equiv FeOH + PO_4^{3-} + 3H^+ \rightleftharpoons \equiv FeH_2PO_4 + H_2O$	35.5	(Smith et al., 2008)
$\equiv FeHPO_4^-$	$\equiv FeOH + PO_4^{3-} + 2H^+ \rightleftharpoons \equiv FeHPO_4^- + H_2O$	30	(Smith et al., 2008)
$\equiv FePO_4^{2-}$	$\equiv FeOH + PO_4^{3-} + H^+ \rightleftharpoons \equiv FePO_4^{2-} + H_2O$	20.5	(Smith et al., 2008)
$\equiv FeH_2AsO_4$	$\equiv FeOH + AsO_4^{3-} + 3H^+ \rightleftharpoons \equiv FeH_2AsO_4 + H_2O$	29.31	PHREEQC wateq4f.dat
$\equiv FeHAsO_4^-$	$\equiv FeOH + AsO_4^{3-} + 2H^+ \rightleftharpoons \equiv FeHAsO_4^- + H_2O$	23.51	PHREEQC wateq4f.dat
$\equiv FeOHAsO_4$	$\equiv FeOH + AsO_4^{3-} \rightleftharpoons \equiv FeOH + AsO_4^{3-}$	10.58	PHREEQC wateq4f.dat

*The NIST (2001) contains a range of log K_{sp} values for strengite, depending on particle size and form, of between -21.8 (amorphous) and -26.8 (crystalline).

Table A1.5. PHREEQC input data file example

```
# Example for calculating total concentrations of Fe and P at pH 10 after 24
hours reaction time.

SOLUTION 1
      temp      22
      pH        10
      pe        10.75
      units     mg/l
      density   1                   # density, default 1 Kg/LA
      Fe(3)     128                 # Total concentration of element.
      P         46
      Mg        3.34
      S         3.122
      Ca        0.614
      C         42.89
      Na        220.09              # NaT=NaT+3*PT   For charge balance
      Cl        385.16              # ClT=ClT+3*FeT
      -water    1                   # kg water, default = 1 Kg


PHASES

Struvite

MgNH4PO4:6H2O = Mg+2 + NH4+ + PO4-3 + 6H2O

   log_k           -13.26

Strengite

FePO4:2H2O = Fe+3 + PO4-3 + 2H2O

   log_k    -25

Fe(OH)3(a)

Fe(OH)3 + 3 H+ = Fe+3 + 3 H2O

   log_k    4.891


EQUILIBRIUM_PHASES 1

Fe(OH)3(a)    0.0   0

Vivianite     0.0   0

Calcite       0.0   0

Hydroxyapatite   0.0   0

Siderite      0.0   0

Pyrite       0.0   0

FeS(ppt)     0.0   0
```

```
Strengite   0.0   0
       pH_Fix -10          HCl 10.0
-force_equality true
       pe_Fix -10.75          O2
-force_equality true

SURFACE 1
Hfo_wOH   Fe(OH)3(a)  equilibrium_phase 0.2     1e5
Hfo_sOH   Fe(OH)3(a)  equilibrium_phase 0.005

  End
```

Table A1.6. P release (%) from Fe-P sludge at different aging times at pH 9 and 10

Sludge Age/Day	pH 9	pH 10
1	40 ± 2	90 ± 2
5	26 ± 4	86 ± 1
9	15 ± 2	53 ± 2
11	18 ± 2	57 ± 3

Table A1.7. Percent of exchangeable P obtained by As(V) extraction for 24 hours at pH 6

Sludge Age/Day	1	5	9	11
%Exchangeable P	43.12±0.94	28.27±1.14	26.11±0.08	25.04±0.20

Table A1.8. Summary of estimated max adsorption capacities and surface areas for HFOs

HFO Age	$Q_{m\ (mmol/g)}$	R^2	SA m^2/g
fresh	2.34±0.14	0.9879±0.0121	515±31
5 days	2.00±0.25	0.9923±0.0116	440±51
9 days	0.765±0.032	0.9518±0.0343	168±7
11 days	0.594±0.085	0.9451±0.0243	130±18

References

Jung, Y., Koh, H., Shin, W., Sung, N. **2005**. Wastewater treatment using combination of MBR equipped with non-woven fabric filter and oyster-zeolite column. Environmental Engineering Research, 10, 247-256.

Metcalf and Eddy Inc., Tchobanoglous G., **2014**. Wastewater engineering : treatment and reuse, 5th Edition. McGraw Hill, New York.

WEF. 2011. Nutrient Removal - Manual of Practice. WEF Manual of Practice No. 34.

Smith, S.. Takacs, I., Murthy, S., Daigger, G. T., Szabo, A., **2008**. Phosphate Complexation Model and Its Implications for Chemical Phosphorus Removal. Water Environ. Res. 80 (5): 428−438.

National Institute of Standards and Technology, **2001**. NIST Standard Reference Database 46. National Institute of Standards and Technology: Gaithersburg, Maryland.

Taylor, A. W., Frazier, A. W., Gurney, E. L., **1963**. Solubility products of magnesium ammonium and magnesium potassium phosphates. Transactions Faraday Society, 59, 1580-1584.

Szabo, A., Takács, I., Murthy, S., Daigger, G.T., Licsko, I., Smith, S., 2008. Significance of design and operational variables in chemical phosphorus removal. Water Environ. Res., 80, 407-416.

Nordstrom, D.K., Archer, D.G., **2003**. Arsenic thermodynamic data and environmental geochemistry, in Arsenic in Ground Water. (eds A.H. Welch and K.G. Stollenwerk), Kluwer Academic Publishers, Boston, pp. 1–25.

Appendix 2 (Chapter 4 appendix)

Table A2.1. Inorganic components of synthetic wastewater adapted from Jung et al. (2005).

Chemical Reagent	Concentration (mg/L)
Magnesium sulfate ($MgSO_4.7H_2O$)	24.0
Calcium chloride ($CaCl_2.2H_2O$)	2.40
Sodium bicarbonate ($NaHCO_3$)	300.0
Sodium phosphate tribasic ($Na_3PO_4.12H_2O$) (mg P/L)	50.00

Vivianite synthesis procedure

Synthetic vivianite was prepared by mixing 0.2 M of ($K_2HPO_4 \cdot 3H_2O$, Sigma-Aldrich, ≥99%) and (0.3 M of $FeCl_2 \cdot 4H_2O$, Fisher Scientific, ≥99%) in 60 mL of deoxygenated ultra pure water (Milli-Q®, (Millipore Corporation), <18.2 MΩ resistance) in a 150 mL 2 necked round bottom flask. The solution was stirred at 500 RPM at room temperature with nitrogen purging for 2 days (Roldan et al., 2002; Wilfert et al., 2016). The resulting slurry was centrifuged, and the solid product was washed with deoxygenated ultra pure water 3 times, then dried under vacuum at room temperature. The vivianite product was blue which indicated partial oxidation of Fe^{2+} (Zhang et al., 2022).

Table A2.2. List of soluble species, solid phases, and surface complexation reactions added or/and modified to PHREEQC database with their corresponding logK values.

Soluble species	Reaction	Log K_{eq} at 25℃	Reference
HPO_4^{2-}	$PO_4^{3-} + H^+ \rightleftharpoons HPO_4^{2-}$	11.66	(Smith et al., 2008)
$H_2PO_4^-$	$PO_4^{3-} + 2H^+ \rightleftharpoons H_2PO_4^-$	18.64	(Smith et al., 2008)
H_3PO_4	$PO_4^{3-} + 3H^+ \rightleftharpoons H_3PO_4$	20.65	(Smith et al., 2008)
$FeOH^{2+}$	$Fe^{3+} + H_2O \rightleftharpoons FeOH^{2+} + H^+$	-2.77	(Smith et al., 2008)
$Fe(OH)_2^+$	$Fe^{3+} + 2H_2O \rightleftharpoons Fe(OH)_2^+ + 2H^+$	-6.29	(Smith et al., 2008)
$Fe(OH)_4^-$	$Fe^{3+} + 4H_2O \rightleftharpoons Fe(OH)_4^- + 4H^+$	-21.77	(Smith et al., 2008)
$FeHPO_4^+$	$Fe^{3+} + HPO_4^{2-} \rightleftharpoons FeHPO_4^+$	19.96	(Smith et al., 2008)
$FeH_2PO_4^{2+}$	$Fe^{3+} + H_2PO_4^- \rightleftharpoons FeH_2PO_4^{2+}$	22.11	(Smith et al., 2008)
$H_2C_2O_4$	$2H^+ + C_2O_4^{2-} \rightleftharpoons H_2C_2O_4$	-5.6	(NIST, 2001)
$HC_2O_4^-$	$H^+ + C_2O_4^{2-} \rightleftharpoons HC_2O_4^-$	-4.3	(NIST, 2001)
$Fe(C_2O_4)^+$	$Fe^{3+} + C_2O_4^{2-} \rightleftharpoons Fe(C_2O_4)^+$	9.2	(NIST, 2001)
$Fe(C_2O_4)_2^-$	$Fe^{3+} + 2C_2O_4^{2-} \rightleftharpoons Fe(C_2O_4)_2^-$	15.5	(NIST, 2001)
$Fe(C_2O_4)_3^{3-}$	$Fe^{3+} + 3C_2O_4^{2-} \rightleftharpoons Fe(C_2O_4)_3^{3-}$	19.8	(NIST, 2001)
H_2A	$2H^+ + A^{2-} \rightleftharpoons H_2A$	-11.82	(Gamov et al., 2022)
HA^-	$H^+ + HA^- \rightleftharpoons HA^-$	-4.31	(Gamov et al., 2022)
FeA^+	$Fe^{3+} + A^{2-} \rightleftharpoons FeA^+$	9.5	(Ritacca et al., 2022)
FeOHA	$Fe^{3+} + OH^- + A^{2-} \rightleftharpoons FeOHA$	21.1	(Ritacca et al., 2022)
$Fe(A)_2^-$	$Fe^{3+} + 2A^{2-} \rightleftharpoons Fe(A)_2^-$	18.8	(Ritacca et al., 2022)
$Fe(OH)_2A^-$	$Fe^{3+} + 2OH^- + A^{2-} \rightleftharpoons Fe(OH)_2A^-$	31.63	(Ritacca et al., 2022)
$FeHA^+$	$Fe^{2+} + HA^- \rightleftharpoons FeHA^+$	1.99	(Wersin,1990)
FeA	$Fe^{2+} + HA^- \rightleftharpoons FeA + H^+$	-6.58	(Ulmgen & Wahlberg, 1974)
Eq. Phases (solids, fix pH and pe)	Reaction	Log K_{sp} at 25℃	Reference
Strengite	$FePO_4.2H_2O \rightleftharpoons Fe^{3+} + PO_4^{3-} + 2H_2O$	-25*	(NIST, 2001; Smith et al., 2008)
Struvite	$MgNH_4PO_4.6H_2O \rightleftharpoons Mg^{2+} + NH_4^+ + PO_4^{3-} + 6H_2O$	-13.26	(Taylor et al., 1963)
Scorodite	$FeAsO_4.2H_2O \rightleftharpoons Fe^{3+} + AsO_4^{3-} + 2H_2O$	-20.429	(Nordstrom and Archer 2003)
Vivianite	$Fe_3(PO_4)_2.8H_2O \rightleftharpoons 3Fe^{2+} + 2\ PO_4^{3-} + 8H_2O$	-36	(Nriagu, 1972)
Ferrous oxalate	$FeC_2O_4.2H_2O \rightleftharpoons Fe^{2+} + C_2O_4^{2-} + 2H_2O$	6.5	(Liu et al., 2019)
Magnesium oxalate	$MgC_2O_4.H_2O \rightleftharpoons Mg^{2+} + C_2O_4^{2-} + H_2O$	5.68	(NIST, 2001)
Calcium oxalate	$CaC_2O_4.H_2O \rightleftharpoons Ca^{2+} + C_2O_4^{2-} + H_2O$	8.75	(NIST, 2001)

pH_Fix	H+ = H+	0.0	Define pH fixing mineral
pe_Fix	e- = e-	0.0	Define pe fixing mineral
HFO surface complexation	Reaction	LogK at 25℃	Reference
$\equiv FeH_2PO_4$	$\equiv FeOH+PO_4^{3-}+3H^+ \rightleftharpoons \equiv FeH_2PO_4 + H_2O$	35.5	(Smith et al., 2008)
$\equiv FeHPO_4^-$	$\equiv FeOH+PO_4^{3-}+2H^+ \rightleftharpoons \equiv FeHPO_4^- + H_2O$	30	(Smith et al., 2008)
$\equiv FePO_4^{2-}$	$\equiv FeOH+ PO_4^{3-}+ H^+ \rightleftharpoons \equiv FePO_4^{2-} + H_2O$	20.5	(Smith et al., 2008)

*The NIST (2001) contains a range of log K_{sp} values for strengite, depending on particle size and form, of between -21.8 (amorphous) and -26.8 (crystalline).

Table A2.3. PHREEQC input data file example

```
# Example for calculating total concentrations of Fe and P at pH 10 after 24
hours reaction time.

SOLUTION 1
      temp      22
      pH        7
      pe        0.422
      units     mg/l
      density   1                   # density, default 1 Kg/LA
      Fe(3)     128                 # Total concentration of element.
      P         46
      AAT       789                 # Total conc. of Ascorbic acid
      Mg        3.34
      S         3.122
      Ca        0.614
      C         42.89
      Na        220.09              # NaT=NaT+3*PT   For charge balance
      Cl        385.16              # ClT=ClT+3*FeT
      -water    1                   # kg water, default = 1 Kg


PHASES

Struvite

MgNH4PO4:6H2O = Mg+2 + NH4+ + PO4-3 + 6H2O

   log_k           -13.26

Strengite

FePO4:2H2O = Fe+3 + PO4-3 + 2H2O
```

```
   log_k    -25
Fe(OH)3(a)
Fe(OH)3 + 3 H+ = Fe+3 + 3 H2O
   log_k    4.891
Vivianite
Fe3(PO4)2:8H2O = 3Fe+2 + 2PO4-3 + 8H2O
   Log_k    -36
EQUILIBRIUM_PHASES 1
Fe(OH)3(a)   0.0   0
Vivianite    0.0   0
Calcite      0.0   0
Hydroxyapatite   0.0   0
Siderite     0.0   0
Pyrite       0.0   0
FeS(ppt)     0.0   0
Strengite    0.0   0
       pH_Fix -7          HCl 7.0
-force_equality true
       pe_Fix -0.422          O2
-force_equality true

SURFACE 1
Hfo_wOH   Fe(OH)3(a)  equilibrium_phase 0.2     1e5
Hfo_sOH   Fe(OH)3(a)  equilibrium_phase 0.005

  End
```

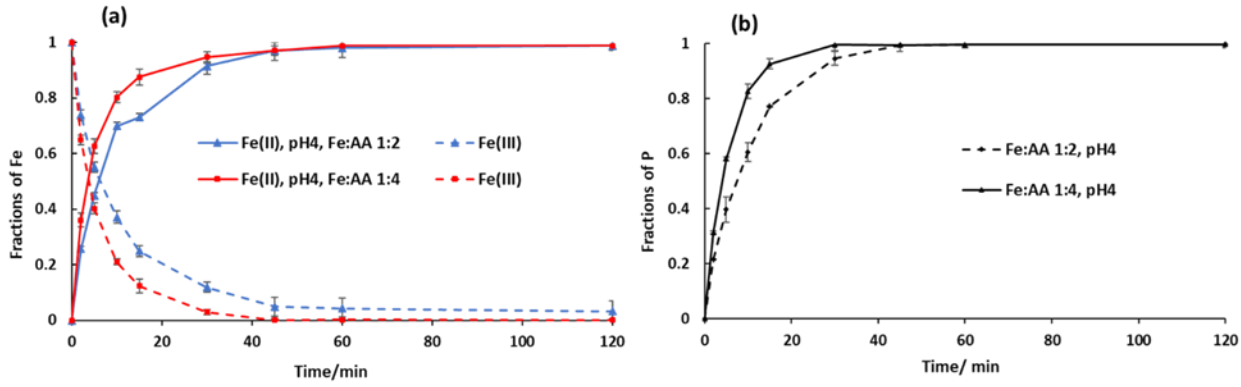

Fig. A2.1 Fractions of (a) iron(III) and iron(II), (b) total phosphorus versus time for treatment of fresh Fe-P sludge with ascorbic acid at Fe/AA molar ratios of 1:2 and 1:4 at pH 4. ORP values were +86±5 and +83±5 mV/Ag/AgCl respectively. Error bars correspond to 95% confidence level.

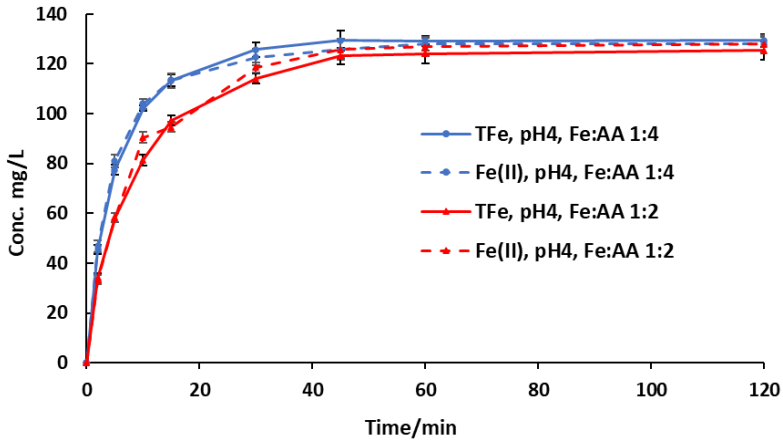

Fig. A2.2 Concentrations (mg/L) of total soluble Fe and Fe^{2+} versus time for treatment of fresh Fe-P sludge with ascorbic acid at Fe/AA molar ratios 1:2 and 1:4 at pH 4. Error bars correspond to 95% confidence level.

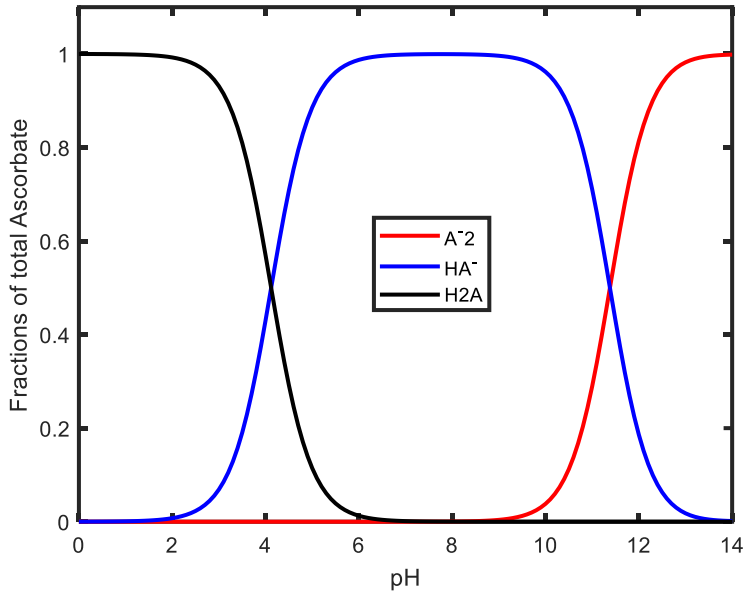

Fig. A2.3 Distribution diagram of ascorbic acid (H_2A) species as a function of pH (pK_{a1} =4.16, pK_{a2} = 11.55, Mahata et al., 2019). Plotted using PHREEQC software.

Table A2.4. Fe and P species after AA treatment at pH4: Observed vs model predictions

	%TP	%TFe^{3+}	%TFe^{2+}	%Free [Fe^{2+}]	%$FeH_2PO_4^{+*}$	%[Fe(II)-HA]$^{+*}$
Modeled	100	3	97	68	22	7
Experimental	97±1	2±1	98±1	---	---	---

* Percent of Fe^{2+} in the form of a complex

Table A2.5. Measured %TP and %TFe release from Fe-P sludge for different treatments.

	Ascorbic acid	Oxalic acid	H_2SO_4	HNO_3	HCL	Hydroxylamine
%TP	(97±1)	(95±2)	(3.1±0.2)	(2.5±0.1)	(1±0.3)	(3.4±0.2)
%TFe	(98±1)	(90±1)	(2±0.1)	(1.5±0.2)	(0.71±0.07)	(1±0.1)

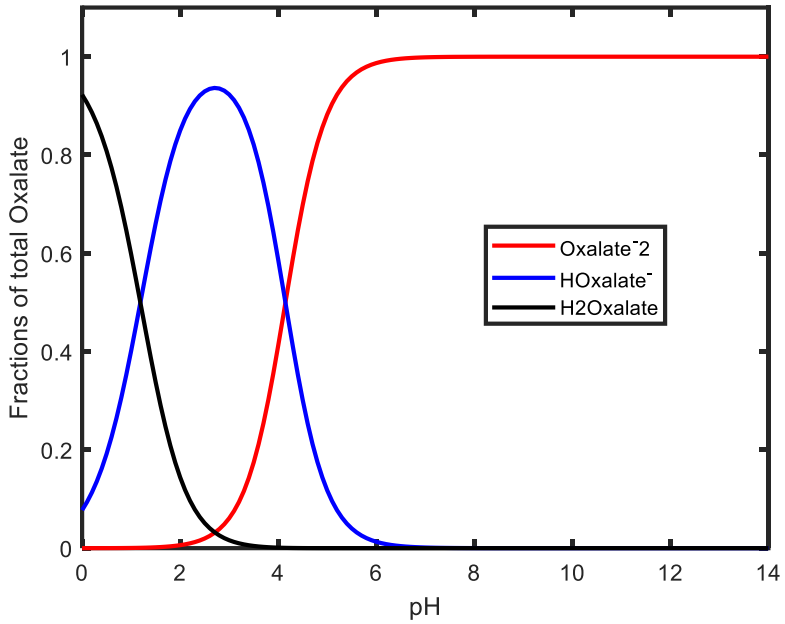

Fig. A2.4 Distribution diagram of oxalate species as a function of pH ((pK_{a1} =1.27, pK_{a2} = 4.28, Lee et al., 2007). Plotted using PHREEQC software

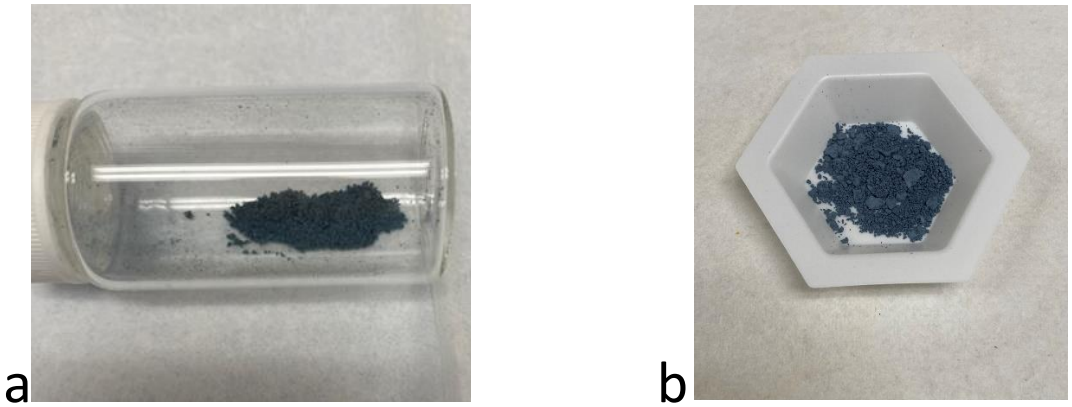

Fig. A2.5 (a) precipitated vivianite, (b) synthesized vivianite.

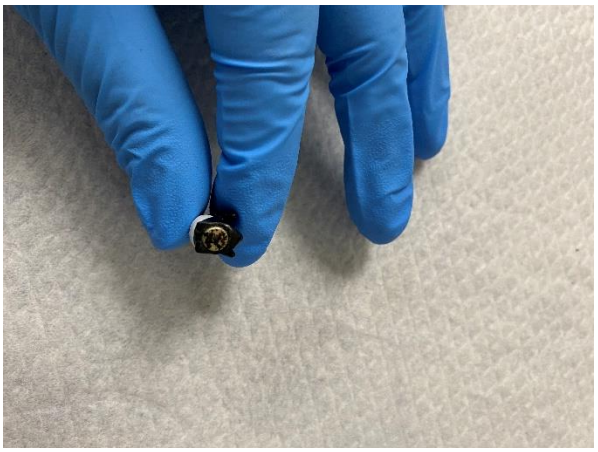

Fig. A2.6 Precipitated vivianite attracted to magnet used in the PHREEQC modelling.

References

Gamov, G. A., Yarullin, D. N., Gudyrina, M. A., Pogodina, E. I., Medvedeva, A. S., Zavalishin, M. N., **2022**. Protonation of l-Ascorbic Acid in an Aqueous Solution at T = 298.2 K, p = 0.1 MPa, and I = 0.10–5.0 mol L^{-1} (NaCl). Journal of Chemical & Engineering Data 2022 67 (6), 1358-1364. doi: 10.1021/acs.jced.2c00034.

Jung, Y., Koh, H., Shin, W., Sung, N., **2005**. Wastewater treatment using combination of MBR equipped with non-woven fabric filter and oyster-zeolite column. Environmental Engineering Research, 10, 247-256.

Lee, S. O., Tran, T., Jung, B. H., Kim, S. J., Kim, M. J., **2007**. Dissolution of iron oxide using oxalic acid, Hydrometallurgy, Volume 87, Issues 3–4, Pages 91-99, doi.org/10.1016/j.hydromet.2007.02.005.

Liu, F., Peng, C., Wilson, B. P., & Lundström, M., **2019**. Oxalic acid recovery from high iron oxalate waste solution by a combination of ultrasound-assisted conversion and cooling crystallization. ACS Sustainable Chemistry and Engineering, 20(7), 17372-17378. doi.org/10.1021/acssuschemeng.9b04351.

Mahata, S., Mitra, I., Mukherjee, S., Pera Reddy B. V., Ghosh, G. KR., Linert, W., and S. Ch. Moi, S. Ch., **2019**. Speciation Study of L-ascorbic Acid and its Chelated Cu(II) & Ni(II) Complexes: an Experimental and Theoretical Model of Complex Formation. S. Afr. J. Chem., 72, 229–236, doi./10.17159/0379-4350/2019/v72a30.

Metcalf and Eddy Inc., Tchobanoglous G., **2014**. Wastewater engineering : treatment and reuse, 5th Edition. McGraw Hill, New York.

National Institute of Standards and Technology, **2001**.NIST Standard Reference Database 46. National Institute of Standards and Technology: Gaithersburg, Maryland.

Nordstrom, D.K., Archer, D.G., **2003**. Arsenic thermodynamic data and environmental geochemistry, in Arsenic in Ground Water. (eds A.H. Welch and K.G. Stollenwerk), Kluwer Academic Publishers, Boston, pp. 1–25.

Nriagu, J.O., **1972**. Stability of vivianite and ion-pair formation in the system $Fe_3(PO_4)_2$-$H_3PO_4H_3PO_4$-H_2o. Geochem. Cosmochim. Acta 36 (4), 459–470.

Ritacca, A. G., Malacaria, L., Sicilia, E., Furia, E., Mazzone, G., **2022**. Experimental and theoretical study of the complexation of Fe^{3+} and Cu^{2+} by l-ascorbic acid in aqueous solution. Journal of Molecular Liquids, Volume 355, 118973, doi.org/10.1016/j.molliq.2022.118973.

Roldan, R., Barron, V., Torrent, J., **2002**. Experimental alteration of vivianite to lepidocrocite in a calcareous medium. Clay Minerals 37 (4), 709-718.

Smith, S., Takacs, I., Murthy, S., Daigger, G. T., Szabo, A., **2008**. Phosphate Complexation Model and Its Implications for Chemical Phosphorus Removal. Water Environ. Res. 80 (5): 428−438.

Szabo, A., Takács, I., Murthy, S., Daigger, G.T., Licsko, I., Smith, S., **2008**. Significance of design and operational variables in chemical phosphorus removal. Water Environ. Res., 80, 407-416.

Taylor, A. W., Frazier, A. W., Gurney, E. L., **1963**. Solubility products of magnesium ammonium and magnesium potassium phosphates. Transactions Faraday Society, 59, 1580-1584.

Ulmgen, P. and Wahlberg, O., **1974**. Equilibrium Studies of L-Ascorbate Ions. IX. Equilibria between Iron(II) Ions, Ascorbate Ions, and Protons in 3 M $(Na)ClO_4$ Medium. Acta Chem Scand. A28. Pages: 631-637.doi:10.3891/acta.chem.scand.28a-063.

WEF., **2011**. Nutrient Removal - Manual of Practice. WEF Manual of Practice No. 34.

Wersin, P., **1990**. Ph.D. Thesis, No. 9230, Swiss Federal Institute of Technology (ETH Zu¨ rich).

Wilfert, P., Mandalidis, A., Dugulan, A.I., Goubitz, K., Korving, L., Temmink, H., Witkamp, G.J.,Van Loosdrecht, M.C.M., 2016. Vivianite as an important iron phosphate precipitate in sewage treatment plants. Water Research 104, 449-460.

Zhang. J, Chen. Z, Liu. Y, Wei. W, Ni. B-J., **2022**. Phosphorus recovery from wastewater and sewage sludge as vivianite, Journal of Cleaner Production. doi.org/10.1016/j.jclepro.2022.133439.

Appendix 3 (Chapter 5 appendix)

Table A3.1. Chemical components of "Syntho" synthetic wastewater recipe adapted from Boeije et al. (1999).

Chemical reagent	Concentration (mg/L)
Na acetate	120
Meat extract	15
Low fat milk powder	120
Potato starch	50
Glycerol	40
Peptone	15
NH_4Cl	11
Urea	75
Uric acid	9
$K_3PO_4 \cdot H_2O$	20
$MgHPO_4 \cdot 3H_2O$	25
Alcohol ethoxylate	10
Diatomaceous earth	10
Diet fibres	80
LAS	10
Lyophilised AS	50
$CaCl_2$	5
$NaHCO_3$	25
$FeSO_4 \cdot 3H_2O$	10
$CoCl_2 \cdot 6H_2O$	0.05
$Cr(NO_3)_3 \cdot 9H_2O$	0.68
$CuCl_2 \cdot 2H_2O$	0.48
EDTA	0.22
K_2MoO_4	0.02
$MnSO_4 \cdot H_2O$	0.1
$NiSO_4 \cdot 6H_2O$	0.3
$ZnCl_2$	0.18

Table A3.2. Characteristics of Syntho recipe

pH	T.COD	TOC	TSS	TN	TP	P_{ortho}	COD/TOC	C/N/T	Alkalinity
7.5	392.67	116.94	91	50.9	8.96	5.20	3.36	100:7:2	99.3

Unit: mg/L

Table A3.3. Inorganic components of synthetic wastewater adapted from Jung et al. (2005).

Chemical Reagent	Concentration (mg/L)
Magnesium sulfate ($MgSO_4.7H_2O$)	24.0
Calcium chloride ($CaCl_2.2H_2O$)	2.40
Sodium bicarbonate ($NaHCO_3$)	300.0
Sodium phosphate tribasic ($Na_3PO_4.12H_2O$) (mg P/L)	5.00

Table A3.4. Calculated total masses (mg) of proteins, carbohydrates, and fats included in all carbon and nitrogen components per 1L of Syntho recipe.

Component	Proteins (mg)	Carbohydrates (mg)	Fats (mg)
*Meat extract	3	0.18	0.75
**Low fat milk powder	34.8	55.2	13.2
Potato starch	0	50	0
Glycerol	0	0	40
Peptone	15	0	0
Total mass (mg)	52.8	105.38	53.95

*Meat extract contains 20% proteins, 5% carbohydrates, and 1.2% fat.
**Low fat milk powder contains 29% proteins, 46% carbohydrates, and 25% fat. (Handbook of Food Chemistry) (Cheung & Bhavbhuti, 2015).

Sample calculation for proteins in 15 mg meat extract as in (Syntho)

Proteins in 15 mg meat extract = $\frac{15 \times 20}{100}$=3 mg

Sample calculation for mgs required for proteins in this study recipe equivalent to 52.8 mg :

Protein sources are peptone and meat extract.

Mass of protein needed from peptone = 15 mg

Mass of peptone needed = 15 mg

Mass of protein needed from meat extract = 52.8-15 = 37.8 mg

Mass of meat extract equivalent to 37.8 mg protein = $\frac{37.8 \times 100}{20}$=189 mg.

Table A3.5. Typical composition of raw municipal wastewater with minor contributions of industrial wastewater (in g/m^3) adopted from Volcke et al, (2023).

Parameter	Low	Medium	High
COD total	500	750	1,200
COD soluble	200	300	480
COD suspended	300	450	720
BOD	230	350	560
VFAs (as acetate)	10	30	80
N total	30	60	100
Ammonia N	20	45	75
Nitrate + Nitrite N	0.1	0.2	0.5
Organic N	10	15	25
P total	6	15	25
Ortho-P	4	10	15
Organic P	2	5	10
Sulphate	24	36	72
TSS	250	400	600
VSS	200	320	480

Table A3.6. pH values at P removal tests conducted with different recipes

Recipe	pH ± 0.03
Control	7.23
Full	7.30
All-C	7.17
All-N	7.25
Urea	7.29
Peptone	7.26
NH_4Cl	7.29
ME	7.14
Starch	7.31
Glycerol	7.30
LM	7.14
ME + All-N	7.22
Starch + All-N	7.31
Glycerol + All-N	7.28
LM + All-N	7.34

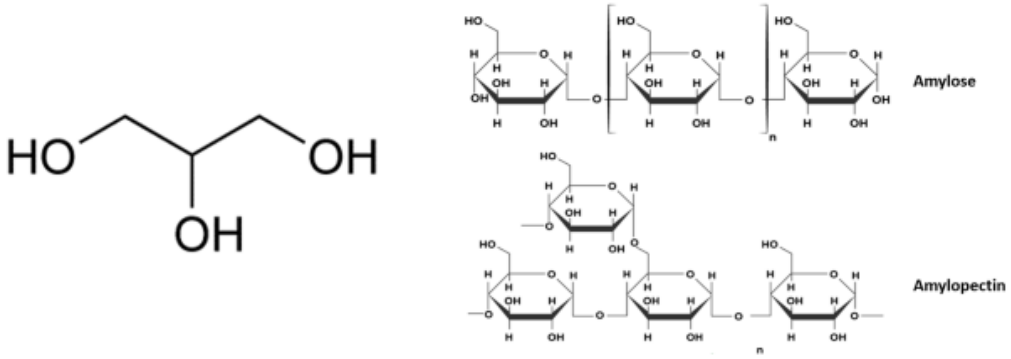

Glycerol **Starch (amylose + amylopectin)**

Figure A3.1. Chemical structure for glycerol and starch (amylose & amylopectin) molecules.

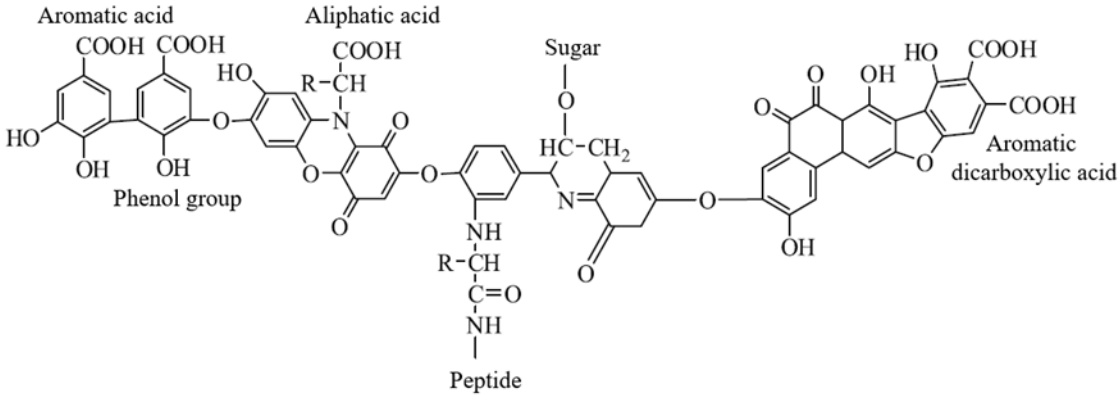

Figure A3.2. Proposed chemical structure for humic acid molecule. (Adopted from Stevenson, 1994).

Table A3.7. TOC concentrations (mg C/L) for different synthetic wastewater recipes before and after P removal tests.

Recipe	TOC (mg C/L) Before	TOC (mg C/L) After
Control	0.00	0.00
Full	120±3	122±2
All-C	114±2	112±3
All-N	18±1	16±3
Urea	16±2	17±1
Peptone	8±1	7±2
NH_4Cl	0.00	0.00
ME	74±4	72±3
Starch	26±3	24±1
Glycerol	18±4	16±2
LM	10±1	10±3
ME-N	98±5	96±3
Starch-N	43±2	40±1
Glycerol-N	39±3	39±2
LM-N	27±3	26±2

References

Boeije, G., Corstanje, R., Rottiers, A., Schowanek, D., **1999**. Adaptation of the CAS test system and synthetic sewage for biological nutrient removal: Part I: development of a new synthetic sewage. Chemosphere. 38(4):699–709. doi:10.1016/s0045-6535(98)00311-7.

Cheung, Peter C. K., and Bhavbhuti M. Mehta, eds., **2015**. Handbook of Food Chemistry. Heidelberg: Springer Reference. Print.

Jung, Y., Koh, H., Shin, W., Sung, N., **2005**. Wastewater treatment using combination of MBR equipped with non-woven fabric filter and oyster-zeolite column. Environmental Engineering Research, 10, 247-256.

Stevenson, F. J., **1994**. Humus Chemistry: Genesis, Composition, Reactions, 2nd ed; Wiley: New York.

Volcke, E. I. P., Solon, K., Comeau, Y., Henze, M., **2023**. Wastewater Characteristics. Edited by Guanghao Chen; Mark C.M. van Loosdrecht; George A. Ekama; Damir Brdjanovic., Biological Wastewater Treatment: Principles, Modelling and Design. Chapter 3 (77-110). IWA Publishing. doi.org/10.2166/9781789060362_0077.

Appendix 4 (Chapter 3 extra discussion)

1- PHREEQC modeling

PHREEQC modeling showed poor fit for P release from Fe-P solids at pH values between 7 and 9 because it considered only P binded to the final surfaces that formed and did not consider P trapped inside HFO particles. However, another modeling software could be used to model the release of internal P like SUMO modeling software (Dynamita S.A.R.L). Moreover, PHREEQC has the capability to model slow irreversible sorption (Parsons et al., 2013).

2- Effect of NaCl on P release from Fe-P solids

The effect of Cl^- ion on P release could be also explained by the type of surface complexes PO_4^{3-} is forming with HFO. For example, it had been reported that electrolyte ions can compete with ions that form outer-sphere complexes for adsorption sites leading to decrease in their adsorption. Conversely, the competition effect of electrolyte ions is very weak toward ions that form inner-sphere complexes where they are directly coordinated to the surface sites (Antelo et al., 2005; Hiemstra, 2018). Thus the negligible effect of Cl^- on P release indicates that PO_4^{3-} anion is forming inner-sphere complexes with HFO surface and the adsorption is less affected by the increase of solution ionic strength.

3- Effect of aging on HFO surface area

As mentioned in chapter 3, aging of HFOs allows for structural transformations to occur altering their surface area and thus their adsorptive/desorption capacity. In fact, changes of HFOs surface area over time due to particle evolution with aging could be explained by Ostwald ripening which describes particle growth by simultaneous precipitation and dissolution processes. Hiemstra

et al, (2019) studied the dynamic change of the reactive surface area of wet ferrihydrite over time. They revealed that when ferrihydrite is initially formed, the particles are ultra-small and subject to Oswald ripening in which the smallest particles dissolve and the larger ones grow, resulting in a decrease of the reactive surface area.

References

Antelo, J., Avena, M., Fiol, S., López, R., Arce, F., 2005. Effects of pH and ionic strength on the adsorption of phosphate and arsenate at the goethite–water interface. Journal of Colloid and Interface Science. 285 (2): 476-486. doi.org/10.1016/j.jcis.2004.12.032.

Hiemstra, T., 2018. Ferrihydrite interaction with silicate and competing oxyanions: Geometry and Hydrogen bonding of surface species. Geochimica et Cosmochimica Acta. (238): 453-476. doi.org/10.1016/j.gca.2018.07.017.

Hiemstra, T., Mendez, J. C., Li, J., 2019. Evolution of the reactive surface area of ferrihydrite: time, pH, and temperature dependency of growth by Ostwald ripening. Environ. Sci.: Nano. 6, 820-833. doi:10.1039/C8EN01198B.

Parsons, C. T., Raoul-Marie Couture, R.-M., Omoregie, E. O., Bardelli, F., Greneche, J.-M., Roman-Ross, G., Laurent Charlet, L., 2013. The impact of oscillating redox conditions: Arsenic immobilisation in contaminated calcareous floodplain soils. Environmental Pollution. 178: 254-263.doi.org/10.1016/j.envpol.2013.02.028.